Molecular Meccano. 3. Constitutional and Translational Isomerism in [2]Catenanes and [n]Pseudorotaxanes[1]

David B. Amabilino,[†] Pier-Lucio Anelli,[‡] Peter R. Ashton,[†] George R. Brown,[⊥] Emilio Córdova,[∥] Luis A. Godínez,[∥] Wayne Hayes,[†] Angel E. Kaifer,[∥] Douglas Philp,[†] Alexandra M. Z. Slawin,[§] Neil Spencer,[†] J. Fraser Stoddart,*[,†] Malcolm S. Tolley,[†] and David J. Williams*[,§]

Contribution from The School of Chemistry, The University of Birmingham, Edgbaston, Birmingham B15 2TT, U.K., BRACCO, via Egidio Folli 50, 20134 Milano, Italy, ZENECA Pharmaceuticals, Mereside, Alderley Park, Macclesfield, Cheshire, SK10 4TG, U.K., Department of Chemistry, University of Miami, Coral Gables, Florida 33124, and Department of Chemistry, Imperial College, London SW7 2AY, U.K.

Received December 2, 1994. Revised Manuscript Received August 17, 1995[⊗]

Abstract: The mutual molecular recognition expressed between two classes of compounds has led to the self-assembly of a range of [2]catenanes, composed of cyclic polyethers intercepted by π-electron donors, and a range of [n]-pseudorotaxanes, composed of similar acyclic polyethers, and various tetracationic cyclophanes. These molecular self-assembly processes rely upon the recognition between (i) π-electron rich and π-electron deficient aromatic units and (ii) hydrogen bond donors and acceptors, within the different components. The constitution of the π-electron rich and the π-electron deficient structural components in these molecular and supramolecular structures has a profound effect on the organization of the various assemblies and on their dynamic properties with respect to each other both in solution and in the solid state. The techniques of X-ray crystallography, fast-atom bombardment mass spectrometry, ^{1}H, ^{13}C, and dynamic nuclear magnetic resonance, ultraviolet/visible spectroscopies, and electrochemistry have been used in the solid and solution states to assess the nature of the structures of the catenanes and the superstructures of the pseudorotaxanes. The successful assembly of these catenanes and pseudorotaxanes, through the transcription of programmed molecular information, in the form of noncovalent bonding interactions, lends support to the contention that self-assembly is a viable paradigm for the construction of nanometer-scale molecular and supramolecular structures incorporating a selection of simple building blocks.

The engineering of nanometer-scale (nanoscale) structures has fascinated and inspired[2] the scientific community for almost a quarter of a century. Although there are no fundamental thermodynamic[3] or quantum mechanical[4] impediments to the development of nanoscale architectures, there is a growing realization[5] that "engineering down" approaches, i.e., a reduction in the size of structures generated by lithographic techniques below the present 1 μm lower limit, are likely to become more impractical. It is therefore becoming increasingly apparent that only by the extension of our knowledge of the self-assembly[6] of large-scale biological structures, which exist and function at and beyond the nanoscale, *downwards* and the development of our expertise regarding the chemical syntheses of small scale structures *upwards*, can the gap between the promise and the reality of nanosystems be closed. This approach to nanoscale structures and systems has been termed the "bottom-up" or "engineering-up" approach.[7] The appearance of synthetic nanometer-scale chemical assemblies has only recently been accomplished as a result of the adoption by chemists of the self-assembly paradigm found in natural systems and its application to the generation of self-assembling,[8] self-organizing,[9] and self-replicating[10] systems. All of these chemical examples have had their success built around an understanding and optimization of molecular recognition[11] processes in synthetic chemical systems. Recently, we have developed[1,12]

[†] University of Birmingham.
[‡] BRACCO.
[⊥] Zeneca Pharmaceuticals.
[∥] University of Miami.
[§] Imperial College.
[⊗] Abstract published in *Advance ACS Abstracts*, October 1, 1995.

(1) Amabilino, D. B.; Ashton, P. R.; Brown, C. L.; Córdova, E.; Godínez, L. E.; Goodnow, T. T.; Kaifer, A. E.; Newton, S. P.; Philp, D.; Pietraszkiewicz, M.; Raymo, F. M.; Reder, A. S.; Rutland, M. T.; Slawin, A. M. Z.; Spencer, N.; Stoddart, J. F.; Williams, D. J. *J. Am. Chem. Soc.* **1995**, *117*, 1271−1293.

(2) (a) Drexler, K. E. *Proc. Natl. Acad. Sci. U.S.A.* **1981**, *78*, 5275−5278 and references therein. (b) Drexler, K. E. *Nanosystems—Molecular Machinery, Manufacturing and Computation*; Wiley Interscience: New York, 1992.

(3) Bennet, C. H. *Int. J. Theor. Phys.* **1982**, *21*, 905−940.

(4) Feynman, R. P. *Found. Phys.* **1986**, *16*, 507−531.

(5) (a) Carter, F. L. *Physica* **1984**, *10D*, 174−194. (b) Haarer, D. *Angew. Chem., Int. Ed. Engl.* **1989**, *28*, 1544−1547 and references cited therein.

(6) (a) Lindsey, J. S. *New J. Chem.* **1991**, *15*, 153−180. (b) Whitesides, G. M.; Mathias, J. P.; Seto, C. T. *Science (Washington DC)* **1991**, *254*, 1312−1319. (c) Amabilino, D. B.; Stoddart, J. F. *Chem. Rev.* In press.

(7) Miller, J. S. *Adv. Mater.* **1990**, *2*, 378−379, 495−497, and references cited therein.

(8) For recent examples of synthetic self-assembling systems, see: (a) Simard, M.; Su, D.; Wuest, J. D. *J. Am. Chem. Soc.* **1991**, *113*, 4696−4698. (b) Geib, S. J.; Vicent, C.; Fan, E.; Hamilton, A. D. *Angew. Chem., Int. Ed. Engl.* **1993**, *32*, 119−121. (c) Copp, S. B.; Subramanian, S.; Zaworotko, M. J. *Angew. Chem., Int. Ed. Engl.* **1993**, *32*, 706−709. (d) Carina, R. F.; Bernardinelli, G.; Williams, A. F. *Angew. Chem., Int. Ed. Engl.* **1993**, *32*, 1463−1465. (e) Constable, E. C.; Edwards, A. J.; Raithby, P. R.; Walker, J. V. *Angew. Chem., Int. Ed. Engl.* **1993**, *32*, 1465−1467. (f) Wyler, R.; de Mendoza, J.; Rebek, J., Jr. *Angew. Chem., Int. Ed. Engl.* **1993**, *32*, 1699−1701. (g) Menger, F. M.; Littau, C. A. *J. Am. Chem. Soc.* **1993**, *115*, 10083−10090. (h) Percec, V.; Heck, J.; Lee, M.; Ungar, G.; Alvarez-Castillo, A. *J. Mater. Chem.* **1993**, *2*, 1033−1039. (i) Krämer, R.; Lehn, J.-M.; Marquis-Rigault, A. *Proc. Natl. Acad. Sci. U.S.A.* **1993**, *90*, 5394−5398. (j) Thonden van Velzen, E. U.; Engbersen, J. F. J.; Reinhoudt, D. N. *J. Am. Chem. Soc.* **1994**, *116*, 3597−3598. (k) Mathias, J. P.; Simanek, E. E.; Whitesides, G. M. *J. Am. Chem. Soc.* **1994**, *116*, 4326−4340. (l) Hanessian, S.; Gomtsyan, A.; Simard, M.; Roelens, S. *J. Am. Chem. Soc.* **1994**, *116*, 4495−4496. (m) Kotera, M.; Lehn, J.-M.; Vigneron, J.-P. *J. Chem. Soc., Chem. Commun.* **1994**, 197−198.

0002-7863/95/1517-11142$09.00/0

an efficient system for the construction of mechanically- interlocked chemical systems, such as catenanes[6c,13] and rotaxanes.[14] This strategy relies upon the molecular recognition observed between π-electron deficient 4,4′-bipyridinium dications and crown ethers containing π-electron rich aromatic rings[15]—usually hydroquinone or 1,5-dioxynaphthalene rings.

We are seeking to understand, at a fundamental level, the influence of constitutional changes upon the outcome of molecular and supramolecular self-assembly processes. At the outset, it may be recalled that the [2]catenane, comprised of bis-*p*-phenylene-34-crown-10 (BPP34C10) and cyclobis(paraquat-*p*-phenylene), is formed[12] in 70% yield at ambient conditions in acetonitrile (Scheme 1). The efficiency of this catenation is derived, at least in part, from the high level of preorganization present in the macrocyclic polyether component, which interacts ultimately with the tetracationic cyclophane component through $\pi-\pi$ stacking,[16] and C−H···O and T-type hydrogen bonding[17] interactions in the [2]catenane. To this end, we report here the attempted self-assembly of the eight constitutional isomers of the prototypical {[2]-[BPP34C10]-[BBIPYBIPXYCY]catenane}$[PF_6]_4$, shown in Scheme 1. The changes in the constitution of this [2]catenane have been made in (i) the π-electron rich units of the macrocyclic polyether and in (ii) the xylyl spacers of the π-electron deficient tetracationic cyclophane. The changes, which have been made (Figure 1), have involved the constitutions—meta or para—of these units and spacers and have led to the self-assembly of seven isomeric [2]catenanes. A detailed investigation of the binding properties of the components of these isomers has provided valuable information on the consequences of constitutional change upon the mutual recognition compatibilities between the macrocyclic polyether and tetracationic cyclophane components. The knowledge gained from this investigation of constitutional isomerism has then been applied to the self-assembly of [2]- and [3]-pseudorotaxanes between cyclobis(paraquat-*p*-phenylene) and a range of acyclic molecular components containing three or more π-electron rich aromatic systems linked by an appropriate number of tetraethylene glycol spacer units. The translational isomerism within these self-assembled superstructures is rationalized in terms of the number and identity—hydroquinone and/or 1,5-dioxynaphthalene residues—of the π-electron rich aromatic systems. Here, we report[18] our findings on the constitutional and translational isomerism in [2]catenanes and [*n*]pseudorotaxanes.

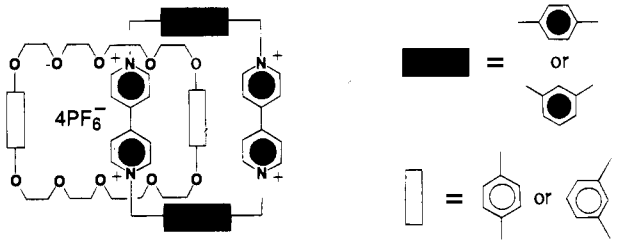

Figure 1. The variable constitutions of the aromatic residues in the macrocyclic polyether and tetracationic cyclophane components of the [2]catenanes. There are nine constitutional isomers.

Scheme 1

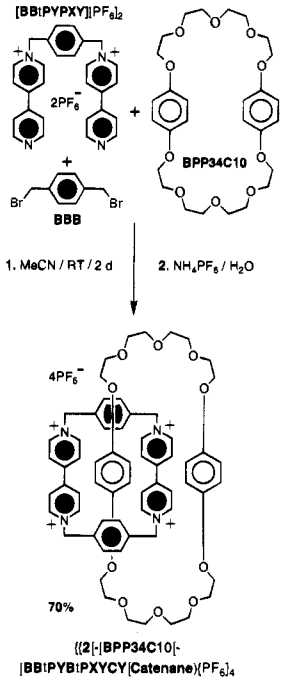

(9) Self-organizing systems have been described: (a) Möbius, D.; Möhwald, H. *Adv. Mater.* **1991**, *3*, 19−24 and references cited therein. (b) Menger, F. M. *Angew. Chem., Int. Ed. Engl.* **1991**, *30*, 1086−1099. (c) Joachimi, D.; Tschierske, C.; Müller, H.; Wendorff, J. H.; Schneider, L.; Kleppinger, R. *Angew. Chem., Int. Ed. Engl.* **1993**, *32*, 1165−1167. (d) Kimizuka, N.; Kawasaki, T.; Kunitake, T. *J. Am. Chem. Soc.* **1993**, *115*, 4387−4388. (e) Lopaz, G. P.; Albers, M. W.; Schreiber, S. L.; Caroll, R.; Peralta, G. M.; Whitesides, G. M. *J. Am. Chem. Soc.* **1993**, *115*, 5877−5878. (f) Fujita, K.; Kimura, S.; Imanishi, Y.; Rump, E.; Ringsdorf, H. *J. Am. Chem. Soc.* **1994**, *116*, 2185−2186.

(10) Self-replicating molecules have been reported: (a) Terfort, A.; von Kiedrowski, G. *Angew. Chem., Int. Ed. Engl.* **1992**, *31*, 654−656. (b) von Kiedrowski, G. In *Bioorganic Chemistry Frontiers*; Dugas, H., Ed.; Springer-Verlag: Berlin, 1993; Vol. 3, pp 113−146. (c) Hong, J.-I.; Feng, Q.; Rotello, V.; Rebek, J., Jr. *Science (Washington DC)* **1992**, *255*, 848−850. (d) Feng, Q.; Park, T. K.; Rebek, J., Jr. *Science (Washington DC)* **1992**, *256*, 1179−1180. (e) Menger, F. M.; Eliseev, A. V.; Khanjin, N. A. *J. Am. Chem. Soc.* **1994**, *116*, 3613−3614. (f) Li, T.; Nicolaou, K. C. *Nature* **1994**, *369*, 218−221. (g) Sievers, D.; von Kiedrowski, G. *Nature* **1994**, *369*, 221−224. (h) Pieters, R. J.; Huc, I.; Rebek, J., Jr. *Tetrahedron* **1995**, *51*, 485−498.

(11) Lehn, J.-M. *Science* **1993**, *260*, 1762−1763.

(12) Anelli, P. L.; Ashton, P. R.; Ballardini, R.; Balzani, V.; Delgado, M.; Gandolfi, M. T.; Goodnow, T. T.; Kaifer, A. E.; Philp, D.; Pietraszkiewicz, M.; Prodi, L.; Reddington, M. V.; Slawin, A. M. Z.; Spencer, N.; Stoddart, J. F.; Vicent, C.; Williams, D. J. *J. Am. Chem. Soc.* **1992**, *114*, 193−218.

(13) (a) Walba, D. M. *Tetrahedron* **1985**, *41*, 3161−3212. More recent reports on catenanes: (b) Hunter, C. A. *J. Am. Chem. Soc.* **1992**, *114*, 5303−5311. (c) Gruter, G.-J. M.; de Kanter, F. J. J.; Markies, P. R.; Nomoto, T.; Akkerman, O. S.; Bickelhaupt, F. *J. Am. Chem. Soc.* **1993**, *115*, 12179−12180. (c) Fujita, M.; Ibukuro, F.; Hagihara, H.; Ogura, K. *Nature* **1994**, *367*, 720−723. (d) Armspach, D.; Ashton, P. R.; Ballardini, R.; Balzani, V.; Godi, A.; Moore, C. P.; Prodi, L.; Spencer, N.; Stoddart, J.-F.; Tolley, M. S.; Wear, T. J.; Williams, D. J. *Chem. Eur. J.* **1995**, *1*, 33−55. (e) Ottens-Hildebrandt, S.; Nieger, M.; Rissanen, K.; Rouvinen, J.; Meier, S.; Harder, G.; Vögtle, F. *J. Chem. Soc., Chem. Commun.* **1995**, 777−778.

(14) Rotaxanes have recently been reported: (a) Isnin, R.; Kaifer, A. E. *J. Am. Chem. Soc.* **1991**, *113*, 8188−8190. (b) Diederich, F.; Dietrich-Buchecker, C.; Nierengarten, J.-F.; Sauvage, J.-P. *J. Chem. Soc., Chem. Commun.* **1995**, 781−782. (c) Córdova, E.; Bissell, R. A.; Kaifer, A. E. *J. Org. Chem.* **1995**, *60*, 1033−1038.

(15) For other self-assembled structures constructed based on this recognition system, see: (a) Philp, D.; Stoddart, J. F. *Angew. Chem., Int. Ed. Engl.* Submitted. For reports by other research groups on this system, see: (b) Vögtle, F.; Müller, W. M.; Müller, U.; Bauer, M.; Rissanen, K. *Angew. Chem., Int. Ed. Engl.* **1993**, *32*, 1295−1297. (c) Gunter, M. J.; Hockless, D. C. R.; Johnston, M. R.; Skelton, B. W.; White, A. H. *J. Am. Chem. Soc.* **1994**, *116*, 4810−4823. (d) Benniston, A. C.; Harriman, A.; Lynch, V. M. *Tetrahedron* Lett. **1994**, *35*, 1473−1476.

(16) For discussions concerning $\pi-\pi$ stacking interactions, see: (a) Hunter, C. A.; Sanders, J. K. M. *J. Am. Chem. Soc.* **1990**, *112*, 5525−5534. (b) Hunter, C. A. *Chem. Soc. Rev.* **1994**, *23*, 101−109.

(17) Jorgensen, W. L.; Severance, D. L. *J. Am. Chem. Soc.* **1990**, *112*, 4768−4774.

(18) Some of the results presented here have appeared as an abbreviated format in the form of preliminary communications. (a) Anelli, P. L.; Ashton, P. R.; Spencer, N.; Slawin, A. M. Z.; Stoddart, J. F.; Williams, D. J. *Angew. Chem., Int. Ed. Engl.* **1991**, *30*, 1036−1039. (b) Ashton, P. R.; Philp, D.; Spencer, N.; Stoddart, J. F. *J. Chem. Soc., Chem. Commun.* **1991**, 1677−1679. (c) Amabilino, D. B.; Ashton, P. R.; Tolley, M. S.; Stoddart, J. F.; Williams, D. J. *Angew. Chem., Int. Ed. Engl.* **1993**, *32*, 1297−1301. (d) Ashton, P. R.; Philp, D.; Spencer, N.; Stoddart, J. F.; Williams, D. J. *J. Chem. Soc., Chem. Commun.* **1994**, 181−184. (e) Amabilino, D. B.; Ashton, P. R.; Brown, G. R.; Hayes, W.; Stoddart, J. F.; Williams, D. J. *J. Chem. Soc., Chem. Commun.* **1994**, 2479−2482.

Scheme 2

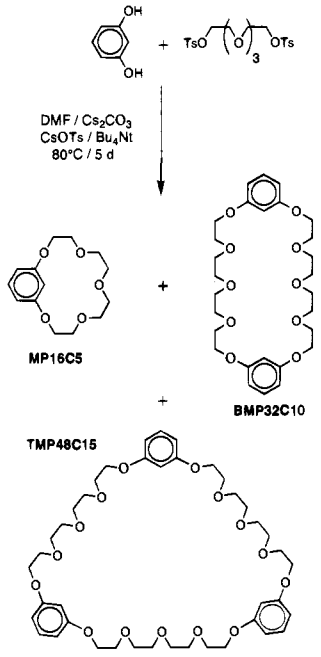

Scheme 3

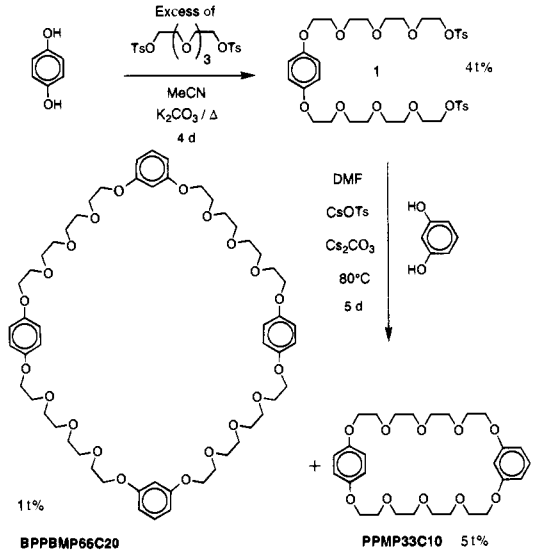

Results and Discussion

Names and Cartoons. The presentation of the results in this paper employs acronyms composed of letters, and occasionally numbers, to identify the neutral and charged compounds displayed in the figures and schemes. The macrocyclic polyethers, bis-*p*-phenylene-34-crown-10, *p*-phenylene-*m*-phenylene-33-crown-10, and bis-*m*-phenylene-32-crown-10, are abbreviated to BPP34C10, PPMP33C10, and BMP32C10, respectively. HQ and NP represent hydroquinone and 1,5-dioxynaphthalene, respectively. The acronym *n*HQ or *n*NP describes compounds containing *n* hydroquinone and 1,5-dioxynaphthalene rings, respectively, linked by $(n-1)$ tetraethylene glycol spacer units and terminated by benzyl ethers. Where NP and HQ appear in the same acronym, e.g., 2NPHQ, the first identifier represents the rings at the chain termini—in the case of the example given, 1,5-dioxynaphthalene rings terminated by benzyl ether groups—and the second identifier represents the ring at the center of the chain—in the case of the example given, a hydroquinone ring. The other acronyms employed in the figures and schemes can be deduced on the basis of the following definitions: B stands for bis when at the beginning, for benzyloxy or bromomethyl when in the middle, and for benzene when at the end of the name. Furthermore, B stands for benzyloxy when it is present in the acronyms of neutral compounds and for bromomethyl when it is present in those of charged compounds. E and H stand for ethoxy and hydroxy, respectively. CY, XY, and BIXY represent cyclophane, xylylene, and bisxylylene units, respectively. In addition, BP and BIPY stand for bipyridine and the bipyridinium ring systems, respectively. Where appropriate, B (benzene) or XY (xylylene) are preceded by M or P, indicating their meta or para substitution patterns, respectively. The formal charges are indicated in the usual manner. In the cartoon versions of the figures and schemes, smaller block rectangles represent disubstituted benzene rings, whereas the larger rectangles represent 4,4′-bipyridinium ring systems, with the positive charges positioned appropriately. In neutral molecules, unshaded rectangles represent hydroquinone rings and unshaded rectangles, bearing a bold horizontal bar, represent 1,5-dioxynaphthalene rings.

I. Constitutionally-Isomeric [2]Catenanes. A. Synthesis. The macrocyclic polyether bis-*m*-phenylene-32-crown-10 (BMP32C10)[19] was prepared by the reaction (Scheme 2) of resorcinol (1,3-dihydroxybenzene) with tetraethylene glycol bistosylate in the presence of cesium carbonate as base under pseudo high-dilution conditions and using cesium ion as an aid[20] to macrocyclic formation. The major product (54%) of this reaction was identified as *m*-phenylene-16-crown-5 (MP16C5),[21] with the desired BMP32C10 being isolated in only 8.4% yield.[22] The trimeric tris-*m*-phenylene-48-crown-15 (TMP48C15) was also obtained (1.7%) from this reaction. The most rapid and efficient synthesis of *p*-phenylene-*m*-phenylene-33-crown-10 (PPMP33C10) (Scheme 3) was achieved by firstly reacting hydroquinone (1,4-dihydroxybenzene) in the presence of an excess of tetraethylene glycol bistosylate. The resulting ditosylate 1 can be easily purified by silica gel chromatography, before being reacted with resorcinol in the presence of cesium carbonate to give PPMP33C10 in 51% yield.[18e] The dimeric macrocyclic polyether BPPBMP66C20, containing two hydroquinone and two resorcinol residues alternating with respect to one another, was also isolated by silica gel chromatography from this reaction mixture in 11% yield. The macrocyclic polyether BPP34C10 was prepared according to a previously reported procedure.[12]

The free tetracationic cyclophane [BBIPYPXYMXYCY]-$[PF_6]_4$ was prepared[18c] by the reaction of [BBIPYMXY]$[PF_6]_2$ with 1,4-bis(bromomethyl)benzene in the presence of BHEEPB in a manner identical to that previously described[12] for the synthesis of [BBIPYBIPXYCY]$[PF_6]_4$. The preparation of the tetracationic cyclophane [BBIPYBIMXYCY]$[PF_6]_4$ has been described previously by Hünig et al.[23] Their published procedure was used for the synthesis of this compound.

The [2]catenane, incorporating BPP34C10 and the tetracationic cyclophane containing one *m*- and one *p*-xylyl spacer,[15c,18c] was self-assembled (Scheme 4) by two different routes. When 1,4-bis(bromomethyl)benzene was reacted with [BBIPYMXY]-$[PF_6]_2$ in the presence of the macrocyclic polyether BPP34C10

(19) Ballardini, R.; Gandolfi, M. T.; Prodi, L.; Ciano, M.; Balzani, V.; Kohnke, F. H.; Shahriari-Zavareh, H.; Spencer, N.; Stoddart, J. F. *J. Am. Chem. Soc.* **1989**, *111*, 7072–7078.

(20) For a review on the "Cesium Effect" in the synthesis of macrocyclic compounds, see: Ostrowicki, A.; Koepp, E.; Vögtle, F. *Top. Curr. Chem.* **1991**, *161*, 37–67.

(21) van Keulen, B. J.; Kellog, R. M.; Piepers, O. *J. Chem. Soc., Chem. Commun.* **1979**, 285–266. For a report of a functionalized crown ether prepared using a similar approach, see: Delaviz, Y.; Gibson, H. W. *Macromolecules* **1992**, *25*, 18–20.

(22) Amabilino, D. B.; Ashton, P. R.; Stoddart, J. F. *Supramolecular Chem.* **1994**, *5*, 5–8.

(23) Geuder, W.; Hünig, S.; Suchy, A. *Tetrahedron* **1986**, *42*, 1665–1677.

Scheme 4

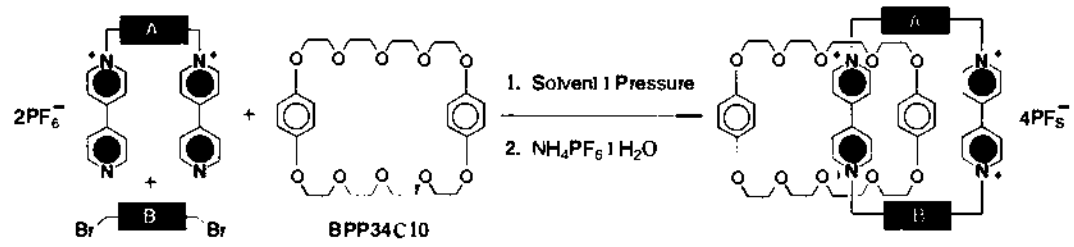

[2]Catenane	A	B	Solvent	Pressure	Yield
{[2]-[BPP34C10]-[BBIPYBIPXYCY]Catenane}$[PF_6]_4$			MeCN	Ambient	70%
			DMF	10 kbar	74%
{[2]-[BPP34C10]-[BBIPYPXYMXYCY]Catenane}$[PF_6]_4$			DMF	Ambient	18%
			DMF	Ambient	40%
			DMF	10 kbar	59%
{[2]-[BPP34C10]-[BBIPYBIMXYCY]Catenane}$[PF_6]_4$			DMF	Ambient	0%
			DMF	10 kbar	28%

Scheme 5

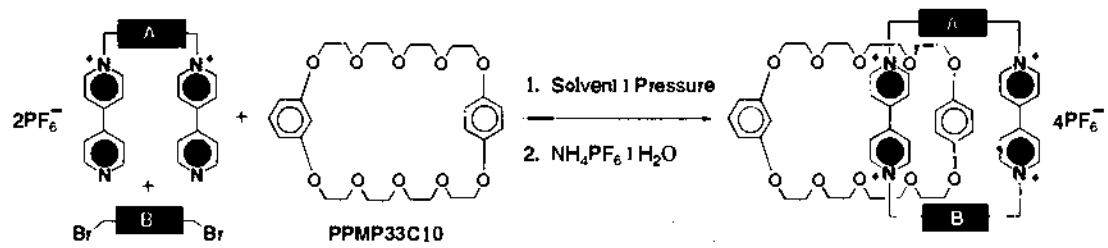

[2]Catenane	A	B	Solvent	Pressure	Yield
{[2]-[PPMP33C10]-[BBIPYBIPXYCY]Catenane}$[PF_6]_4$			DMF	Ambient	15%
{[2]-[PPMP33C10]-[BBIPYPXYMXYCY]Catenane}$[PF_6]_4$			DMF	Ambient	27%
{[2]-[PPMP33C10]-[BBIPYBIMXYCY]Catenane}$[PF_6]_4$			DMF	12 kbar	1.8%

as the template, the [2]catenane was isolated in 40% yield after silica gel chromatography. When the self-assembly process was carried out using 1,3-bis(bromomethyl)benzene and [BBIPYPXY][PF_6]$_2$ in the presence of BPP34C10, in the same solvent at identical concentrations, the [2]catenane was isolated in only 18% yield.[24] When the catenation was performed at high pressure[25] (10 kbars) using 1,4-bis(bromomethyl)benzene and [BBIPYMXY[[PF_6]$_2$ as the tetracationic cyclophane precursors in the presence of BPP34C10, {[2]-[BPP34C10]-[BBIPYPXYMXYCY]catenane}[PF_6]$_4$ was isolated in 59% yield. High pressure conditions are known to accelerate the Menschutkin reaction, and the efficiencies of the final cyclizations[26] to form the [2]catenanes are improved, at least in part, by this acceleration.[27] When 1,3-bis(bromomethyl)benzene was reacted with [BBIPYMXY[[PF_6]$_2$ in solution with an excess of BPP34C10 at ambient temperature and pressure, no catenated products were isolated. Despite the formation of a red solution, indicating the presence of charge transfer interactions between the π-electron rich and π-electron deficient units and hence the possible complexation of a bipyridinium-containing species within the macrocyclic polyether, ring closure to form the catenane is apparently not favored at ambient pressure. Repetition of the reaction at 10 kbars resulted in a 28% yield of the desired {[2]-[BPP34C10]-[BBIPYBIMXYCY[catenane}[PF_6]$_4$ after silica gel chromatography. The effect of pressure upon the efficiencies of these catenations can be compared with that observed during the template-directed synthesis of the {[2]-[BPP34C10]-[BBIPYBIPXYCY]catenane}[PF_6]$_4$. This [2]catenane was self-assembled at 10 kbars in DMF under conditions identical to those employed in the high pressure template-directed synthesis of {[2]-[BPP34C10]-[BBIPYPXYMXYCY]-catenane}[PF_6]$_4$. The prototypical [2]catenane has been isolated previously[12] in 70% yield in acetonitrile solution at atmospheric pressure (Scheme 1). The yield of 74% from the high pressure catenation represents a very modest improvement to the yield reported previously at ambient pressure. In comparison, there is a dramatic increase in the yields obtained in the catenations of the smaller cyclophanes when ultrahigh pressure conditions are employed.

The macrocyclic polyether PPMP33C10 was employed as a template for the synthesis (Scheme 5) of the [2]catenanes, incorporating all three tetracationic cyclophanes. Reaction

(24) Assuming that these catenations proceed under kinetic control, the relative yields of the [2]catenanes indicate that the tricationic intermediate tref 1] containing the *p*-xylyl spacer unit closes faster than the corresponding intermediate in which the *m*-xylyl unit of the cyclophane is located at the ring closure point. For further evidence that catenations of this type are kinetically controlled at ambient temperature and pressure, see: Amabilino, D. B.; Ashton, P. R.; Pérez-García, L.; Stoddart, J. F. *Angew. Chem., Int. Ed. Engl.* In press.

(25) Isaacs, N. S. *Tetrahedron* **1991**, *47*, 8463–8497.

(26) High pressure can be used for enhanced yields in cyclizations involving the Menschutkin reaction, see: Jurczak, J.; Pietraszkiewicz, M. *Top. Curr. Chem.* 1986, *130*, 183–204.

(27) Brown, C. L.; Philp, D.; Stoddart, J. F. *Synlett* **1991**, 459–461.

Scheme 6

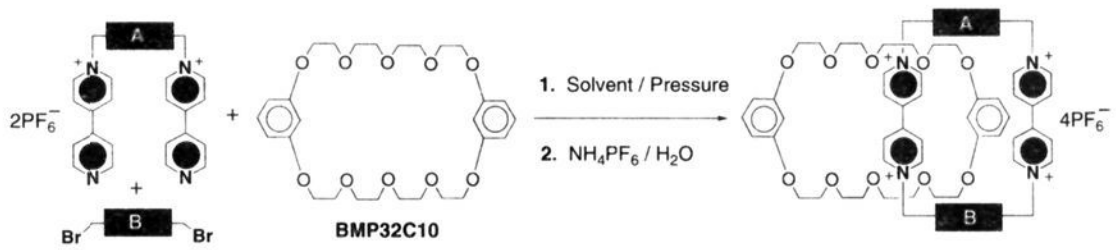

[2]Catenane	A	B	Solvent	Pressure	Yield
{[2]-[BMP32C10]-[BBIPYBIPXYCY]Catenane}$[PF_6]_4$			DMF	Ambient	17%
{[2]-[BMP32C10]-[BBIPYPXYMXYCY]Catenane}$[PF_6]_4$			DMF	Ambient	12%
{[2]-[BMP32C10]-[BBIPYBIMXYCY]Catenane}$[PF_6]_4$			DMF	15 kbar	0%

conditions and isolation procedures were similar to those used for the self-assembly of BPP34C10-containing catenanes. In all cases, the yields of the [2]catenanes obtained in the template-directed reactions were lower than those for the isomeric catenanes in which BPP34C10 was employed as the template. The catenation of PPMP33C10 with $[BBIPYMXY][PF_6]_2$ and 1,3-bis(bromomethyl)benzene requires high pressure (12 kbars), in common with the reaction where BPP34C10 is employed as the template. However, the yield (1.8%) of the [2]catenane obtained, when PPMP33C10 is used as the template, is dramatically lower.

The [2]catenanes incorporating either the $[BBIPYBIPXYCY]^{4+}$ or $[BBIPYPXYMXYCY]^{4+}$ cyclophanes and BMP32C10 were isolated (Scheme 6) as their tetrakis(hexafluorophosphate) salts after column chromatography and counterion exchange. The yields recorded for these catenations were lower than those obtained for the same reactions carried out with either BPP34C10 or PPMP33C10 as the templates. The macrocyclic polyether BMP32C10 does not act as a template for the formation of the [2]catenane incorporating the $[BBIPYBIMXYCY]^{4+}$ cyclophane, even at ultrahigh pressures (15 kbar).

B. Stability Constants. The stability constants and derived free energies of complexation for the 1:1 complexes formed by the tetracationic cyclophanes $[BBIPYPXYMXYCY][PF_6]_4$ and $[BBIPYBIPXYCY][PF_6]_4$ with both BHEEPB and BHEEMB, which were obtained by ^1H NMR spectroscopic titration in CD_3CN at 293 K, are listed in Table 1. The lower yields in catenations involving templates which incorporate resorcinol rings might be explained partially by the fact that the resorcinol derivatives[28] have lower binding constants (K_a) with $[BBIPYBIPXYCY][PF_6]_4$ when compared with their constitutional

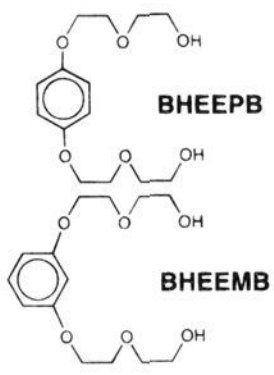

isomers incorporating hydroquinone rings.[12] Decreasing the size of the cavity of the tetracationic cyclophane to $[BBIPYPXYMXYCY][PF_6]_4$ has the effect of reducing the K_a values for the binding of BHEEPB and BHEEMB to 37 and 23 M^{-1}, respectively, in CD_3CN. These observations provide a partial explanation for the relatively low yield of this cyclophane when using BHEEPB as the template. As expected, the smallest tetracationic cyclophane $[BBIPYBIMXYCY][PF_6]_4$ does not form 1:1 complexes with either BHEEPB or BHEEMB in CD_3CN solutions for steric reasons.

Table 1. Stability Constants (K_a) and Derived Free Energies of Complexation ($-\Delta G^\circ$) for the 1:1 Complexes Formed by the Tetracationic Cyclophanes $[BBIPYBIPXYCY][PF_6]_4$ and $[BBIPYPXYMXYCY][PF_6]_4$ with BHEEPB and BHEEMB in CD_3CN Solution at 293 K

1:1 complex	K_a (M^{-1})	$-\Delta G^\circ$ (kcal mol^{-1})
$[BHEEPB{\cdot}BBIPYBIPXYCY][PF_6]_4$	2220 ± 240^a	4.6 ± 0.6
$[BHEEMB{\cdot}BBIPYBIPXYCY][PF_6]_4$	1070 ± 340^b	4.1 ± 0.3
$[BHEEPB{\cdot}BBIPYPXYMXYCY][PF_6]_4$	37 ± 8^b	2.1 ± 0.3
$[BHEEMB{\cdot}BBIPYPXYMXYCY][PF_6]_4$	23 ± 12^b	1.8 ± 0.4

[a] See ref 12. Determined by a spectrophotometric titration in MeCN (298 K) at $\lambda = 478$ nm. [b] Determined by ^1H NMR spectroscopic titration.

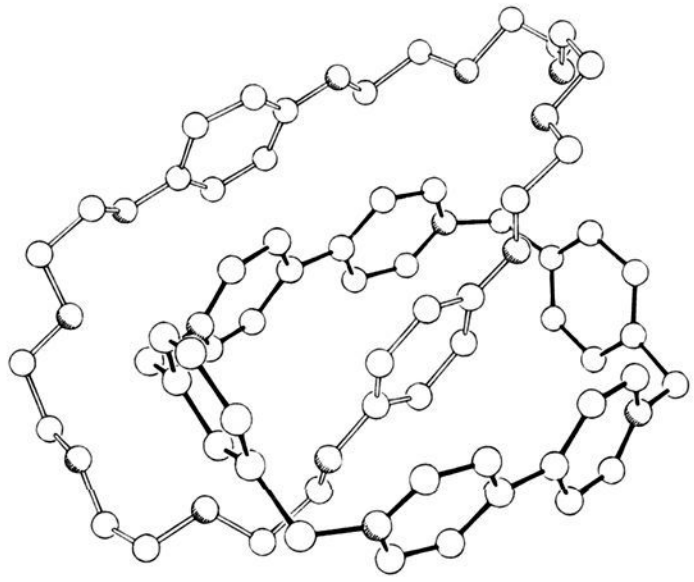

Figure 2. Ball-and-stick representation of the solid-state structure of $\{[2]\text{-}[BPP34C10]\text{-}[BBIPYPXYMXYCY]catenane\}^{4+}$.

C. X-ray Crystal Structures. The solid state structure (Figure 2) of {[2]-[BPP34C10]-[BBIPYPXYMXYCY]catenane}-$[PF_6]_4$ is similar to that of the isomeric catenane[12] containing two *p*-xylyl spacers in the cyclophane component. The π-electron deficient bipyridinium units of the charged component sandwich a hydroquinone ring of the macrocyclic polyether between them, the $-OC_6H_4O-$ unit of the included unit forming an angle of 44° with the mean plane defined by the four methylene carbon atoms of the former. One of the protons of the included hydroquinone ring is directed toward the *p*-xylyl spacer in the tetracationic cyclophane. The length of the C−H···π interaction is 2.75 Å, whereas, in the isomeric [2]-

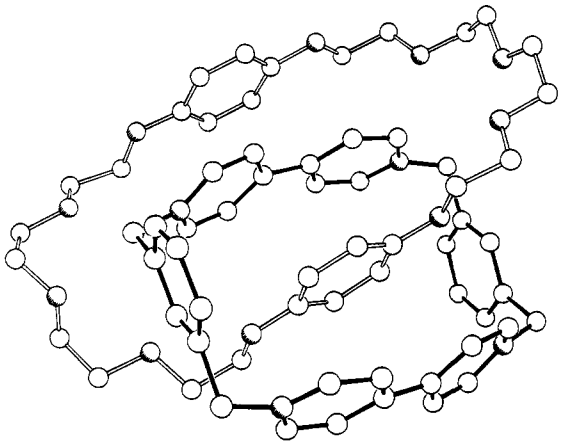

Figure 3. Ball-and-stick representation of the solid-state structure of {[2]-[BPP34C10]-[BBIPYBMXYCY]catenane}$^{4+}$.

catenane containing a [BBIPYBIPXYCY]$^{4+}$ component, the analogous hydrogen atoms are located 2.85 Å from the centroid of the *p*-xylyl spacer. The hydroquinone ring hydrogen atom, which is directed toward the *m*-xylyl unit in the tetracationic cyclophane, is located 2.79 Å from the carbon atom at the 2-position in this spacer. The methylene groups of both the planar "inside" and "alongside" $-CH_2OC_6H_4OCH_2-$ units adopt anti geometries, whereas, in the isomeric [2]catenane[12] containing the [BBIPYBIPXYCY]$^{4+}$ component, the inside unit has an anti and the alongside unit has a syn geometry. In addition, there are stabilizing C−H···O hydrogen bonding interactions between selected hydrogen atoms in the π-electron deficient cyclophane component and some of the oxygen atoms in the BPP34C10 component. The α-CH hydrogen atom—attached to the inside pyridinium unit nearest to the *m*-xylyl spacer—forms a C−H···O hydrogen bond (H···O distance = 2.52 Å, C−H···O angle = 153°) to the central oxygen atom in the tetraethylene glycol spacer of the crown ether. The diametrically opposite oxygen atom forms a hydrogen bond (H···O distance = 2.57 Å, C−H···O angle = 159°) with one of the hydrogen atoms attached to the *p*-xylyl spacer of the tetracationic cyclophane.

The solid state structure (Figure 3) of {[2]-[BPP34C10]-[BBIPYBIMXYCY]-catenane}$[PF_6]_4$ bears a remarkable resemblance to that of the [2]catenane[12] containing two *p*-xylyl spacers in its tetracationic cyclophane. Not only is the $-OC_6H_4O-$ unit inserted through the center of the tetracationic cyclophane component with its axis inclined by 42° to the equatorial plane (Figure 4a) and the geometries of inside and alongside $-CH_2OC_6H_4OCH_2-$ units exhibit anti and syn relationships, respectively, but also, the conformations of the polyether loops are essentially identical (Figure 4b) with those in the [2]catenane containing two *p*-xylyl spacers in its tetracationic cyclophane. Two of the hydrogen atoms attached to the inside hydroquinone ring make essentially orthogonal approaches (H···C distance = 2.72 Å) to the carbon atoms at the 2-positions of each *m*-xylyl spacer in the tetracationic cyclophane component. There are C−H···O hydrogen bonds between the central oxygen atoms in the BPP34C10 component and one of the methylene hydrogen atoms in each of the methylene groups associated with the included bipyridinium unit in the charged component (H···O distance = 2.35 Å, C−H···O angle = 157°) and also between the diametrically opposite central oxygen atom and one of the α-CH hydrogen atoms of the included bipyridinium unit (H···O distance = 2.58 Å, C−H···O angle = 147°).

There are changes in the dimensions of the tetracationic cyclophane components within the [2]catenanes that accompany the sequential replacement of the *p*-xylyl spacers with the meta-

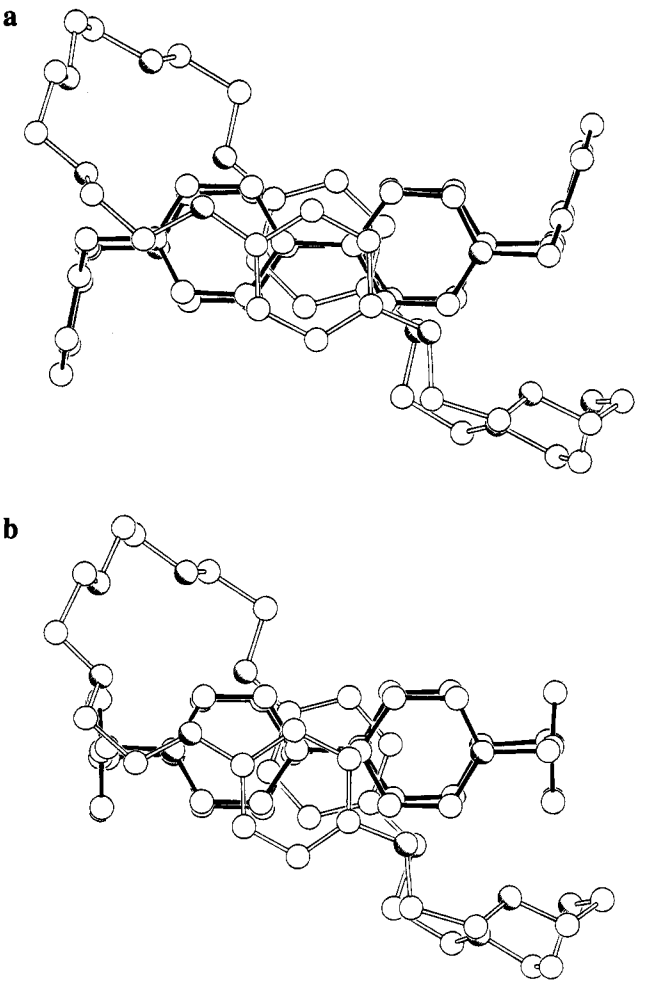

Figure 4. (a) Ball-and-stick representation of the view down the aromatic stack in the molecule {[2]-[BPP34C10][BBIPYBMXYCY]-catenane}$^{4+}$ in the solid state. (b) Ball-and-stick representation of the view down the aromatic stack in the molecule {[2]-[BPP34C10]-[BBIPYBPXYCY]catenane}$^{4+}$ in the solid state.[12]

substituted units. In the structure of {[2]-[BPP34C10]-[BBIPYPXYMXYCY]catenane}$[PF_6]_4$, the decrease in the methylene−methylene distance associated with changing one *p*-xylyl to a *m*-xylyl residue imposes a reduction in the maximum separation between the two bipyridinium units from 7.0 to 6.9 Å. The distance between the two xylyl spacers is decreased from 10.3 to 10.0 Å. The bowing of the bipyridinium units is, however, the same, with the angles subtended by the pairs of CH_2-N bonds being 26°. The replacement of the remaining *p*-xylyl unit with a *m*-xylyl one brings about a reduction in the breadth of the tetracationic cyclophane to 6.76 Å as well as a decrease in the distance between the *m*-xylyl spacers to 9.8 Å. In this [2]catenane, the bowing within each bipyridinium unit is increased noticeably, with the pairs of CH_2-N bonds subtending angles of ca. 31°. Accompanying the reduction in the breadth of the tetracationic cyclophane in the [2]catenane is a decrease to 6.74 Å in the interplanar separation of the inside and alongside hydroquinone rings (cf. values of 6.85 Å in the catenane with *p*- and *m*-xylyl spacers and 6.95 Å in the one with two *p*-xylyl spacers).

The single crystal X-ray structural analysis of {[2]-[PPMP-33C10]-[BBIPYBIPXYCY]catenane}$[PF_6]_4$ reveals a solid state geometry (Figure 5) similar to that of its isomers. Only one of the two possible translational isomers of this [2]catenane is observed, i.e., the isomer in which the hydroquinone ring resides in the cavity of the tetracationic cyclophane. The O−O vector associated with this inside hydroquinone residue is inclined by ca. 46° to the mean plane of the cyclophane which displays a

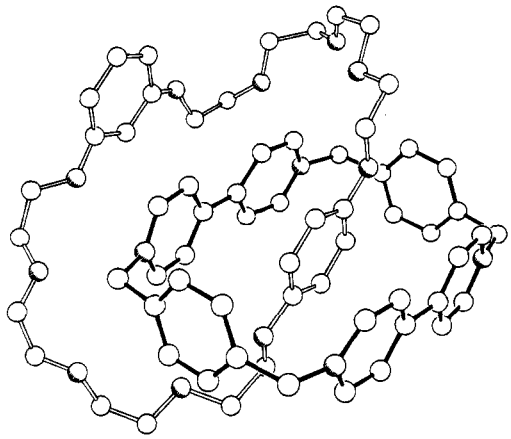

Figure 5. Ball-and-stick representation of the solid-state structure of {[2]-[PPMP33C10][BBIPYBPXYCY]catenane}$^{4+}$, showing the single translational isomer present in the crystal.

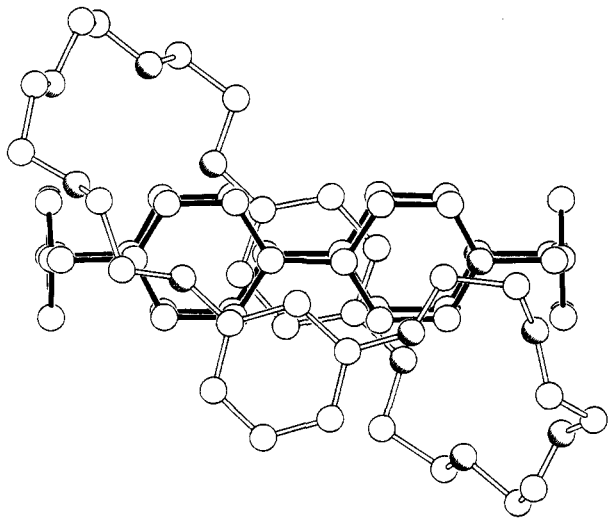

Figure 6. Ball-and-stick representation of the view down the aromatic stack in the molecule {[2]-[PPMP33C10][BBIPYBPXYCY]catenane}$^{4+}$ in the solid state.

characteristic barrel-like distortion. The resorcinol ring positions itself alongside and parallel to one of the bipyridinium residues in the π-electron deficient component. However, the resorcinol ring is offset (Figure 6) such that optimum $\pi-\pi$ overlap is apparently not achieved. Despite this situation, the interplanar separations between both the hydroquinone and resorcinol rings and their accompanying bipyridinium units are all approximately 3.5 Å. In common with the other structures discussed in this paper, two hydrogen atoms on the included hydroquinone ring form C−H···π interactions with the *p*-xylyl spacers in the tetracationic cyclophane (H···ring centroid distance = 2.84 Å), and there are stabilizing C−H···O interactions between the α-CH hydrogen atoms attached to the inside bipyridinium unit and some of the oxygen atoms in the PPMP33C10 component of this [2]catenane.

All of the X-ray crystal structures presented in this paper display unique packing motifs. In common with {[2]-[BPP34C10]-[BBIPYBIPXYCY]catenane}$[PF_6]_4$, the [2]catenane incorporating BPP34C10 and a cyclophane with one *p*-xylyl and one *m*-xylyl spacer forms a continuous polar π-electron donor/π-electron acceptor stack in its crystals. The packing of {[2]-[BPP34C10]-[BBIPYBIMXYCY]catenane}-$[PF_6]_4$ is markedly different.[18c] The [2]catenane molecules form stepped enantiomeric "dimers", which are aligned by virtue of a $\pi-\pi$ stacking interaction between the alongside hydroquinone rings of each molecule in the pair. The interplanar separation between the two alongside π-electron rich residues is 3.62 Å (centroid−centroid separation = 3.99 Å), a geometry which resembles very closely the arrangement[1] of hydroquinone rings inside the cyclobis(paraquat-4,4′-biphenylene)cyclophane incorporating two BPP34C10 macrocycles. The separation between the hydroquinone rings inside this [3]catenane is 3.63 Å (centroid−centroid separation = 3.82 Å). The [3]catenane also stacks in the crystal, so that the alongside hydroquinone residues on neighboring molecules have an interplanar separation of 3.66 Å (centroid−centroid separation = 4.34 Å).[1] The {[2]-[PPMP33C10]-[BBIPYBIPXYCY]catenane}$[PF_6]_4$ forms centro-symmetrically related polar stacks containing alternating π-electron rich and π-electron deficient units. The alongside resorcinol ring in the catenane compensates for its rather poor intramolecular $\pi-\pi$ stacking by forming a more favorable $\pi-\pi$ stacking arrangement with the alongside bipyridinium unit of an adjacent molecule (interplanar separation = 3.4 Å, cf. 3.5 Å in the isomeric catenane incorporating BPP34C10 and the same tetracationic cyclophane), resulting in a slightly "stepped" array.[18e]

D. ^{1}H NMR Spectroscopy. The 1:1 complexes formed between both BHEEPB and BHEEMB and the tetracationic cyclophanes [BBIPYPXYMXYCY]$[PF_6]_4$ and [BBIPYBIPXY-CY]$[PF_6]_4$ were studied by ^{1}H NMR spectroscopy in CD_3CN solutions. The 1:1 complex formed between BHEEPB and [BBIPYBIPXYCY]$^{4+}$ has been studied by ^{1}H NMR spectroscopy previously.[12] This investigation revealed that the π-electron rich residue is located inside the cavity of tetracationic cyclophane at room temperature, exhibiting a signal at δ 3.96 which arises from its hydroquinone protons. The resonances for the resorcinol protons in the ^{1}H NMR spectrum (CD_3CN, 400 MHz) of the BHEEMB in its 1:1 complex with [BBIPY-BIPXYCY]$[PF_6]_4$ are broad at room temperature. However, when a CD_3CN solution of this complex was cooled down to 233 K, well-resolved resonances for the protons attached to the aromatic ring of the guest were observed at δ 1.21, 3.17, and 4.37 for H-2, H-5, and H-4/6, respectively. In addition, the number of resonances arising from the host are doubled, as a result of the imposed C_{2v} symmetry of the resorcinol-based guest upon the host. The chemical shift changes (Table 2) in the resonances arising from the protons attached to the resorcinol ring suggest an average binding geometry of the guest within [BBIPYBIPXYCY]$^{4+}$ similar to that shown in Figure 7a. The coalescence[29] of the resonances arising from the α- and β-CH protons of the bipyridinium units in the tetracationic cyclophane at 247 and 245 K, respectively, along with their limiting chemical shift differences ($\Delta\nu$ = 97 and 41 Hz, respectively), allow the calculation to be made of the free energy of activation ($\Delta G_c^{\ddagger}$) associated with the expulsion of the resorcinol ring of the guest from the cavity of the charged host. The result is an average $\Delta G_c^{\ddagger}$ value of 11.6 kcal mol^{-1}. The 1:1 complexes formed between BHEEPB and BHEEMB and [BBIPYPXYMX-YCY]$[PF_6]_4$ are considerably weaker than those formed between [BBIPYBIPXYCY]$[PF_6]_4$ and the same guests in CD_3CN solutions. Consequently, in addition to resonances for the 1:1 complexes, signals for unbound host and guests are also observed in the low temperature ^{1}H NMR spectra of these complexes. The chemical shift changes (Table 2) in the resonances for the protons in the 1:1 complex formed between [BBIPYPXYMXYCY]$[PF_6]_4$ and BHEEMB suggest a binding geometry similar to that depicted in Figure 7b, in which H-2 on the resorcinol ring is directed towards the *p*-xylyl spacer of the host. The cyclophane [BBIPYBIMXYCY]$[PF_6]_4$ does not form an inclusion complex that could be detected by ^{1}H NMR spectroscopy with either guest in CD_3CN solution.

All the [2]catenanes reported in this paper show temperature-dependent ^{1}H NMR spectra in solution. Three main dynamic

Table 2. Chemical Shift Data [δ Values (Δδ Values)][a] Obtained from the 400 MHz ^{1}H NMR Spectra Recorded on BHEEPB, BHEEMB, [BB]PYB]PXYCY][PF_6]$_4$, and [BB]PYPXYMXYCY][PF_6]$_4$ and their 1:1 Complexes in CD_3CN Solutions

	charged component				neutral component
compound or complex	α-CH	β-CH	C_6H_4[b]	CH_2N^+	ArH
BHEEPB					6.85
BHEEMB					6.49(t)/6.52(dd)/7.17(t)
[BB]PYB]PXYCY)[PF_6]$_4$[c]	8.86	8.16	7.52	5.74	
[BB]PYPXYMXYCY)][PF_6]$_4$	8.82/8.87	8.06/8.08	7.44(s)/7.61(s)[d] 7.67(t)/7.78(d)	5.77	
[BHEEPB·BB]PYB]PXYCY][PF_6]$_4$[e]	8.97 (+0.11)	7.85 (−0.3t)	7.80 t+0.28)	5.69 (−0.05)	3.96 (−2.89)
[BHEEMB·BB]PYB]PXYCY)[PF_6]$_4$[e]	8.82/9.06 (−0.04/+0.20)	7.80/7.91 (−0.36/−0.25)	7.76 (+0.26)	5.63/5.67 (−0.07/−0.11)	1.21(s)/3.17(t)/4.37(d) (−5.29/−4.00)/−2.17)
[BHEEPB·BB]PYPXYMXYCY][PF_6]$_4$[f]	8.84/8.94 (+0.02/−0.07)	7.82 t−0.24/−0.26)	7.77(s)[d,g] (+0.16)	5.67/5.77 (−0.10/0.01)]	3.84 (−3.01)
[BHEEMB·BB]PYPXYMXYCY)][PF_6]$_4$[e]	8.82/8.88 (0.00/+0.01)	8.04/8.07 (−0.02/−0.01)	7.44(s)/7.64(s)[d] 7.68(t)/7.77(d) (0.00/+0.03 +0.01/+0.01)	5.75 (−0.02)	5.93(bs)/6.37(bs)/ 7.04(bs) (−0.56/−0.15/−0.13)

[a] The Δδ values indicated in parentheses under the respective δ values relate to the changes in chemical shift exhibited by the probe protons upon complex formation, a negative value indicates a movement of the resonance to the high field. [b] The C_6H_4 refers to the m-xylyl and *p*-xylyl components of [BB]PYB]PXYCY]$^{4+}$ and [BB]PYPXYMXYCY)$^{4+}$, respectively. [c] See ref 12. [d] This resonance corresponds to the protons attached to the *p*-xylyl spacer in the cyclophane. [e] Values given refer to the spectrum of this complex recorded at 233 K. [f] Values given refer to the spectrum of this complex recorded at 243 K. The free components of the complex are also observed in the solution. [g] The resonances reported for this complex are averaged on the ^{1}H NMR time scale at 283K. [h] The resonances arising from the m-xylyl spacer are broad and obscured in this spectrum.

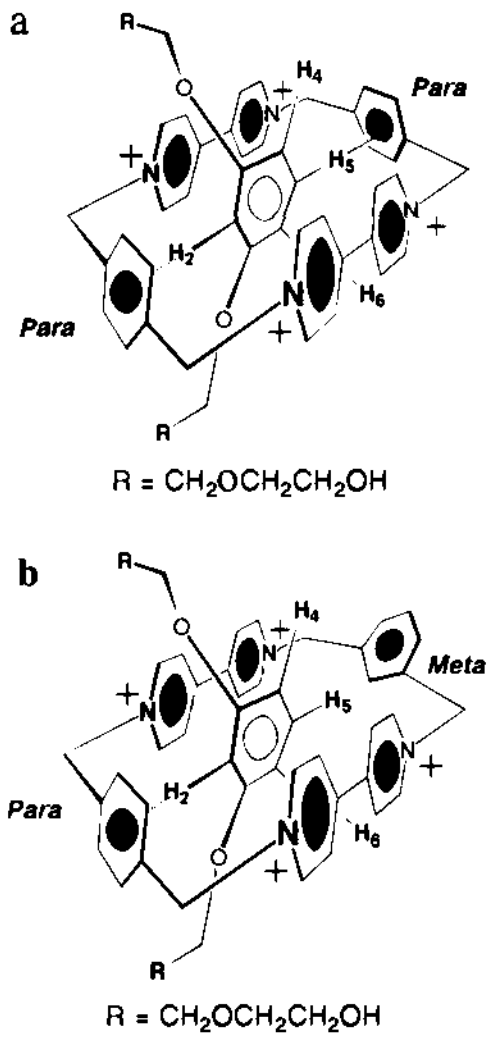

Figure 7. (a) Proposed binding geometry from ^{1}H NMR data of BHEEMB within the cavity of the tetracationic cyclophane incorporating two *p*-xylyl spacers. (b) Proposed binding geometry from ^{1}H NMR data of BHEEMB within the cavity of the tetracationic cyclophane incorporating one *p*-xylyl and one m-xylyl spacer.

processes are observable.[12] They are all associated with the motions of their charged and neutral components with respect to each other and involve (Scheme 7) the following: (i) exchange of the π-electron rich units A and B within the cavity of the tetracationic cyclophane, as a result of circumrotation of the neutral component through the charged component (process I), (ii) exchange of the π-electron deficient units A and B within the less rigid cavity of the neutral component as a result of it pirouetting around the charged component (process II), and (iii) "rocking" of the included π-electron rich hydroquinone ring within the cavity of the tetracationic cyclophane, a process which

Scheme 7

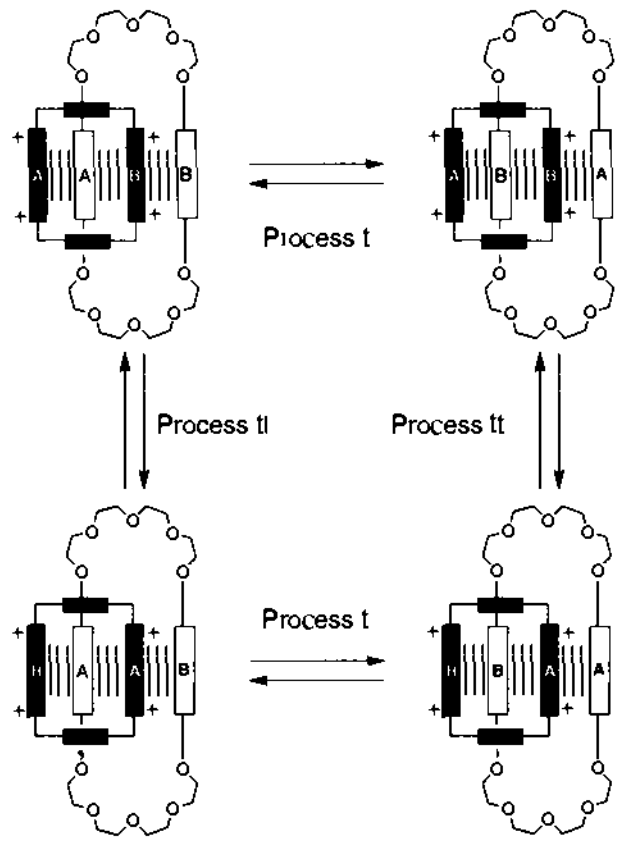

Scheme 8

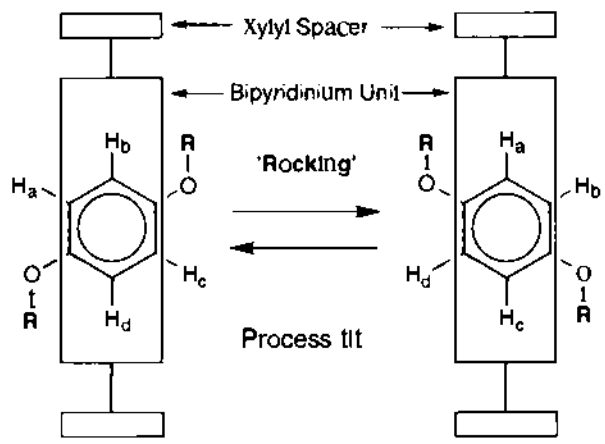

involves site exchange of protons H_a and H_c with protons H_b and H_d, respectively (process III, Scheme 8). The most meaningful (for comparison) and accessible (in terms of rates on the ^{1}H NMR time scale) dynamic realm in which to quote chemical shift data is when process I is slow and the other dynamic processes (II and III) are fast on the ^{1}H NMR time scale. Therefore, all the chemical shift data relating to the

Scheme 9

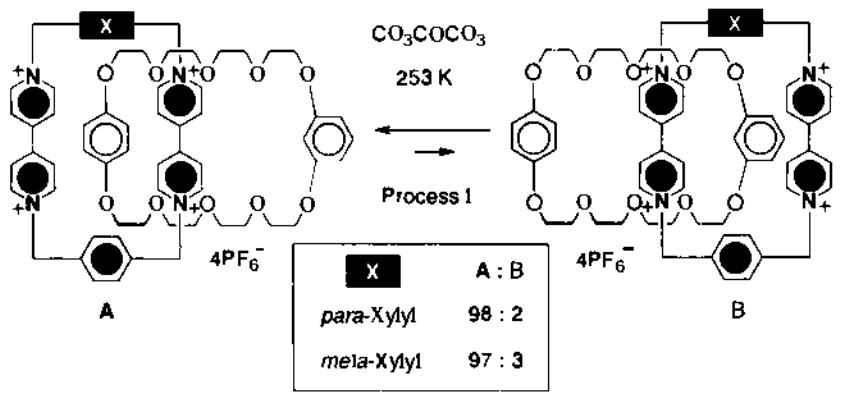

constitutionally-isomeric [2]catenanes are presented on this basis in Table 3. Comparison of the chemical shift data for the series of isomeric [2]catenanes incorporating BPP34C10 reveals significant changes in the $\Delta\delta$ values for both inside and alongside hydroquinone ring protons. The ^{1}H NMR spectrum of the [2]catenane incorporating [BBIPYPXYMXYCY][$^{4+}$ shows two resonances for the inside hydroquinone ring protons at 300 K, corresponding to its two "sides". When the CD_3COCD_3 solution of the [2]catenane is cooled down to 213 K, four well-resolved signals are observed for the inside hydroquinone ring protons, indicating that the rocking process (Scheme 8) is slow on the ^{1}H NMR time scale at this temperature. The protons H_a, H_b, H_c, and H_d in Scheme 8 are anisochronous, giving rise to resonances (i) at δ 1.78 for the proton directed toward the *p*-xylyl spacer, (ii) at δ 3.17 for the proton directed toward the *m*-xylyl spacer, and (iii) at δ 5.42 and 5.53 for the protons directed away from the π-electron deficient cavity. The resonances arising from the inside hydroquinone ring protons in the [2]catenane incorporating [BBIPYBIMXCY][$^{4+}$ and BPP34C10 are shifted by 2.42 ppm to high field. At temperatures below 273 K, process III (Scheme 8) for this [2]catenane is slow on the ^{1}H NMR time scale, as witnessed by resonances at δ 3.19 and 5.63 for the hydroquinone protons directed toward, respectively, the *m*-xylyl spacers and away from the center of the tetracationic cyclophane. Once again, this observation indicates that this [2]catenane adopts a highly ordered structure in the solution state.

Crystals of the [2]catenane incorporating PPMP33C10 and [BBIPYBIPXYCY][PF_6]$_4$ contain exclusively the translational isomer in which the hydroquinone ring of the macrocyclic polyether is included within the cavity of the tetracationic cyclophane and the resorcinol ring in the neutral component is located alongside one of the bipyridinium units. This situation also predominates in solution, where the equilibration between the two translational isomers (A and B in Scheme 9) arising from process I (Scheme 7) takes place readily. At room temperature in CD_3COCD_3 solution, process I is slow on the ^{1}H NMR time scale, as witnessed by the observation of slightly broadened resonances at δ 5.56, 6.28, and 7.10, arising from the H-2, H-4/6, and H-5 protons, respectively, attached to the resorcinol ring in PPMP33C10. These resonances correspond to isomer A in Scheme 9. Indeed, no indication of isomer B could be found in the ^{1}H NMR spectrum at room temperature. However, at 273 K, a small, broad singlet was observed at 6.41. Irradiation of this very low intensity resonance resulted in a transfer of saturation to the inside hydroquinone ring proton resonance centered on δ 3.78. Integration of the ^{1}H NMR spectrum at 253 K of the compound gave a ratio of 98:2 in favor of the translational isomer in which the hydroquinone ring resides inside the cavity of the tetracationic cyclophane. When the [2]catenane was dissolved in CD_3SOCD_3, the ^{1}H NMR spectrum once again revealed the presence of essentially one translational isomer. Thus, this [2]catenane does not display the same dramatic solvent dependence in its translational isomerism, as does the [2]catenane[10] in which hydroquinone and 1,5-dioxynaphthalene units are incorporated into the macrocyclic polyether component.

At temperatures below 298 K, the [2]catenane incorporating PPMP33C10 and the [BBIPYPXYMXYCY][$^{4+}$ cyclophane also shows a remarkable preference for the translational isomer in which the hydroquinone ring resides within the cavity of the charged component in CD_3COCD_3. A ratio of 97:3 for hydroquinone residues inside:alongside (Scheme 9) was determined at 253 K by integration of the ^{1}H NMR spectrum at this temperature. Irradiation of a low intensity singlet at δ 6.38 resulted in a transfer of saturation to two broad resonances at δ 3.67 and 4.41, respectively. This observation confirms that the signal at δ 6.38 arises from the protons on the alongside hydroquinone ring in the minor isomer (B in Scheme 9). Irradiation of the inside hydroquinone proton resonance resulted in an apparent transfer of saturation to the resonance at δ 6.26 corresponding to the H-4/6 protons of the alongside resorcinol ring in the major isomer. This observation suggests that the resonance, arising from the inside resorcinol ring H-4/6 protons of the major isomer, is accidentally coincident with the inside hydroquinone ring proton resonance at δ 4.41. An extremely high ratio of included hydroquinone to resorcinol residues was also observed within the cavity of the [BBIPYBIMXYCY][$^{4+}$ cyclophane in the [2]catenane comprised of this tetracation and PPMP33C10. The complexity of the spectra and the small quantity of material available to us from this low yielding reaction prevented the determination of the exact ratio of the two translational isomers.

An ^{1}H NMR spectroscopic experiment involving competition between BHEEPB and BHEEMB for the cavity of [BBIPYBIPXYCY][PF_6]$_4$ in CD_3CN solution was performed in order to investigate the selectivity exhibited in the [2]catenanes incorporating PPMP33C10 and to deduce whether the inclusion of the hydroquinone ring in preference to that of the resorcinol ring is a result of catenation. The ratio of BHEEPB:BHEEMB bound within the tetracationic cyclophane—approximately 85:15—is lower than that observed in the catenanes. This result indicates that the conformation of the catenated macrocyclic polyethers in solution influences the ratio of translational isomers that is observed.

The [2]catenane incorporating BMP32C10 and the [BBIPYBIPXYCY][$^{4+}$ tetracationic cyclophane gives a ^{1}H NMR spectrum in CD_3COCD_3 at room temperature in which none of the resonances for the protons attached to the resorcinol rings of the macrocyclic polyether component can be observed. However, process I is slow on the ^{1}H NMR time scale at 273 K, as indicated by the appearance of resonances at δ 6.86, 6.23, and 5.63 for the H-5, H-4/6, and H-2 protons, respectively, attached to the alongside resorcinol ring and at δ 3.32, 4.75, and 1.69 for the analogous protons attached to the inside ring. These resonances undergo significant chemical shift changes upon further cooling of the CD_3COCD_3 solution of the [2]catenane. In particular, the resonances arising from the H-2 and H-5 protons attached to the inside resorcinol ring are shifted dramatically in opposite directions, while the resonance arising from the H-4/6 protons is unaffected. These results suggest a binding geometry for the π-electron rich unit very similar to that proposed for the complex [BHEEMB·BBIPYBIPXYCY]-[PF_6]$_4$, where the H-2 and H-5 protons are directed into the π-faces (Figure 8) of the *p*-xylyl spacers of the tetracationic cyclophane. The resonance arising from the alongside resorcinol ring protons also display dramatic temperature dependency, the most affected resonances being those for H-5 and H-4/6. This observation suggests a greater alongside $\pi-\pi$ interaction of the resorcinol ring with the bipyridinium units as the temperature of the CD_3COCD_3 solution is lowered.

Table 3. Chemical Shift Data [δ Values ($\Delta\delta$ Values)][a] Obtained from the 400 MHz ^{1}H NMR Spectra Recorded on Constititutionally Isomeric [2]Catenanes and Their Components in CD_3COCD_3 Solution at 298 K (Unless Stated Otherwise)

	charged component				crown component	
compound or catenane	α-CH	β-CH	C_6H_4[b]	CH_2N^+	ArH alongside	ArH inside
[BBIPYBIPXYCY][PF_6]$_4$	9.38	8.58	7.76	6.15		
[BBIPYPXYMXYCY][PF_6]$_4$	9.31/9.34	8.40/8.45	7.70(t)/7.82(s)[c] 7.89(s)/7.95(d)	6.18/6.19		
[BBIPYBIMXYCY][PF_6]$_4$	9.23	8.45	7.92(d)/7.76(t) 7.31(s)	6.22		
BPP34C10					6.77	
{[2]-[BPP34C10][BBIPYBIPXYCY]catenane}[PF_6]$_4$[d]	9.28 (−0.10)	8.18 (−0.40)	8.04 (+0.28)	6.01 (−0.14)	6.22 (−0.55)	3.76 (−3.01)
{[2]-[BPP34C10][BBIPYPXYMXYCY]catenane}[PF_6]$_4$	9.15/9.27 (−0.16/−0.07)	8.18/8.25 (−0.22/−0.20)	7.87(t)/7.89(s) 8.04(s)[c]/8.16(d) (+0.17/0.00 +0.15/+0.21)	6.03/6.10 (−0.15/−0.09)	6.27 (−0.50)	3.64/4.42[e] (−3.13/−2.35)
{[2]-[BPP34C10][BBIPYBIMXYCY]catenane}[PF_6]$_4$	9.16 (−0.07)	8.27 (−0.18)	7.90(t)/8.06(s) 8.18(d) (+0.14/+0.75 +0.26)	6.18 (−0.04)	6.31 (−0.46)	4.35 (−2.42)
PPMP33C10					6.48(t)/6.50(dd) 6.81(s)/7.14(t)	
{[2]-[PPMP33C10][BBIPYBIPXYCY]catenane}[PF_6]$_4$[f,g]	9.36 (−0.02)	8.14 (−0.44)	8.02 (+0.26)	6.01 (−0.14)	5.48(t)/6.27(dd) 7.07(t) (−1.00/−0.23/−0.07)	3.7 (−3.03)
{[2]-[PPMP33C10][BBIPYPXYMXYCY]catenane}[PF_6]$_4$[g]	9.20/9.30 (−0.11/−0.04)	8.09/8.22 (−0.31/−0.23)	7.87(t)/8.01(s) 8.01(s)[c]/8.17(d) (+0.17/+0.12 +0.12/+0.22)	6.00/6.07 (−0.18/−0.12)	5.55(t)/6.25(dd) 7.06(t) (−0.93/−0.25/0.08)	3.64/4.41[f] (−3.16/−2.40)
{[2]-[PPMP33C10][BBIPYBIMXYCY]catenane}[PF_6]$_4$	9.19 (−0.04)	8.16 (−0.29)	7.80(bt)/8.02(s) 8.03(m) (−0.2/+0.26 /+0.72)	6.11 (−0.11)	5.69(d)/6.25(d) 7.03(t) (−0.79/−0.25 /−0.11)	3.90/4.5 (−2.91/−2.31)
BMP32C10					6.49(d)/6.51(t)/7.12(t)	
{[2]-[BMP32C10][BBIPYBIPXYCY]catenane}[PF_6]$_4$[g]	9.38 (0.00)	8.32 (−0.26)	8.03 (+0.27)	6.08 (−0.07)	5.60/6.23/6.86	1.69/3.32/4.75
{[2]-BMP32C10][BBIPYPXYMXYCY][catenane}[PF_6]$_4$	9.26/9.35 (−0.05/+0.01)	8.26/8.34 (−0.14/−0.11)	7.84(t)/8.04(s) 8.08(s)[c]/8.17(d) (+0.14/+0.05 +0.26/+0.22)	6.09/6.13 (−0.09/−0.06)	5.63/6.14/6.93	2.60/4.17/4.54

[a] The $\Delta\delta$ values indicated in parentheses under the respective δ values relate to the changes in chemical shift exhibited by the probe protons upon complex formation. A negative value indicates the movement of the resonance to high field. [b] The C_6H_4 refers to the *m*-xylyl and *p*-xylyl components of [BBIPYBIPXYCY]$^{4+}$ and [BBIPYPXYMXYCY]$^{4+}$, respectively. [c] This resonance corresponds to the *p*-xylyl spacer in the tetracationic cyclophane component. [d] See ref 1. [e] Located by a saturation transfer experiment at 300 K. [f] The chemical shifts quoted are those for the translational isomer in which the hydroquinone ring is located within the cavity of the charged component. [g] Located by a saturation transfer experiment at 273 K. [h] Values given refer to the spectrum of the catenane recorded at 273 K. [i] Values given refer to the spectrum of the catenane recorded at 283 K.

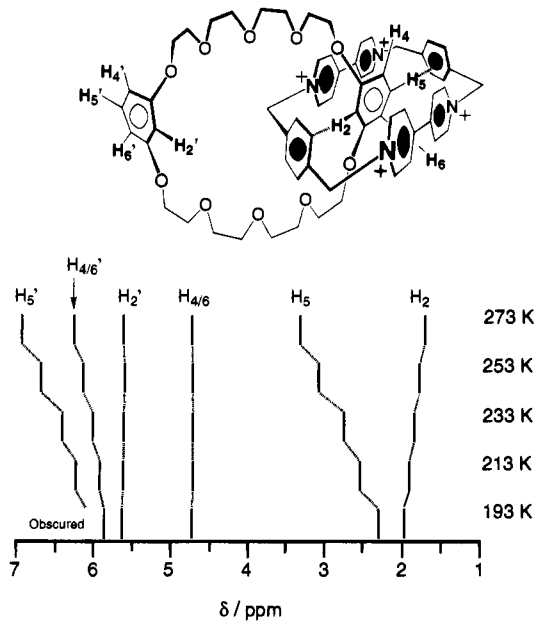

Figure 8. The temperature dependent ^{1}H NMR spectra of {[2]-[BMP32C10]-[BBIPYBIPXYCY]catenane}$[PF_6]_4$ in CD_3COCD_3.

The kinetic and thermodynamic data for the dynamic processes taking place in the isomeric [2]catenanes were calculated from the temperature dependent ^{1}H NMR spectra of the molecules using approximate expressions[29,31] and are listed in Table 4. These data provide some interesting information when considered in combination with the results of X-ray crystallography and binding constant measurements.

The series of isomers incorporating the BPP34C10 component illustrate that *reducing* the dimensions of the tetracationic cyclophane, by successive replacement of *p*-xylyl spacers for *m*-xylyl ones, *increases* the barriers to circumrotation of the neutral component through the cavity of the charged component (process I, Scheme 7) and also raises the activation energy to

Scheme 10

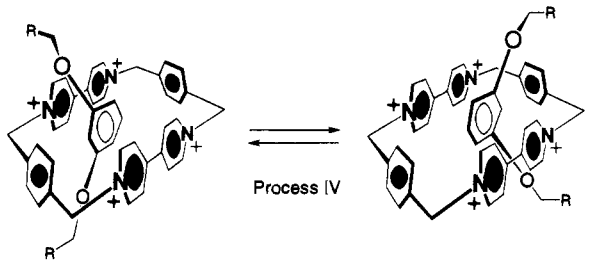

the rocking of the included π-electron rich ring within the π-electron deficient cavity. The energy barrier to process I increases from 15.6 for the largest, through 16.3 for the intermediate, to 17.6 kcal mol^{-1} for the smallest tetracationic cyclophane. The activation barrier to the rocking of the inside hydroquinone ring (process III, Scheme 8) rises from 9.0 kcal mol^{-1} for the $[BBIPYBIPXYCY]^{4+}$ cyclophane,[32] through 10.5 kcal mol^{-1} for the $[BBIPYPXYMXYCY]^{4+}$ cyclophane, to 11.7 kcal mol^{-1} for the $[BBIPYBIMXYCY]^{4+}$ cyclophane. These data suggest that the hydroquinone ring is held more firmly in the tetracationic cyclophane, as the distance between the methylene "corners" of the cyclophane is reduced.

The free energy of activation required for the circumrotation of the BMP32C10 macrocyclic polyether through $[BBIPYBIPXYCY]^{4+}$ (process I, Scheme 7) in the [2]catenane comprised of these components is substantially lower than in either of the isomeric catenanes incorporating the same tetracationic cyclophane. This observation supports the assertion that resorcinol rings exhibit much weaker $\pi-\pi$ interactions with the outside faces of the tetracationic cyclophane when compared to hydroquinone rings. In addition to process I, a fourth type of dynamic process (process IV, Scheme 10) is observed in the [2]catenanes incorporating only resorcinol rings as the π-electron rich units in the macrocyclic polyether component. This process[33] corresponds to the displacement of the included π-electron rich unit, followed by its reorientation and re-entry

Table 4. Kinetic and Thermodynamic Parameters Obtained from the Temperature-Dependent 400 MHz ^{1}H NMR Spectra Recorded on the Isomeric Series of [2]Catenanes

[2]catenane components	probe protons	$\Delta\nu^a$ (Hz) $(\Delta\nu)^b$	k_c^a (s^{-1}) $(k)^b$	T_c^a (K) $(T)^b$	$\Delta G_c^{\ddagger a}$ (kcal mol^{-1}) $(\Delta G^{\ddagger})^b$	process	solvent
BPP34C10	OC_6H_4O	678	1505	354	15.6	I	CD_3CN
BBIPYBIPXYCY		(19.0)	(60)	(313)	(15.7)		
	α-CH	74.3	165	250	12.0	II	$(CD_3)_2CO$
		(26.9)	(85)	(250)	(12.3)		
	β-CH	34.3	76	247	12.2	II	$(CD_3)_2CO$
		(25.1)	(79)	(247)	(12.3)		
	CH_2N^+	45.8	102	248	12.1	II	$(CD_3)_2CO$
		(30.7)	(97)	(248)	(12.2)		
BPP34C10	OC_6H_4O	206	458	350	16.3	I	CD_3CN
BBIPYPXYMXYCY	alongside	(13)	(40)	(317)	(16.3)	I	CC_3CN
	OC_6H_4O	(8.2)	(26)	(313)	(16.3)	I	CD_3CN
	inside	944		245	10.5	III	$(CD_3)_2CO$
BPP34C10	OC_6H_4O	(7.7)	(24)	(335)	(17.6)	I	CD_3CN
BBIPYBIMXYCY	alongside	(12)	(36)	(340)	(17.6)	I	CD_3CN
	OC_6H_4O	976	2169	271	11.7	III	$(CD_3)_2CO$
	inside						
PPMP33C10	2-CH in meta	(23.4)	(73.5)	(307)	(15.4)	I	$(CD_3)_2CO$
BBIPYBIPXYCY	OC_6H_4O						
	CH_2N^+	47	105	228	11.1	II	$(CD_3)_2CO$
PPMP33C10	2-CH in meta	(21.5)	(65.4)	(233)	(15.7)	I	$(CD_3)_2CO$
BBIPYPXYMXYCY	OC_6H_4O						
BMP32C10	4- and 6-CH	457	1015	304	13.6[c]	I	$(CD_3)_2CO$
BBIPYBIPXYCY	in OC_6H_4O						
	α-CH	26.9	60	240	12.0	IV	$(CD_3)_2CO$
	CH_2N^+	58.1	129	251	12.2	IV	$(CD_3)_2CO$
BMP32C10	4- and 6-CH	676	1502	321	14.2	I	$(CD_3)_2CO$
BBIPYPXYMXYCY	in OC_6H_4O						

[a] Data not in parentheses relate to the coalesence method (see ref 29). [b] Data in parentheses relate to the exchange method (see ref 31). [c] Data were calculated from the chemical shift difference of the probe protons at 213 K.

into the π-electron deficiency cavity. In the [2]catenane incorporating [BBIPYBIPXYCY]$^{4+}$ and BMP32C10, this process is associated with a full energy of activation of 12.2 kcal mol^{-1}.

E. Electrochemistry. The voltammetric behavior of the [BBIPYBIPXYCY]$^{4+}$ cyclophane has been reported previously.[12] Briefly, the two paraquat residues behave as independent electroactive subunits, and two consecutive two-electron waves are observed. The first one corresponds to the PQT^{2+}/PQT^{+} conversion by both paraquat residues, and the second wave results from the PQT^{+}/PQT conversion. The half-wave potentials ($E_{1/2}$) for these two processes are substantially less negative than those for the parent compound, paraquat (methyl viologen). In the tetracationic cyclophane, the electrostatic repulsions between the four positive charges is considerable. Its ease of reduction compared to paraquat must then originate from the relief of these electrostatic repulsions. As the substitution pattern in the xylyl spacers of the cyclophane is changed from para to meta, the overall reduction pattern is little affected. However, two significant trends are clearly observed. Firstly, the apparent half-wave potentials for the two consecutive two-electron reduction processes shift to more negative values on going from the [BBIPYBIPXYCY]$^{4+}$ cyclophane (the corresponding $E_{1/2}$ values are -0.251 and -0.689 V vs Ag/AgCl) to the [BBIPYBIMXYCY]$^{4+}$ cyclophane (-0.294 and -0.756 V vs Ag/AgCl). The $E_{1/2}$ values for the [BBIPYPXYMXYCY]$^{4+}$ cyclophane are intermediate (-0.278 and -0.745 V vs Ag/AgCl). Secondly, the two-electron wave at more negative potentials noticeably broadens on going from the [BBIPYBIPXYCY]$^{4+}$ cyclophane to [BBIPYBIMXYCY]$^{4+}$ cyclophane. This broadening is probably arising from partial splitting of the second reduction wave. The electrochemistry of [BBIPYBIMXYCY]$^{4+}$ cyclophane reported by Hünig,[23] using MeOH as solvent (vs Ag/AgNO$_3$/MeCN/glassy carbon) described a two-electron reduction (-0.31 V) followed by two single-electron reductions (-0.71 and -0.94 V, these being disturbed by adsorption and slow charge transfer). The voltammogram presented in that publication is also extremely broad. The observed trend in the $E_{1/2}$ values for the electrochemistry of the cyclophanes found in the present investigation is probably related to the relative strengths of the electrostatic repulsions among the positive charges and the spatial relationships between the paraquat residues in the three different tetracations. In the [BBIPYBIPXYCY]$^{4+}$ cyclophane, X-ray diffraction data and CPK space-filling molecular models indicate that the paraquat residues are approximately parallel. In fact, this molecule has a plane of symmetry which is equidistant and parallel to both paraquat residues. In contrast, the same models indicate that the paraquat residues are increasingly offset and/or angled on changing the substitution pattern associated with the xylyl spacer, firstly to meta–para and then to meta–meta. These constitutional differences, perhaps combined with differences in the solvation of the cyclophane's four positive charges, suggest that the extent of electrostatic repulsion is largest in the [BBIPYBIPXYCY]$^{4+}$ cyclophane, which would explain the observed trend in the half-wave potentials. By comparison, Hünig and co-workers[23] found that the tetracationic cyclophanes, incorporating (i) one *o*- and one *m*-xylyl and (ii) two *o*-xylyl spacers are increasingly easy to reduce as the dimensions of the cyclophane are decreased. This trend can be ascribed to the significantly greater electrostatic repulsions as the two π-electron deficient units are brought even closer together.

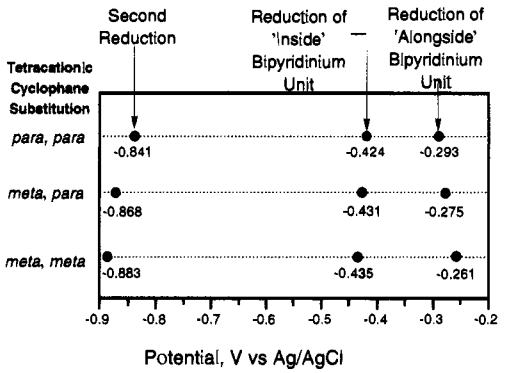

Figure 9. Apparent half-wave potentials for the reduction of [2]-catenanes formed between BPP34C10 and the tetracationic cyclophanes with the xylyl substitution indicated by the labels next to the left vertical axis. All values obtained with 1.0 mM solution of the [2]catenane in 0.1 M [TBA][PF$_6$]/MeCN.

The voltammetric behavior of the [2]catenane incorporating [BBIPYBIPXYCY]$^{4+}$ and BPP34C10 has been reported previously.[12] The PQT^{2+}/PQT^{+} redox couple is split into two waves, corresponding to the reduction of the alongside and inside paraquat residues. The same is true of the [2]catenanes incorporating the same macrocyclic polyether and [BBIPYPXYMXYCY]$^{4+}$ and [BBIPYBIMXYCY]$^{4+}$, respectively (the potentials are given in Figure 9). However, while the inside paraquat residue is reduced at very similar potential values for all three catenanes, the half-wave potential for reduction of the alongside paraquat residue clearly shifts to less negative values as the cyclophane's xylyl substitution pattern is changed from para–para to meta–meta. This trend indicates that the extent of charge transfer stabilization of the alongside paraquat residue is smaller in the [2]catenane incorporating the [BBIPYBIMXYCY]$^{4+}$ cyclophane than it is in the one incorporating the [BBIPYBIPXYCY]$^{4+}$ cyclophane. The uptake of the third and fourth electrons by the [2]catenane incorporating [BBIPYBIPXYCY]$^{4+}$ and BPP34C10 take place at similar half-wave potential values, and the two waves cannot be resolved clearly. These two waves have been barely resolved in the case of the [2]catenane containing the [BBIPYPXYMXYCY]$^{4+}$ cyclophane (Figure 10), while their resolution is again not possible in the [2]catenane incorporating the [BBIPYBIMXYCY]$^{4+}$ cyclophane. This trend is probably related to the opposing effects of the intrinsic proximity of these two waves in the corresponding uncatenated cyclophanes and the varying degrees of internal organization within the catenanes.

(28) Odell, B.; Reddington, M. V.; Slawin, A. M. Z.; Spencer, N.; Stoddart, J. F.; Williams, D. J. *Angew. Chem., Int. Ed. Engl.* **1988**, *27*, 1547–1550.

(29) Determination of the kinetic and thermodynamic data using the *coalescence method* involved calculating values for the rate constant k_c at the coalescence temperature (T_c) (Sutherland, I. O. *Annu. Rep. NMR Spectrosc.* **1971**, *4*, 71–235) from the approximate expression, $k_c = \pi(\Delta\nu)/(2)^{1/2}$, where $\Delta\nu$ is the chemical shift difference (in Hertz) between the coalescing signals at low temperatures in the absence of exchange. The Eyring equation was subsequently employed to calculate $\Delta G_c^{\ddagger}$ at T_c.

(30) Ashton, P. R.; Blower, M.; Philp, D.; Spencer, N.; Stoddart, J. F.; Tolley, M. S.; Balzani, V.; Gandolfi, M. T.; Prodi, L.; McLean, C. H. *New J. Chem.* **1993**, *17*, 689–695.

(31) Determination of the kinetic and thermodynamic data using the *exchange method* involved calculating values of k (Sandström, J. *Dynamic NMR Spectroscopy*; Academic Press: London, 1982; Chapter 6) from the approximate expression $k = \pi(\Delta\nu)$, where $\Delta\nu$ is the difference (in Hertz) between the line width at a temperature T, where exchange of sites is taking place, and the line width in the absence of exchange. The Eyring equation was subsequently employed to calculate $\Delta G^{\ddagger}$ at T.

(32) Ashton, P. R.; Preece, J. A.; Stoddart, J. F.; Tolley, M. S.; White, A. J. P.; Williams, D. J. *Synthesis* **1994**, 1344–1352.

(33) A similar process has been observed in a [2]catenane incorporating the tetracationic cyclophane [BBIPYBIPXYCY]$^{4+}$ and a macrocyclic polyether containing two 1,5-dioxynaphthalene residues. See: Ashton, P. R.; Brown, C. L.; Chrystal, E. J. T.; Goodnow, T. T.; Kaifer, A. E.; Parry, K. P.; Philp, D.; Slawin, A. M. Z.; Spencer, N.; Stoddart, J. F.; Williams, D. J. *J. Chem. Soc., Chem. Commun.* **1991**, 634–639.

(34) See, for example: Ashton, P. R.; Brown, C. L.; Chapman, J. R.; Gallagher, R. T.; Stoddart, J. F. *Tetrahedron Lett.* **1992**, *33*, 7771–7774.

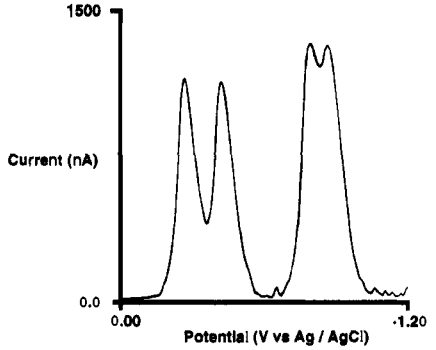

Figure 10. Differential pulse votlammogram obtained on a glassy carbon electrode (0.0079 cm^3) with 1.0 mM solution of the [2]catenane formed between BPP34C10 and [BBIPYPXYMXYCY][PF_6]$_4$ in 0.1 M [TBA][PF_6]/MeCN: pulse amplitude, 10 mV; pulse width, 50 ms; pulse period, 1 s; scan rate, 2 mV/s.

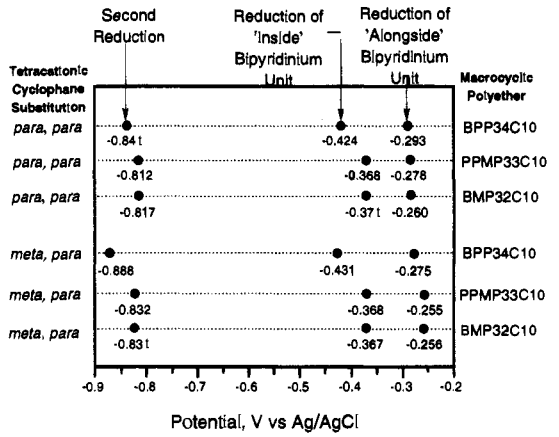

Figure 11. Apparent half-wave potentials for the reduction of [2]catenanes formed by various tetracationic cyclophanes (see labels next to left axis) and the crown ethers (see labels next to right axis). All values obtained with 1.0 mM solution of the [2]catenane in 0.1 M [TBA][PF_6]/MeCN.

Finally, it is interesting to contrast the cathodic voltammetric behavior of the [2]catenane incorporating [BBIPYBIPXYCY]$^{4+}$ and BPP34C10 with those of the isomeric compounds containing the same tetracationic cyclophane and either PPMP33C10 or BMP32C10. The reduction patterns are similar in all compounds, but the half-wave potentials for each one of the reduction processes are less negative for the [2]catenanes containing PPMP33C10 and BMP32C10 (Figure 11). This difference reveals the greater degree of molecular organization of the [2]catenane containing BPP34C10, a feature which results in a larger degree of stabilization for the paraquat residues in this structure. In particular, the striking similarities between the voltammograms of the [2]catenanes incorporating PPMP-33C10 and BMP32C10 indicates that the alongside interaction is important in determining the reduction potentials for the paraquat residues. The ^{1}H NMR spectroscopic studies have shown that resorcinol residues have a much weaker alongside interaction than the hydroquinone ring analogues. A similar comparison between the corresponding isomeric [2]catenanes, where the [BBIPYPXYMXYCY]$^{4+}$ formation has been templated by the same three macrocyclic polyethers, reveals analogous results. BPP34C10 fosters a greater degree of molecular organization and, thus, exhibits a larger stabilization of the paraquat residues than is observed in the PPMP33C10 and BMP32C10 isomers. These results complement the ^{1}H NMR spectroscopic and X-ray structural data for the catenanes.

II. **Translationally-Isomeric [*n*]Pseudorotaxanes.** The prototypical [2]-[BPP34C10]-[BBIPYBIPXYCY]catenane (Figure 1) displays a remarkable degree of ordering, both in solution

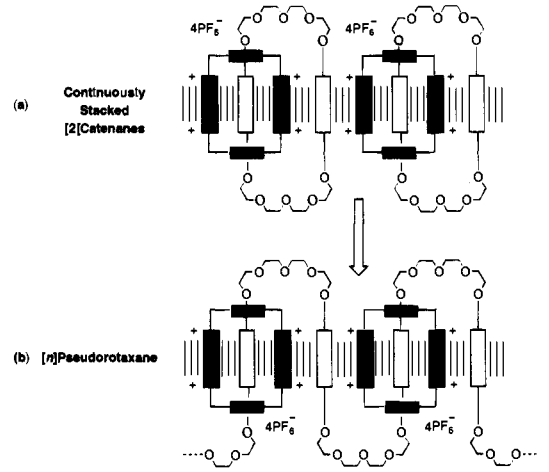

Figure 12. The theoretical conversion of (a) continuously stacked [2]-catenanes to (b) an [*n*]pseudorotaxane.

and in the solid state, as a direct consequence of the noncovalent bonding interactions between the π-electron deficient 4,4′-bipyridinium dications and the π-electron rich hydroquinone rings, crucial to the efficient self-assembly of the [2]catenane and "living on" in the final structure. The X-ray crystal structure of the [2]catenane, shown schematically in Figure 12a, reveals a continuous donor−acceptor stack parallel to one of the crystallographic axes. The mean planes of the π-donors and π-acceptors are separated by an essentially uniform distance of 3.5 Å, both within the [2]catenane molecules and between adjacent molecules in the stack. We envisaged that this type of continuous stacking behavior may be present in other types of supramolecular structures. The translation of one set of the tetraethylene glycol spacer units in the BPP34C10 rings of the [2]catenane in Figure 12a by 7.0 Å along the stack direction gives rise to the structure shown in Figure 12b. This structure consists of an acyclic polyether chain intercepted by π-electron donors threaded through many [BBIPYBIPXYCY]$^{4+}$ cyclophanes. We call this structure an [*n*]pseudorotaxane. In light of the effects observed in the self-assembly and properties of [2]catenanes upon alteration of the constitution of the molecular components, we decided to investigate the self-assembly of [*n*]-pseudorotaxanes and, in particular, to compare their supramolecular behavior with the molecular dynamic properties of the constitutionally-isomeric [2]catenanes by addressing the following questions: (i) The principal stabilizing features of the [*n*]pseudorotaxane superstructure are the noncovalent bonding interactions between its matching molecular components. There is a minimal contribution from the entwining, i.e., mechanical entanglement, of the molecular components. How stable are the pseudorotaxane superstructures in solution? (ii) The tetracationic [BBIPYBIPXYCY]$^{4+}$ cyclophanes can exchange between different π-donor sites on the acyclic molecular component. What are the dynamics of this exchange process in the pseudorotaxanes? (iii) In principle, dynamic properties give rise to a range of possible superstructures, given an acyclic unit with a sufficient number of π-donors. Is the self-assembly process, which creates these superstructures, selective, i.e., will it select and assemble a particular superstructure from a range of possible superstructures? (iv) The acyclic molecular component of the pseudorotaxane may be intercepted by a variety of π-donors which are constitutionally different. What is the effect of different π-donors on the superstructures generated and on the nature of the dynamic behavior of the pseudorotaxanes?

Thus, we set out to investigate the questions raised above by examining the self-assembly of the tetracationic cyclophane [BBIPYBIPXYCY][PF_6]$_4$ with a range of acyclic molecular

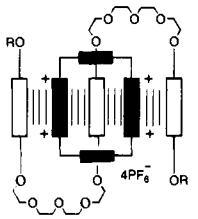

Figure 13. A prototypical [2]pseudorotaxane.

components containing three or more π-donor units linked by an appropriate number of tetraethylene glycol spacer units.

A. Systems Containing Three π-Donors. The simplest case in which [BBIPYBIPXYCY]$^{4+}$ can form a discrete donor–acceptor stack with a system containing π-donor units occurs (Figure 13) when the acyclic system contains three π-donors, i.e., the superstructure obtained is a [2]pseudorotaxane. In order to investigate the effect of the nature of the π-donors on the superstructures and dynamics of pseudorotaxanes, we had to develop a simple, yet efficient, synthetic strategy for the construction of the π-donor-containing compounds which permits easy substitution of a hydroquinone ring by an alternative π-donor. The benzyl group was chosen as the protecting group (R) terminating the three π-donor systems because of its stability and also in view of the synthetic modifications we wished to perform on the three π-donor system later. In addition, it provides an excellent NMR probe in the form of the benzylic methylene protons. The marked dependencies of chemical shifts in ^{1}H NMR spectra on the electronic environment of the probe proton makes ^{1}H NMR spectroscopy a sensitive method for the detection of interactions between two systems containing aromatic π-systems. The observation of mutually induced chemical shift changes (CSC) in the proton resonances of the two systems, which characterize the ^{1}H NMR spectrum of the 1:1 complex, can therefore give a wealth of information about the disposition of functional groups in three-dimensional space. The benzylic methylene protons resonate with chemical shifts in ^{1}H NMR spectra well removed from the other resonances of both the π-donor and π-acceptor systems and hence can serve as useful ^{1}H NMR probes. The characterization of the [2]pseudorotaxane superstructures can be performed by employing FAB mass spectrometry and UV–vis and ^{1}H NMR spectroscopies, with additional support being drawn from ^{13}C NMR spectroscopy and X-ray crystallography, where appropriate.

The general synthesis of the four compounds studied, namely 3HQ, 2HQNP, 2NPHQ, and 3NP, is outlined in Scheme 11. Reaction of hydroquinone (HQ) or 1,5-dihydroxynaphthalene (NP) with 2-(2-chloroethoxy)ethanol under mildly basic conditions affords the diols **2** and **3** in 63% and 46% yields, respectively. Similarly, reaction of 4-benzyloxyphenol (**4**) or 1-benzyloxy-5-hydroxynaphthalene (**5**) with 2-(2-chloroethoxy)-ethanol under mildly basic conditions affords the alcohols **6** and **7**, which were then tosylated (TsCl/Et_3N/CH_2Cl) to afford the tosylates **8** and **9** in overall yield of 85% and 70%, respectively. The syntheses of 3HQ, 2HQNP, 2NPHQ, and 3NP were then completed by reaction of the requisite diols, either **2** or **3**, with the appropriate tosylate, either **8** or **9**, under strongly basic conditions (NaH/refluxing THF).

When [BBIPYBIPXYCY][PF_6]$_4$ and either 3HQ, 2HQNP, 2NPHQ, or 3NP are mixed together in equimolar quantities in acetonitrile solution at room temperature, the solution becomes highly colored instantaneously. The appearance of this color can be attributed to the appearance of a CT band in the UV–vis spectrum of the samples. The presence of the CT band, characteristic of the interaction between 4,4′-bipyridinium dications and π-electron rich aromatic rings, signals the formation of the [2]pseudorotaxanes. The stability of the [2]-pseudorotaxanes so formed may be easily assessed by means of spectrophotometric titration at the wavelength of the CT bands (Table 5).

Scheme 11

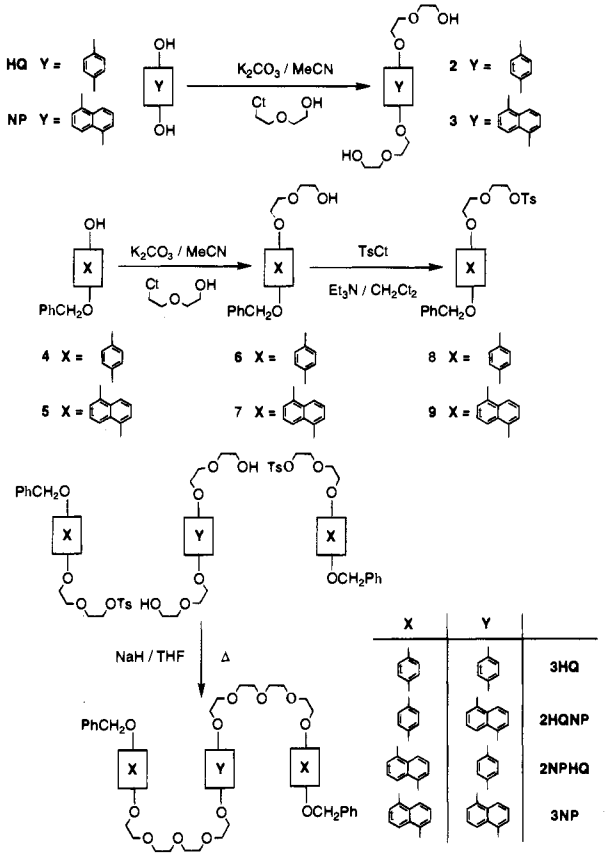

Table 5. Stability Constants for [2]Pseudorotaxanes

[2]pseudorotaxane	λ_{max} (nm)[a]	K_a (M^{-1})[b]	$-\Delta G^o$ (kcal mol^{-1})[c]
[3HQ•BBIPYBIXYCY]$^{4+}$	469	2800	4.75
[2HQNP•BBIPYBIXYCY]$^{4+}$	518	9750	5.48
[2NPHQ•BBIPYBIXYCY]$^{4+}$	502	4900	5.07
[3NP•BBIPYBIXYCY]$^{4+}$	527	11150	5.56

[a] Tetrakis(hexafluorophosphate) salt in MeCN solution at 300 K. [b] Quoted values of K_a are the average of two determinations. [c] Calculated from values of K_a.

Evaporation of MeCN solutions of the [2]pseudorotaxanes [3HQ•BBIPYBIPXYCY][PF_6]$_4$, [2NPHQ•BBIPYBIPXYCY]-[PF_6]$_4$, [2HQNP•BBIPYBIPXYCY][PF_6]$_4$, and [3NP•BBIPYBIPXYCY][PF_6]$_4$ afforded highly colored powders. These powders were subjected to analysis by FAB mass spectrometry. In addition to peaks at relatively low mass (m/z < 1000), corresponding to the individual components of the [2]pseudorotaxanes, peaks corresponding (Table 6) to the loss of one and two PF_6^- counterions, respectively, from the intact 1:1 complexes were observed in all four cases, indicating the comparative stability of the [2]pseudorotaxanes. Strong peaks at m/z 2055, 1910, and 1765, arising from the loss of one, two, and three PF_6^- counterions from a cluster consisting of two [BBIPYBIPXYCY]$^{4+}$ cyclophanes and eight PF_6^- counterions, were also observed in the cases of [3HQ•BBIPYBIPXYCY]-[PF_6]$_4$, [2NPHQ•BBIPYBIPXYCY][PF_6]$_4$. The origin of this supramolecular assembly is unknown, but such cluster ions are well documented[34] by FAB mass spectrometry. Indeed, spectrometers are generally calibrated using CsI cluster ions.

The solution state behavior of the tetrakis(hexafluorophosphate) salts of [3HQ•BBIPYBIPXYCY]$^{4+}$, [2HQNP•-

Table 6. Fast Atom Bombardment Mass Spectrometric Data for [2]Pseudorotaxanes

[2]pseudorotaxane[a]	M[a,b]	[M-PF_6][c]	[M-2PF_6][c]
[3HQ•BBIPYBIXYCY]$^{4+}$	1926	1781	1636
[2HQNP•BBIPYBIXYCY]$^{4+}$	1976	1831	1686
[2NPHQ•BBIPYBIXYCY]$^{4+}$	2026	1881	1736
[3NP•BBIPYBIXYCY]$^{4+}$	2076	1932	1787

[a] Tetrakis(hexafluorophosphate) salt. [b] Nominal molecular mass of the [2]pseudorotaxane. These peaks are not observed. [c] Observed peaks.

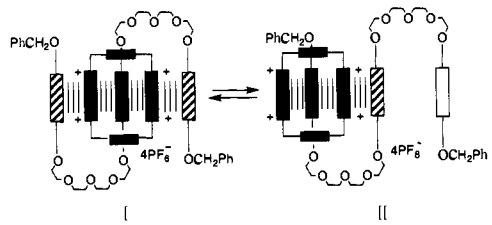

Figure 14. The two possible translational isomers (I and II) of [3HQ•BBIPYBIXYCY][PF_6]$_4$.

BBIPYBIPXYCY]$^{4+}$, [2NPHQ•BBIPYBIPXYCY]$^{4+}$, and [3NP•BBIPYBIPXYCY]$^{4+}$ were investigated by variable temperature ^{1}H NMR spectroscopy in CD_3CN and CD_3COCD_3 solution.

[3HQ•BBIPYBIPXYCY][PF_6]$_4$. There are two possible isomeric superstructures (Figure 14) for the [2]pseudorotaxane, [3HQ•BBIPYBIPXYCY][PF_6]$_4$. These isomers may be interconverted by the translational motion of the [BBIPYBIPXYCY]$^{4+}$ cyclophane from the central hydroquinone ring to one of the two terminal hydroquinone rings. Translational isomer I maximizes $\pi-\pi$ interactions by forming a complete donor–acceptor stack across the superstructure and would be expected to give rise to a relatively simple ^{1}H NMR spectrum, with resonances for the two types—shaded and striped (Figure 14)—of hydroquinone ring and one resonance for the benzylic methylene protons, because of the relatively high degree of symmetry present in the superstructure. Translational isomer II does not contain a complete $\pi-\pi$ stack and is less symmetric, a feature which is probably more favorable entropically. The ^{1}H NMR spectrum would be expected to contain resonances for three types—unshaded, shaded, and striped (Figure 14)—of hydroquinone rings and two resonances for the benzylic methylene protons. At room temperature (293 K), the 400 MHz ^{1}H NMR spectrum of [3HQ•BBIPYBIPXYCY][PF_6]$_4$ in CD_3CN shows considerable broadening, especially for the hydroquinone proton resonances of 3HQ, as a consequence of the exchange between I and II, and indeed with [BBIPYBIPXYCY]$^{4+}$ in free solution.[35] This line broadening is a result of the exchange processes being slow on the ^{1}H NMR time scale. On cooling the CD_3CN solution down from 293 to 233 K, we first of all observed further broadening of the resonances for the protons on two of the hydroquinone rings of 3HQ and then sharpening of the same resonances, until, at 233 K, they appear as an AA′BB′ system (J_{AB} = 9 Hz). These signals may be assigned to the protons on the striped hydroquinone rings of I (Figure 14). The benzylic methylene protons resonate as one singlet at this temperature, providing further strong evidence for the presence of only the translational isomer I in solution at this temperature. Irradiation of the two broad signals centered on δ 6.50 at 263 K produced a transfer of saturation[36] to a broad signal located at δ 3.43, thus identifying this signal as arising from the protons on the hydroquinone ring included within the cavity of [BBIPYBIPXYCY]$^{4+}$ (vide supra). This resonance is shifted further to high field (δ 3.37) at 233 K. In addition, a strong positive nuclear Overhauser enhancement (NOE) was observed in the benzylic methylene signal at δ 4.85, confirming the assignment of the irradiated signal as that produced by the

Table 7. Induced Chemical Shift Changes for the [2]Pseudorotaxane [3HQ•BBIPYBIXYCY][PF_6]$_4$ in CD_3CN Solution

component	proton	δ_{uc}[a]	δ_c(233 K)[b]	$\Delta\delta$[c]
[BBIPYBIXYCY]$^{4+}$	α-CH[d]	8.86	8.70	−0.07
	β-CH[d]	8.16	7.57	−0.59
	C_6H_4	7.52	7.69	+0.17
	N^+-CH_2	5.74	5.60	−0.14
3HQ	Ph-CH_2	7.29–7.44	7.31–7.41	
	ArH (HQ)	6.89/6.82	6.35/6.58	−0.31/−0.47
		6.80	3.33	−3.47
	Ph-CH_2	5.00	4.85	−0.15
	α-OCH_2[e]	3.99	see text	
	β-OCH_2[e]	3.91	see text	
	γ-/δ-OCH_2[e]	3.54–3.61	see text	

[a] δ_{uc} is the chemical shift in the 400 MHz ^{1}H NMR spectrum recorded in CD_3CN of the protons of each component in the uncomplexed state. The concentration of the solution used to determine δ_{uc} was in the range $5-8 \times 10^{-3}$ M. [b] δ_c(233 K) is the chemical shift of the protons observed in the 400 MHz ^{1}H NMR spectrum of the 1:1 complex [3HQ•BBIPYBIXYCY][PF_6]$_4$ recorded in CD_3CN at 233 K. The concentration of the solution used to determine δ_c(233 K) was in the range $5-8 \times 10^{-3}$ M. [c] $\Delta\delta = \delta_c$(233 K) − δ_{uc}. [d] Relative to pyridinium ring nitrogen atom. [e] Relative to oxygen atom attached to the hydroquinone ring.

protons in the striped hydroquinone rings in I (Figure 14). A strong positive NOE was also observed for the *N*-methylene protons of [BBIPYBIPXYCY]$^{4+}$, perhaps indicating the close proximity of the striped hydroquinone rings to the outer π-surface of the 4,4′-bipyridinium dications in [BBIPYBIPXYCY]$^{4+}$, as is indeed the case in I. The induced chemical shift changes observed at this temperature in both [BBIPYBIPXYCY]$^{4+}$ and 3HQ are recorded in Table 7. There is an extremely large upfield shift ($\Delta\delta$ −3.47 ppm) of the resonance for the protons on the hydroquinone ring (shaded in Figure 14) included within the cavity of the [BBIPYBIPXYCY]$^{4+}$ cyclophane. The chemical shift changes observed ($\Delta\delta$ −0.31 and −0.47 ppm) in the resonances for the protons on the two terminal hydroquinone rings, although smaller in magnitude, are entirely consistent with the stacked structure of I in Figure 14. The upfield shift of the resonance for the benzylic methylene protons is consistent with their location within the shielding region, i.e., above the plane, of the 4,4′-bipyridinium π-systems of [BBIPYBIPXYCY]$^{4+}$. The induced chemical shift changes observed for the proton resonances in the [BBIPYBIPXYCY]$^{4+}$ component of the complex are also entirely consistent with the superstructure proposed. Upfield shifts of the resonances for α-CH ($\Delta\delta$ −0.07 ppm) and β-CH ($\Delta\delta$ −0.59 ppm) protons of the 4,4′-bipyridinium dicationic units of [BBIPYBIPXYCY]$^{4+}$ are observed as a result of the "sandwiching" of these units between the faces of two hydroquinone rings. In addition, the protons of the bridging C_6H_4 ring experience a downfield shift by virtue of their lying in the plane of the included hydroquinone ring. The upfield shift ($\Delta\delta$ −0.14 ppm) of the *N*-methylene protons[37] is consistent with their location close to the alongside hydroquinone rings (vide infra). This observation is in agreement with the NOE data and supports the completely π-stacked superstructure proposed for the [2]pseudorotaxane [3HQ•BBIPYBIPXYCY][PF_6]$_4$. The distinction between inside and alongside hydroquinone rings in the [2]pseudorotaxane is reflected in the observation that all of the OCH_2 proton signals, in each equivalent polyether chain linking the inside hydroquinone ring to the alongside ones, are anisochronous and resonate in the region between δ 3.40 and δ 3.90, although unambiguous assignment of the individual signals is not possible. The overall picture of the [2]pseudorotaxane, which emerges from these experiments, is of a highly organized superstructure in solution. At room temperature, the [BBIPYBIPXYCY]$^{4+}$ cyclophane can exchange relatively freely between the two translationally isomeric states, I and II.

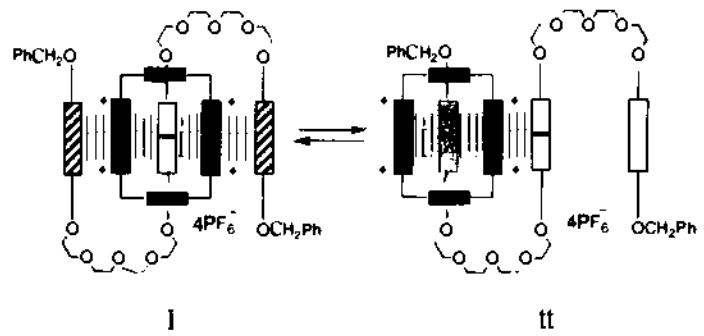

Figure 15. The two possible translational isomers (I and II) of [2HQNP·BBIPYBIXYCY][PF_6]4.

[2HQNP·BBIPYBIPXYCY][PF_6]4. The extensive line broadening observed in the 400 MHz ^{1}H NMR spectrum of [2HQNP·BBIPYBIPXYCY][PF_6]$_4$ in CD_3CN solution recorded at 293 K indicates that the exchange between translational isomers I and II (Figure 15) is slow on the ^{1}H NMR time scale. However, on cooling the CD_3CN solution down to 261 K, the signals, which are extremely broad at 293 K, become sharp. The simplicity of the ^{1}H NMR spectrum at 261 K indicates that, almost certainly, only translational isomer I is present in solution. Translational isomer I has a completely π-stacked structure and would be expected to display proton resonances for one type of hydroquinone ring (striped in Figure 15) as well as resonances for the 1,5-disubstituted naphthalene protons commensurate with that ring (unshaded with a bar in Figure 15) being included within the cavity of [BBIPYBIPXYCY]$^{4+}$. In addition, only one resonance would be expected for the benzylic methylene protons of the 2HQNP component of translational isomer I. By contrast, the spectrum of translational isomer II would be expected to contain (i) resonances for two types of hydroquinone ring protons, (ii) resonances for the protons on the 1,5-disubstituted naphthalene ring commensurate with it being located in the alongside position, and (iii) two resonances for the benzylic methylene protons. Table 8 summarizes the induced chemical shift change data from the 400 MHz ^{1}H NMR spectrum of [2HQNP·BBIPYBIPXYCY]-[PF_6]$_4$ recorded in CD_3CN at 261 K. There is a strong dispersion of the resonances arising from protons in the [BBIPYBIPXYCY]$^{4+}$ component of the [2]pseudorotaxane. Two resonances are apparent for each of the α-CH and the β-CH protons as well as for the protons of the bridging C_6H_4 units in [BBIPYBIPXYCY]$^{4+}$. The resonance for the *N*-methylene

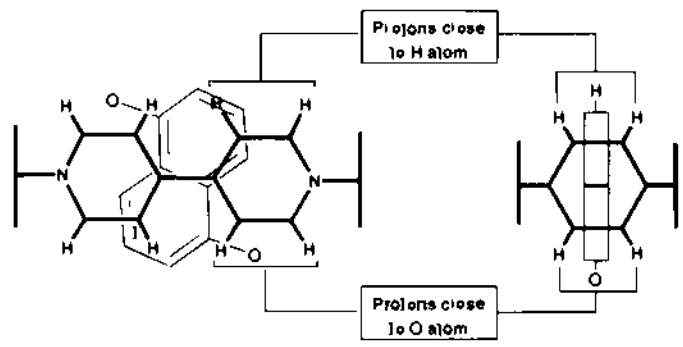

Figure 16. The diagonal and vertical relationships between protons in [BBIPYBIXYCY]$^{4+}$ when a 1,5-dioxynaphthalene ring is included in the cavity of the cyclophane.

Table 8. Induced ^{1}H NMR Chemical Shift Changes for the [2]Pseudorotaxane [2HQNP·BBIPYBIXYCY][PF_6]$_4$ in CD_3CN Solution

	proton	δ_{uc}[a]	δ_c(261 K)[b]	$\Delta\delta$[c]
[BBIPYBIXYCY]$^{4+}$	α-CH[d]	8.86	8.93	+0.07
			8.50	−0.36
	β-CH[d]	8.16	7.17	−0.99
			7.08	−1.08
	C_6H_4	7.52	7.99	+0.47
			7.79	+0.27
	N^+-CH_2	5.74	5.72	−0.02
			5.58	−0.16
2HQNP[e]	HQ ArH	6.87	6.63	−0.24
		6.79	6.41	−0.38
	H-2/H-6[f]	6.91	6.15	−0.76
	H-3/H-7[f]	7.37	5.86	−1.51
	H-4/H-8[f]	7.80	2.26	−5.54
	Ph-CH_2	5.00	4.89	−0.11

[a] δ_{uc} is the chemical shift in the 400 MHz ^{1}H NMR spectrum recorded in CD_3CN of the protons of each component (ca. 5×10^{-3} M) in the uncomplexed state. [b] δ_c(261K) is the chemical shift of the protons observed in the 400 MHz ^{1}H NMR spectrum of the 1:1 complex [2HQNP·BBIPYBIXYCY][PF_6]$_4$ (ca. 5×10^{-3} M) recorded in CD_3CN at 261 K. [c] $\Delta\delta = \delta_c(261K) - \delta_{uc}$. [d] Relative to pyridinium ring nitrogen atom. [e] Selected resonances only. [f] Naphthalene ring protons numbered relative to the oxygen atom at position 1.

protons appears as an AB signal. The signal dispersion is a direct consequence of the inclusion of the 1,5-disubstituted naphthalene ring (Figure 16) within the cavity of [BBIPYBIPXYCY]$^{4+}$. The averaged C_{2h} symmetry enforced on the superstructure by the 2HQNP guest is such that it renders anisochronous vertically opposite pairs of protons within [BBIPYBIPXYCY]$^{4+}$ as represented in Figure 16. We observe separate signals for the protons in [BBIPYBIPXYCY]$^{4+}$ which are located next to the oxygen substituents of the naphthalene ring and those which are located next to a hydrogen atom on the naphthalene ring. From Figure 16, those protons within the 4,4′-bipyridinium units, which are diagonally related between pyridinium rings are equivalent, and those which are vertically related within each bipyridinium ring are nonequivalent.

The chemical shift changes (Table 8), observed in the [BBIPYBIPXYCY]$^{4+}$ component of the [2]pseudorotaxane, are an indication of the increased shielding effect of the included 1,5-disubstituted naphthalene ring, when compared to the ring current of a hydroquinone ring. Very large upfield shifts ($\Delta\delta$ −0.99 and −1.08 ppm) of the resonances for the β-CH protons indicate that the 4,4′-bipyridinium dications of [BBIPYBIPXYCY]$^{4+}$ are strongly sandwiched between the included central naphthalene ring and the two alongside hydroquinone rings of the 2HQNP component. The strong downfield shifts ($\Delta\delta$ +0.27 and +0.47 ppm) of the protons of the C_6H_4 bridging unit are a result of them lying in the plane of the strong naphthalene ring current. The protons of the naphthalene ring of 2HQNP are, in turn, strongly perturbed by inclusion within the cavity of [BBIPYBIPXYCY]$^{4+}$. Most remarkable is the chemical shift change induced ($\Delta\delta$ −5.54 ppm) in the resonance for the H-4 and H-8 protons on the included naphthalene ring.

(35) The concentration of the solution used to record the ^{1}H NMR spectra was ca. 5×10^{-3} M. At this concentration, given a stability constant of ca. 3×10^3 M^{-1}, approximately 50% of the [BBIPYBIXYCY]$^{4+}$ will be bound to the 3HQ at any given instant.

(36) Sanders, J. K. M.; Hunter, B. K. *Modern NMR Spectroscopy*, 2nd ed.; Oxford University Press; Oxford, 1993; pp 222−230.

(37) In simple 1:1 complexes, e.g., with 1,4-dimethoxybenzene, the *N*-methylene protons of [BBIPYBIXYCY]$^{4+}$ show no significant CSCs.

(38) Assuming a similar inclusion geometry to that observed in the X-ray crystal structure of [3NP·BBIPYBIXYCY][PF_6]$_4$.

(39) Attempts to fit 2:1 binding isotherms to the titration data resulted in very poor fits suggesting that, if the complex [BBIPYBIXYCY·4HQ·-BBIPYBIXYCY]$^{8+}$ exists in solution, it is extremely weak.

(40) The relative integral remains constant at 2.5:1 on cooling the CD_3-$COCD_3$ solution of the [2]pseudorotaxane from 253 K down to 213 K.

(41) The line shape analysis was carried out using the DNMR program [Burdon, J.; Hotchkiss, J. C.; Jennings, W. B. *J. Chem. Soc., Perkin Trans. 2* **1976**, 1052−1057) running on an IBM-compatible PC. We thank Prof. W. B. Jennings for instruction on the use of this program.

(42) The ^{1}H NMR spectrum of free 5HQ, recorded in CD_3COCD_3 solution, does not change appreciably on cooling through the same temperature range.

(43) Ashton, P. R.; Reder, A. S.; Spencer, N.; Stoddart, J. F. *J. Am. Chem. Soc.* **1993**, *115*, 5286−5287.

(44) Ashton, P. R.; Chrystal, E. J. T.; Mathias, J. P.; Parry, K. P.; Slawin, A. M. Z.; Spencer, N.; Stoddart, J. F.; Williams, D. J. *Tetrahedron Lett.* **1987**, *28*, 6367−6370.

(45) Brown, C. L.; Philp, D.; Spencer, N.; Stoddart, J. F. *Israel J. Chem.* **1992**, *432*, 61−67.

(46) Sheldrick, G. M. SHELTXL PLUS PC; Version 4.2, Siemens Analytical X-ray Instruments Inc., Madison, WI, 1990.

Table 9. Induced ^{13}C NMR Chemical Shift Changes for the [2]Pseudorotaxane [2HQNP•BBIPYBIXYCY][PF_6]$_4$ in CD_3CN Solution

	carbon	δ_{uc}[a]	δ_c(261 K)[b]	$\Delta\delta$[c]
[BBIPYBIXYCY]$^{4+}$	γ-C[d]	150.4	145.3	−5.1
	α-CH[d]	146.2	145.2	−1.0
			144.7	−1.5
	CH(C_6H_4)	131.4	131.7	+0.3
			132.0	+0.6
	β-CH[d]	128.3	126.4	−1.9
			124.9	−3.2
	N^+-CH_2	65.7	65.6	−0.1
2HQNP[e]	C-3/C-7[f]	129.5	128.7	−0.8
	HQ (CH)	116.8	116.2	−0.6
	HQ (CH)	116.4	115.7	−0.7
	C-4/C-8[f]	115.1	108.7	−6.4
	C-2/C-6[f]	107.0	104.7	−2.3

[a] δ_{uc} is the chemical shift in the 100 MHz ^{13}C NMR spectrum recorded in CD_3CN of the protons of each component (ca. 5×10^{-3} M) in the uncomplexed state. [b] δ_c(261 K) is the chemical shift of the protons observed in the 100 MHz ^{13}C NMR spectrum of the 1:1 complex [2HQNP•BBIPYBIXYCY][PF_6]$_4$ (ca. 5×10^{-3} M) recorded in CD_3CN at 261 K. [c] $\Delta\delta = \delta_c(261\ K) - \delta_{uc}$. [d] Relative to pyridinium ring nitrogen atom. [e] Only resonances which could be assigned unambiguously in both complexed and uncomplexed states are included. [f] Naphthalene ring carbon atoms, numbered relative to the carbon bearing an oxygen atom at position 1.

This observation reflects the fact that these protons are located deep within the π-electron cloud of the C_6H_4 bridging units of [BBIPYBIPXYCY]$^{4+}$, only 2.6 Å above the aromatic ring[38] plane of this unit. The chemical shift changes in the other naphthalene protons are less dramatic, i.e., $\Delta\delta$ −0.76 ppm for H-2 and H-6 and $\Delta\delta$ −1.51 ppm for H-3 and H-7. However, they are entirely consistent with the inclusion of the naphthalene ring in the cavity of [BBIPYBIPXYCY]$^{4+}$. The chemical shift changes observed in the resonances for the hydroquinone ring protons ($\Delta\delta$ −0.24 and −0.38 ppm) and the benzylic methylene protons ($\Delta\delta$ −0.11 ppm) of 2HQNP and, in addition, those for the *N*-methylene protons ($\Delta\delta$ −0.02 and −0.16 ppm) of [BBIPYBIPXYCY]$^{4+}$ support the assertion that the [2]pseudorotaxane has a time-averaged π-stacked superstructure characteristic of translational isomer I in CD_3CN solution at 261 K. Further evidence for a π-stacked superstructure for the [2]-pseudorotaxane comes, once again, from the observation that all eight OCH_2 groups, in each of the polyether chains linking the π-donors, are anisochronous at 261 K.

The chemical shift changes observed at 261 K in the 400 MHz ^1H NMR spectrum are closely mirrored by those observed in the 100 MHz ^{13}C NMR spectrum (Table 9) recorded in CD_3CN at the same temperature. The resonances for all of the carbon atoms of the 4,4′-bipyridinium dications in [BBIPYBIPXYCY]$^{4+}$ display strong upfield shifts, the largest ($\Delta\delta$ −5.1 ppm) being that observed for the quaternary γ carbon atoms linking the two pyridinium rings of the 4,4′-bipyridinium dication. This carbon atom lies directly above the center of the naphthalene π-system. There are concomitant, large downfield shifts observed in the carbon resonances of the naphthalene and hydroquinone rings. In common with the ^1H NMR spectrum, the largest ^{13}C chemical shift change ($\Delta\delta$ −6.4 ppm) is observed in the resonance for C-4 and C-8 of the naphthalene ring. Upfield shifts ($\Delta\delta$ +0.3 and +0.6 ppm) are observed in the resonances for the aromatic CH carbon atoms of the C_6H_4 bridging units within [BBIPYBIPXYCY]$^{4+}$. This observation is commensurate with these units lying in the plane—and hence in the deshielding region—of the naphthalene ring current.

The nature of the $\pi-\pi$ stacked superstructure (Figure 15) of the [2]pseudorotaxane in CD_3CN solution was further supported by a $^1H-^{13}C$ heteronuclear correlation experiment performed at 261 K. It revealed that the proton resonances of the OCH_2 groups in the bridging polyether chains of 2HQNP correlate to eight carbon resonances in the range δ 68.0 to δ 71.0, in agreement with the observations made from ^1H NMR spectroscopic experiments. In addition, further insight into the dynamics of the [2]pseudorotaxane in CD_3CN solution at 261 K could be gained by considering the results of the $^1H-^{13}C$ heteronuclear correlation experiment. Correlations can be observed between the proton resonances of the α-CH protons at δ 8.50 and 8.93 of [BBIPYBIPXYCY]$^{4+}$ and two carbon resonances at δ 145.2 and 144.7, respectively. Further correlations are evident between the β-CH proton resonances (δ 7.17 and 7.08) and the two β-CH carbon resonances (δ 124.9 and 126.4). The two proton resonances (δ 7.79 and 7.99) of the bridging C_6H_4 unit of [BBIPYBIPXYCY]$^{4+}$ also correlate to two carbon resonances (δ 131.7 and 132.0). However, the proton resonances (δ 5.72 and 5.58) for the *N*-methylene group of [BBIPYBIPXYCY]$^{4+}$ correlate to the same carbon resonance (δ 65.6). These observations indicate that the naphthalene ring is locked in the cavity of [BBIPYBIPXYCY]$^{4+}$ on both the ^1H and ^{13}C NMR time scales at 261 K. Thus, the averaged C_{2h} symmetry (Figure 16), generated by the inclusion geometry of the central 1,5-dioxynaphthalene unit, is expressed in both the ^1H and ^{13}C NMR spectra. However, if there were no dynamic processes occurring within the [2]pseudorotaxane, two carbon resonances would be expected for the *N*-methylene groups of [BBIPYBIPXYCY]$^{4+}$. The different resonances would arise (Figure 17) from the *N*-methylene groups at diagonally opposite corners of the [BBIPYBIPXYCY]$^{4+}$ cyclophane, since two of these groups (■) are close to a polyether chain of 2HQNP and the other two (▲) are not. The observation of only one *N*-methylene carbon resonance is commensurate with an equilibration process which exchanges the alongside hydroquinone rings (A and B), shown in Figure 17, and is fast on the ^{13}C NMR time scale. The equilibration process may be thought of as a pirouetting motion of the hydroquinone rings—and the associated polyether chains—about the C−O bonds attaching them to the included 1,5-disubstituted naphthalene ring. This motion has the effect of exchanging diagonally opposite corners (▲ and ■) of the [BBIPYBIPXYCY]$^{4+}$ cyclophane and hydroquinone rings (A and B). The diagonal asymmetry imposed on [BBIPYBIPXYCY]$^{4+}$ by the inclusion of a naphthalene ring within the tetracationic cyclophane is expressed in the ^1H NMR spectrum, since one proton of the methylene group is invariably close to the polyether chain and the other proton is invariably in a position remote from the polyether chain.

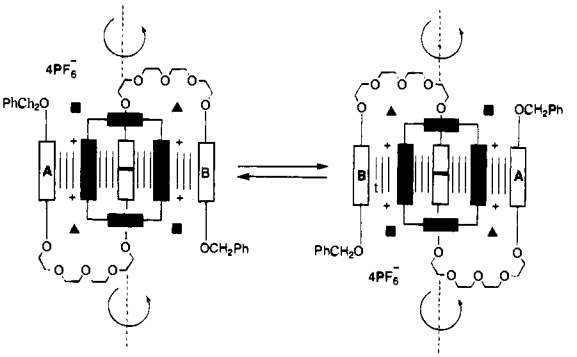

Figure 17. Dynamic pirouetting process which exchanges the *N*-methylene protons of [BBIPYBIXYCY]$^{4+}$ in of [2HQNP•-BBIPYBIXYCY][PF_6]$_4$ at 261 K in CD_3CN.

The activation barrier to reorientation of the naphthalene ring within the cavity of [BBIPYBIPXYCY]$^{4+}$ may be estimated[29] by the application of variable temperature ^1H NMR spectroscopy to the [2]pseudorotaxane. Observation of the coalescence of the signals corresponding to the β-CH, *N*-methylene, and the aromatic C_6H_4 protons of [BBIPYBIPXYCY]$^{4+}$ affords (Table

Table 10. Thermodynamic Parameters for the Equilibrium of Translational Isomers I and II in [2HQNP·BBIPYBIXYCY][PF_6]$_4$

probe protons	$\Delta\nu$ (Hz)	k_C (s^{-1})[a]	T_C (K)[b]	$\Delta G^{\ddagger}_C$ (kcal mol^{-1})[c]
β-CH	34.5	77	296	14.8
C_6H_4	76.5	170	301	14.5
N^+-CH_2	55.0	122	297	14.6

[a] Calculated from the approximate expression, $k_C = \pi(\Delta\nu)/2^{1/2}$. [b] Temperature of the spectrometer probe at coalescence, measured using an electronic thermometer. [c] Calculated using the Eyring equation (ref 29).

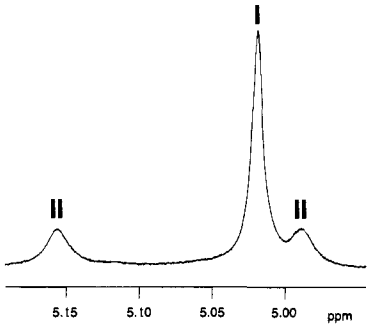

Figure 18. Partial 400 MHz ^{1}H NMR spectrum, recorded in CD_3CN at 233 K, of [2NPHQ·BBIPYBIXYCY][PF_6]$_4$ showing the signals corresponding to the benzylic methylene protons of 2NPHQ.

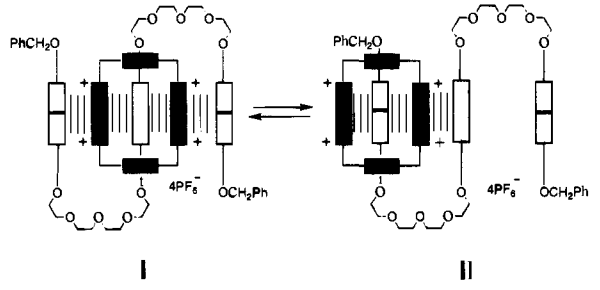

Figure 19. The two possible translational isomers (I and II) of [2NPHQ·BBIPYBIXYCY][PF_6]$_4$.

10) an averaged value for $\Delta G_c^{\ddagger}$ of 14.6 kcal mol^{-1}. In summary, the [2]pseudorotaxane of [2HQNP·BBIPYBIPXYCY]-[PF_6]$_4$ exists exclusively in CD_3CN solution at 261 K as translational isomer I (Figure 15). This conclusion is inescapabale, taking into account both the ^{1}H and ^{13}C NMR spectroscopic data. Although, on a time-average, the superstructure is completely $\pi-\pi$ stacked, the alongside hydroquinone rings are exchanging rapidly on the ^{13}C NMR time scale at 261 K by a process which involves a pirouetting motion.

[2NPHQ·BBIPYBIPXYCY][PF_6]$_4$. Examination of the 400 MHz ^{1}H NMR spectrum of [2NPHQ·BBIPYBIPXYCY][PF_6]$_4$ recorded in CD_3CN solution at 293 K reveals extensive line broadening as a consequence of slow exchange between equilibrating translational isomers. On cooling the solution down to 233 K, there is no obvious simplification of the spectrum. Indeed, it would appear from closer examination of the spectrum that there are at least two different supramolecular species present in solution at this temperature. A detailed examination of the resonances arising from the benzylic methylene protons (Figure 18) confirms that, in fact, we are observing equilibration between the two possible translational isomers (Figure 19) of [2NPHQ·BBIPYBIPXYCY][PF_6]$_4$ which is slow on the ^{1}H NMR time scale at 233 K. The signal pattern observed in the resonances for the benzylic methylene protons may be explained if we accept that, in addition to the presence of a significant amount of the $\pi-\pi$ stacked translational isomer I, there is a finite population of the asymmetric translational isomer **II** in CD_3CN solution at 233 K. If this is the case, then the two smaller benzylic methylene signals, resonating at δ 5.17 and 4.98, must correspond to the two nonequivalent benzylic methylene groups of translational isomer II, and the larger signal, resonating at δ 5.01, must correspond to the single resonance for the equivalent benzylic methylene groups of translational isomer I. Thus, it is apparent that the [2]pseudorotaxane [2NPHQ·BBIPYBIPXYCY][PF_6]$_4$ exists as an ca. 2:1 mixture—as judged from integration of the benzylic methylene signals—of the completely $\pi-\pi$ stacked translational isomer I and the asymmetric translational isomer II in CD_3CN solution at 233 K.

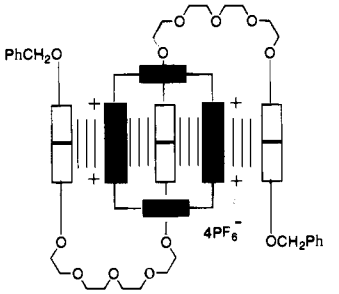

Figure 20. π-Stacked structure of the [2]pseudorotaxane of [3NP·-BBIPYBIXYCY][PF_6]$_4$.

[3NP·BBIPYBIPXYCY][PF_6]$_4$. Examination of the 400 MHz ^{1}H NMR spectrum of [3NP·BBIPYBIPXYCY][PF_6]$_4$ recorded in CD_3CN solution at 293 K reveals some degree of line broadening as a consequence of slow exchange between equilibrating translational isomers. On cooling the solution down to 243 K, there is considerable simplification of the spectrum. The simplicity of the ^{1}H NMR spectrum at 243 K suggests that the [2]pseudorotaxane exists exclusively as the completely π-stacked translational isomer (Figure 20). This assertion is confirmed by consideration of the chemical shift changes observed (Table 11) in the 400 MHz ^{1}H NMR spectrum, recorded in CD_3CN at 243 K, of [3NP·-BBIPYBIPXYCY][PF_6]$_4$. The appearance of two resonances in each case for the α-CH, β-CH, aromatic C_6H_4, and *N*-methylene protons of the [BBIPYBIPXYCY]$^{4+}$ component of the [2]pseudorotaxane may be explained by the inclusion of a 1,5-dioxynaphthalene residue within the cavity of the tetracationic cyclophane since this guest enforces averaged C_{2h} symmetry on the host component of the superstructure. Upfield shifts are observed for the α-CH ($\Delta\delta$ −0.18 and −0.74 ppm) and *N*-methylene ($\Delta\delta$ −0.19 and −0.31 ppm) protons of the [BBIPYBIPXYCY]$^{4+}$ which are considerably larger in magnitude than those observed for the [2]pseudorotaxane incorporating 2HQNP. This observation reflects the enhanced shielding effect of the naphthalene rings in the alongside positions of the [3NP·-BBIPYBIPXYCY][PF_6]$_4$ pseudorotaxane, which is also reflected in the extremely large upfield shifts ($\Delta\delta$ −1.53 and −1.59 ppm) of the β-CH protons. The downfield shifts of the aromatic C_6H_4 protons of [BBIPYBIPXYCY]$^{4+}$ are of comparable magnitude to that observed in the case of [2HQNP·BBIPYBIPXYCY]-[PF_6]$_4$, reflecting the fact that the *p*-phenylene rings are hardly affected by the stacking of the two alongside naphthalene rings on the outer π-faces of the 4,4′-bipyridinium dications of [BBIPYBIPXYCY]$^{4+}$.

The chemical shift changes observed (Table 11) in the proton resonances of the 3NP component of the [2]pseudorotaxane are also entirely consistent with the structure shown in Figure 20. The largest chemical shift changes ($\Delta\delta$ −5.41 ppm) are observed for the protons of the included 1,5-dioxynaphthalene ring, the most notable being that for H-4 and H-8. This large $\Delta\delta$ value is commensurate with the location of these protons within 2.7 Å of the mean ring plane of the C_6H_4 bridging units in [BBIPYBIPXYCY]$^{4+}$ and agrees well with the $\Delta\delta$ value observed (−5.54 ppm) in the case of [2HQNP·BBIPYBIPXYCY]-

Table 11. Induced ^{1}H NMR Chemical Shift Changes for the [2]Pseudorotaxane [3NP·BBIPYBIXYCY][PF_6]$_4$ in CD_3CN Solution

	proton	δ_{uc}[a]	δ_c(243 K)[b]	$\Delta\delta$[c]
[BBIPYBIXYCY]$^{4+}$	α-CH[d]	8.86	8.68	−0.18
			8.12	−0.74
	β-CH[d]	8.16	6.63	−1.53
			6.57	−1.59
	C_6H_4	7.52	7.84	+0.32
			7.71	+0.19
	N^+-CH_2	5.74	5.43	−0.21
			5.33	−0.31
3NP[e]	alongside H-4[f]	7.77	7.32	−0.45
	alongside H-8[f]	7.79	7.33	−0.46
	alongside H-7[f]	7.34	7.16	−0.18
	alongside H-3[f]	7.32	7.07	−0.25
	alongside H-6[f]	6.88	6.69	−0.17
	alongside H-2[f]	6.82	6.40	−0.42
	included H-2/H-6[f]	6.95	5.90	−1.05
	included H-3/H-7[f]	7.34	5.60	−1.74
	included H-4/H-8[f]	7.82	2.41	−5.41
	Ph-CH_2	5.23	5.03	−0.20

[a] δ_{uc} is the chemical shift in the 400 MHz ^{1}H NMR spectrum recorded in CD_3CN of the protons of each component (ca. 4×10^{-3} M) in the uncomplexed state. [b] δ_c(243 K) is the chemical shift of the protons observed in the 400 MHz ^{1}H NMR spectrum of the 1:1 complex [3NP·BBIPYBIXYCY][PF_6]$_4$ (ca. 4×10^{-3} M) recorded in CD_3CN at 243 K. [c] $\Delta\delta = \delta_c(243\text{ K}) - \delta_{uc}$. [d] Relative to pyridinium ring nitrogen atom. [e] Selected resonances only. [f] Naphthalene ring protons, numbered relative to the oxygen atom at the 1 position of the naphthalene ring.

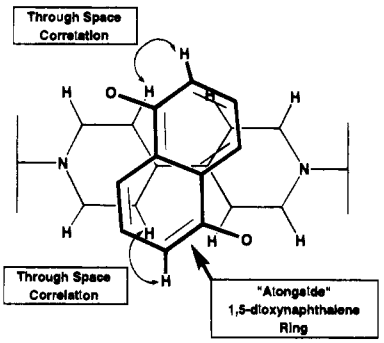

Figure 21. Through space correlations, based on the results of a 2-D NOESY experiment performed in CD_3CN at 233 K, between protons on the alongside 1,5-dioxynaphthalene ring of 3NP and the β protons of the [BBIPYBIXYCY]$^{4+}$ cyclophane in the [2]pseudorotaxane [3NP·BBIPYBIXYCY][PF_6]$_4$.

[PF_6]$_4$ and other related systems.[38] The chemical shift changes observed in the resonances for the protons of the alongside naphthalene ring, although smaller in magnitude, are entirely consistent with the completely π-stacked superstructure proposed (Figure 20) for the [2]pseudorotaxane.

Further evidence for a completely π-stacked structure for the [2]pseudorotaxane comes from examination of the results of a 2D-NOESY experiment performed in CD_3CN at 243 K. In addition to cross peaks arising from through-space correlations within the individual components of [3NP·BBIPYBIPXYCY]-[PF_6]$_4$, cross peaks were also in evidence arising from a through-space correlation between H-2 of the alongside naphthalene ring and one of the two resonances for the β-CH protons of [BBIPYBIPXYCY]$^{4+}$ and between H-6 of the alongside naphthalene ring and the other resonance for the β-CH protons of [BBIPYBIPXYCY]$^{4+}$. These intercomponent through-space correlations suggest that the interaction of the alongside naphthalene ring with the outer π-faces of the 4,4′-bipyridinium dication of [BBIPYBIPXYCY]$^{4+}$ is as shown in Figure 21. The averaged symmetry of the superstructure[22] is increased if the central naphthalene unit is ejected from the cavity of [BBIPY-BIPXYCY]$^{4+}$ and then returns to the cavity with the opposite orientation (Figure 22). This process results in the exchange

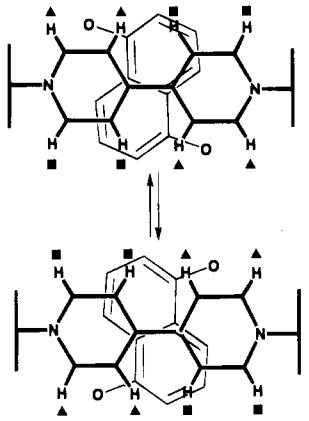

Figure 22. The exchange of vertically opposite pairs of protons in the [BBIPYBIXYCY]$^{4+}$ cyclophane by reorientation of the included 1,5-dioxynaphthalene ring.

Table 12. Thermodynamic Parameters for Naphthalene Ring Reorientation in [3NP·BBIPYBIXYCY][PF_6]$_4$

probe protons	Δν (Hz)	k_C (s^{-1})[a]	T_C (K)[b]	$\Delta G_C^{\ddagger}$ (kcal mol^{-1})[c]
β-CH	24.0	53	303	15.4
C_6H_4	52.0	116	314	15.5

[a] Calculated from the approximate expression, $k_C = \pi(\Delta\nu)/2^{1/2}$. [b] Temperature of the spectrometer probe at coalescence, measured using an electronic thermometer. [c] Calculated using the Eyring equation (ref 29).

of vertically opposite α-CH, β-CH, aromatic C_6H_4, and *N*-methylene protons (Figure 22). The activation barrier for this exchange process in [3NP·BBIPYBIPXYCY][PF_6]$_4$ was estimated by the application of variable temperature ^{1}H NMR spectroscopy to the [2]pseudorotaxane in CD_3CN solution. Observation of the coalescence of the signals arising from the β-CH and aromatic C_6H_4 protons of [BBIPYBIPXYCY]$^{4+}$ affords (Table 12) an average value for the activation barrier, $\Delta G_c^{\ddagger}$, of 15.5 kcal mol^{-1}. The picture of the [2]pseudorotaxane [3NP·BBIPYBIPXYCY][PF_6]$_4$ which emerges from the spectroscopic data is that of a completely π−π stacked superstructure in CD_3CN solution at 243 K. In summary, [3NP·-BBIPYBIPXYCY][PF_6]$_4$ has the most stable and highly organized solution state superstructure of the [2]pseudorotaxanes formed in CD_3CN solution between three π-donor systems and [BBIPYBIPXYCY][PF_6]$_4$.

The solid state structures of the [2]pseudorotaxanes [3HQ·-BBIPYBIPXYCY][PF_6]$_4$ and [3NP·BBIPYBIPXYCY][PF_6]$_4$ were determined using single crystals, grown by vapor diffusion of *i*-Pr_2O into MeCN solutions of the appropriate 1:1 mixtures of the components of the pseudorotaxanes.

[3HQ·BBIPYBIPXYCY][PF_6]$_4$. The solid state structure (Figure 23) of [3HQ·BBIPYBIPXYCY][PF_6]$_4$ reveals π−π stacking interactions between the inside hydroquinone ring of 3HQ and the bipyridinium residues of the [BBIPYBIPXYCY]$^{4+}$ cyclophane (separation 3.55 Å) and between the alongside hydroquinone rings of 3HQ also and one of the pyridinium rings of [BBIPYBIPXYCY]$^{4+}$ (mean interplanar separation 3.55 Å, tilt angle 7°, centroid−centroid distance 3.81 Å). In addition, there are other C−H···O and C−H···π interactions which stabilize the overall structure of the [2]pseudorotaxane. C−H···O hydrogen bonds are observed between both the benzylic methylene groups (C−H···O distance 2.53 Å, C−H···O angle 141°) and the aromatic ring of the *p*-xylyl unit (C−H···O distance 2.64 Å, C−H···O angle 164°). In addition, there are more remote contacts between α-bipyridinium protons and the second and third oxygen atoms in the polyether chain of 3HQ. A C−H···π interaction between the protons of the inside

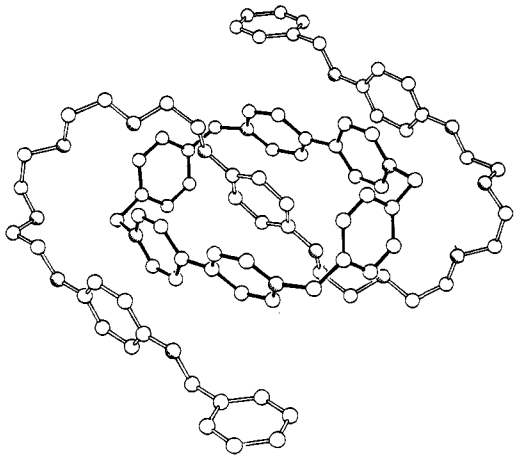

Figure 23. X-ray crystal structure of [3HQ·BBIPYBIXYCY][PF_6]$_4$. Ball-and-stick representation.

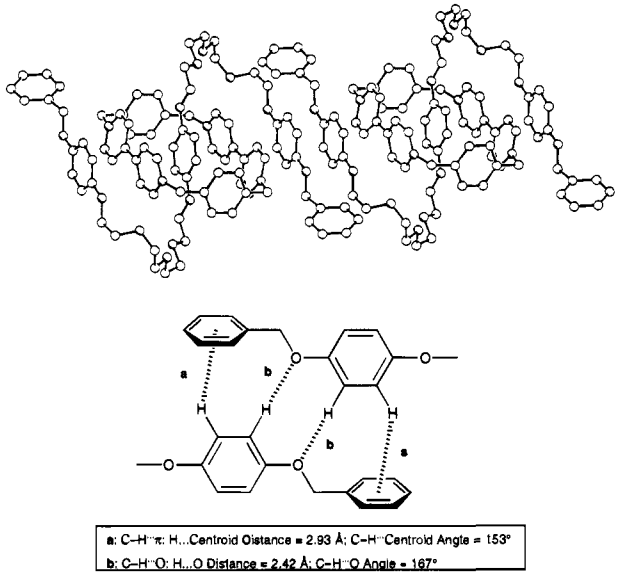

Figure 24. (a) Stepped array of [3HQ·BBIPYBIXYCY][PF_6]$_4$ in the solid state. (b) Schematic representation of the cooperative C−H···O interactions in the stepped array of [3HQ·BBIPYBIXYCY][PF_6]$_4$ in the solid state.

hydroquinone ring of 3HQ and the aromatic ring of the *p*-xylyl spacer (C−H···centroid distance 2.82 Å) is also observed. The [2]pseudorotaxanes form a stepped array in the solid state (Figure 24a) which is stabilized by cooperative C−H···O and C−H···π interactions (Figure 24b) between the alongside hydroquinone rings and the aromatic rings of the benzyl ether groups in adjacent [2]pseudorotaxanes which lie in an almost orthogonal (interplanar angle 76°) arrangement within the crystal lattice.

[3NP·BBIPYBIPXYCY][PF_6]$_4$. The solid state structure (Figure 25) of [3NP·BBIPYBIPXYCY][PF_6]$_4$ reveals $\pi-\pi$ stacking interactions between both the inside and alongside 1,5-dioxynaphthalene rings of 3NP and the bipyridinium residues of the [BBIPYBIPXYCY]$^{4+}$ cyclophane (mean interplanar separation 3.40 Å). In addition, there are other C−H···O and C−H···π interactions which stabilize the overall structure of the [2]pseudorotaxane. Weak C−H···O hydrogen bonds are observed between both the benzylic methylene group (C−H···O distance 2.82 Å, C−H···O angle 152°) and the aromatic ring of the *p*-xylyl unit (C−H···O distance 2.69 Å, C−H···O angle 139°). In addition, there are also close contacts between α-bipyridinium protons in the [BBIPYBIPXYCY]$^{4+}$ cyclophane and the second and third oxygen atoms in the polyether chain of 3NP (second O atom: C−H···O distance 2.58 Å, C−H···O angle 141°; third O atom: C−H···O distance 2.73 Å, C−H···O angle 149°). There is also an exceptionally short contact between the H4 and H8 of the inside 1,5-dioxynaphthalene ring of 3NP and the aromatic ring of the *p*-xylyl spacer (C−H··· centroid distance 2.54 Å). The [2]pseudorotaxanes form a continuous layered array (Figure 26)—adjacent [2]pseudorotaxanes are turned by 90° with respect to their neighbors in the sheet. The continuous array is supported by face-to-face $\pi-\pi$ interactions between the alongside 1,5-dioxynaphthalene ring of one [2]pseudorotaxane and the *p*-xylyl spacer of the [BBIPYBIPXYCY]$^{4+}$ cyclophane of the adjacent [2]pseudorotaxane (mean interplanar separation 3.55 Å).

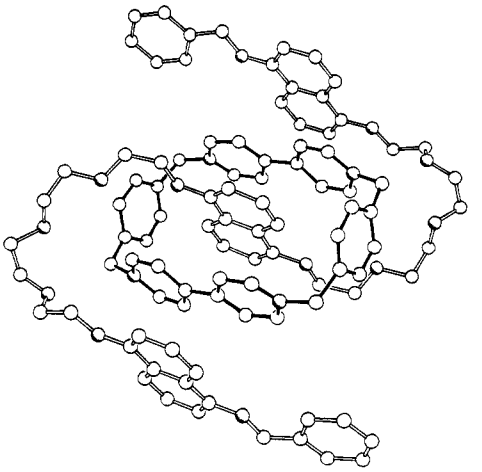

Figure 25. X-ray crystal structure of [3NP·BBIPYBIXYCY][PF_6]$_4$. Ball-and-stick representation.

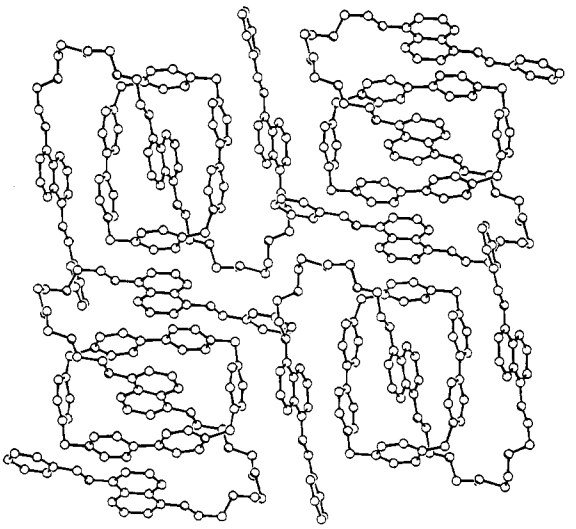

Figure 26. Layered array of the [2]pseudorotaxane [3NP·BBIPYBIXYCY][PF_6]$_4$ in the solid state. Ball-and-stick representation.

B. A System Containing Four π-Donors. The four π-donor system 4HQ, containing four hydroquinone rings linked by three tetraethylene glycol chains, was synthesized by two different routes (Scheme 12) using identical methodology employed for the synthesis of the three π-donor systems.

The mixing of equimolar quantities of [BBIPYBIPXYCY]-[PF_6]$_4$ and 4HQ in MeCN solution at room temperature results in the instantaneous appearance of a reddish-orange color in the solution. The intense color of the sample arises from the appearance of a CT absorption band in the visible region of the spectrum, characteristic of the formation of the complex [4HQ·-BBIPYBIPXYCY][PF_6]$_4$. The 1:1 stoichiometry of the complex was established,[39] and a K_a value of 3010 M^{-1} obtained by means of a spectrophotometric titration performed in MeCN

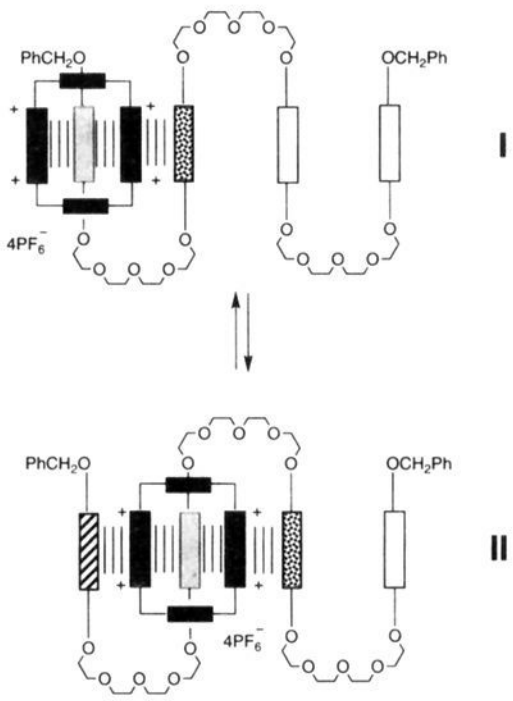

Figure 27. The two possible translational isomers (I and II) of [4HQ·BBIPYBIXYCY][PF_6]$_4$.

solution at 300 K. This stability constant corresponds to a $-\Delta G^\circ$ value 4.77 kcal mol^{-1} at 300 K.

Examination of the 400 MHz ^{1}H NMR spectrum of [4HQ·BBIPYBIPXYCY][PF_6]$_4$ recorded in CD_3CN at 293 K reveals line broadening of the resonances of the hydroquinone ring protons, indicating exchange of the [BBIPYBIPXYCY]$^{4+}$ cyclophane between hydroquinone rings within 4HQ, or, indeed, exchange with [BBIPYBIPXYCY]$^{4+}$ in free solution. On cooling the solution down from 293 to 233 K, there is considerable sharpening of all of the resonances in the spectrum. Two resonances are observed for both the α-CH protons (δ 8.79 and 8.76; $\Delta\delta$ −0.07 and −0.10 ppm) and the β-CH (δ 7.55 and 7.51; $\Delta\delta$ −0.61 and −0.65 ppm). By contrast, only one resonance is observed (δ 7.68; $\Delta\delta$ +0.16 ppm) for the aromatic C_6H_4 protons of [BBIPYBIPXYCY]$^{4+}$. The observation of two resonances for the α-CH and β-CH protons arises not from a lowering of symmetry by inclusion of the hydroquinone ring (cf. the inclusion of a 1,5-dioxynaphthalene ring) within the cavity of [BBIPYBIPXYCY]$^{4+}$ but rather from a constitutional asymmetry generated by the stacking of the aromatic rings within the [2]pseudorotaxane. This phenomenon can be best understood by considering the two possible translational isomers (Figure 27) of [4HQ·BBIPYBIPXYCY][PF_6]$_4$. In both translational isomers I and II, there are two environments for the 4,4′-bipyridinium units of [BBIPYBIPXYCY]$^{4+}$ within the $\pi-\pi$ stack. Thus, if exchange is slow on the ^{1}H NMR time scale, we would expect to observe two sets of resonances for each of the α-CH and β-CH protons of [BBIPYBIPXYCY]$^{4+}$. Although there are formally two environments for both the *N*-methylene and aromatic C_6H_4 protons of [BBIPYBIPXYCY]$^{4+}$, the constitutional asymmetry manifests itself in the ^{1}H NMR spectrum only in the resonance for the *N*-methylene protons. These protons resonate as an AB system (δ 5.61 and 5.56; $\Delta\delta$ −0.13 and −0.18 ppm) at 233 K. In order to decide which of the two translational isomers shown in Figure 27 is the one observed in solution at 233 K, we must consider the behavior of the resonances for the hydroquinone ring protons as the temperature is decreased. At 293 K, 12 of the 16 hydroquinone protons resonate as two broad signals in the region δ 6.45 to 6.75. However, at 233 K the resonances for 12 of the 16 hydroquinone ring protons now appear in three discrete signals in the range δ 6.20 to 6.90. Eight of the hydroquinone ring protons resonate as two AA′BB′ systems (δ 6.55 and 6.33; δ 6.37 and 6.24). The remaining four protons from this group of 12 resonate as a broad signal in the range δ 6.65 to 6.90. The resonance for the protons on the included hydroquinone ring has been located by means of a saturation transfer experiment performed in CD_3CN solution at 260 K. Irradiation of the broad signals in the range δ 6.30 to 6.80 produced some transfer of saturation to a broad resonance located at δ 3.40, identifying this resonance as that for these protons. Examination of the available ^{1}H NMR spectroscopic data strongly implies that the superstructure of [4HQ·BBIPYBIPXYCY][PF_6]$_4$ in CD_3CN solution at 233 K is that of translational isomer II in Figure 27. The spectrum of this translational isomer would be expected to display a resonance for one set of hydroquinone ring protons (unshaded in Figure 27) which resonate close to their chemical shift in free 4HQ. We can assign the broad signal, which integrates for 4H, in the range δ 6.65 to 6.90, to the protons on this hydroquinone ring. There are two hydroquinone rings in translational isomer II which enter into a $\pi-\pi$ stacking interaction with the [BBIPYBIPXYCY]$^{4+}$ cyclophane (striped and dotted in Figure 27). The two AA′BB′ systems observed in the range δ 6.20 to 6.60 may be assigned to the protons on these two hydroquinone rings. Finally, the resonance observed at 260 K by saturation transfer at δ 3.40 may be assigned to the protons of the included hydroquinone ring (shaded in Figure 27). The appearance of two equal intensity singlets (δ 4.91 and 4.82) for the benzylic methylene protons is also consistent with the proposed superstructure for [4HQ·BBIPYBIPXYCY][PF_6]$_4$.

The activation barrier to the exchange of degenerate translationally isomeric states of II within the [2]pseudorotaxane was estimated by application of variable temperature 400 MHz ^{1}H NMR spectroscopy. Observation of the coalescence of the signals, corresponding to the β-CH protons of [BBIPYBI-

Scheme 12

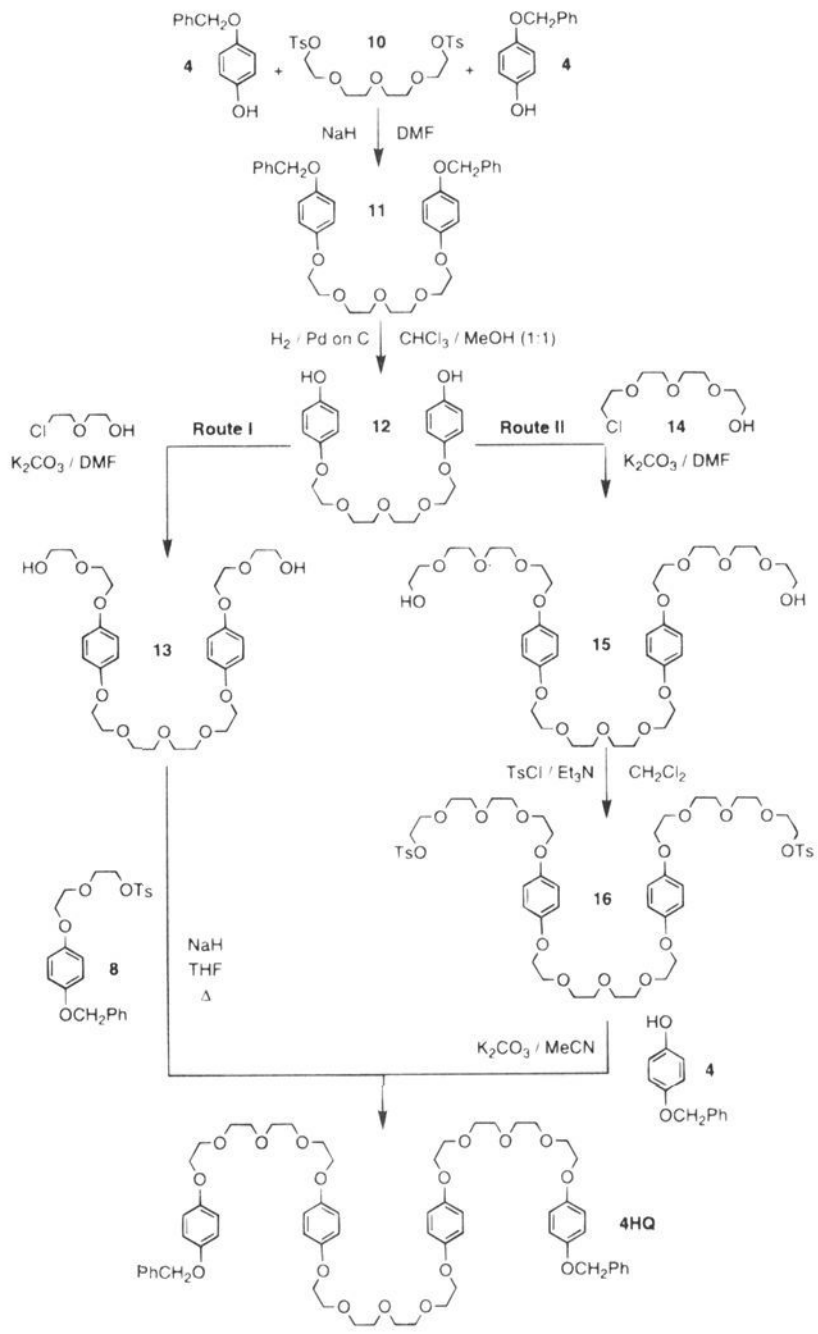

Table 13. Thermodynamic Parameters for the Equilibration of the Degenerate States of Translational Isomers II in [4HQ·BBIPYBIXYCY][PF_6]$_4$

probe protons	$\Delta\nu$ (Hz)	k_C (s^{-1})[a]	T_C (K)[b]	$\Delta G_C^{\ddagger}$ (kcal mol^{-1})[c]
β-CH	17.5	39	251	12.8
Ph-CH_2	36.0	80	261	13.0

[a] Calculated from the approximate expression, $k_C = \pi(\Delta\nu)/2^{1/2}$. [b] Temperature of the spectrometer probe at coalescence, measured using an electronic thermometer. [c] Calculated using the Eyring equation (ref 29).

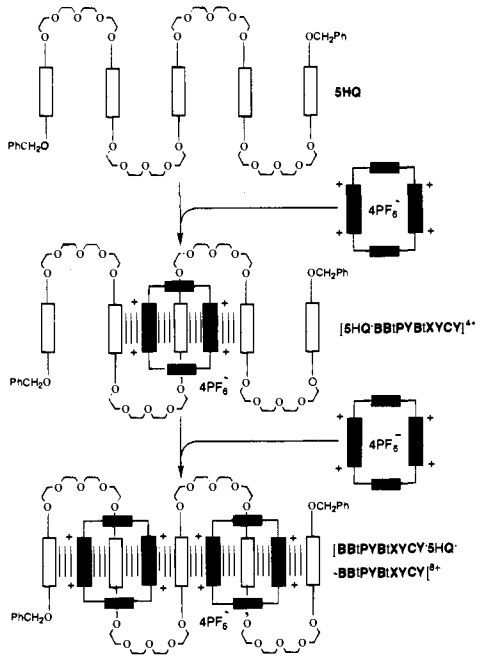

Figure 28. The consecutive self-assembly of [5HQ·BBIPYBIXYCY]-[PF_6]$_4$ followed by [BBIPYBIXYCY·5HQ·BBIPYBIXYCY][PF_6]$_8$.

PXYCY]$^{4+}$ and the benzylic methylene protons of 4HQ (Table 13), affords an average value for $\Delta G_c^{\ddagger}$ of 12.9 kcal mol^{-1}.

The self-assembly of the [2]pseudorotaxane [4HQ·-BBIPYBIPXYCY][PF_6]$_4$ demonstrates that this strategy for the construction of large, ordered superstructures in solution can be extended to systems which contain more than the minimum number of π-donors to achieve a completely π-stacked structure. In CD_3CN solution at 233 K, [4HQ·BBIPYBIPXYCY][PF_6]$_4$ adopts exclusively the superstructure which offers maximum $\pi-\pi$ stacking interactions, i.e., translational isomer II.

C. A System Containing Five π-Donors. The five π-donor system 5HQ, containing five hydroquinone rings separated by four tetraethylene glycol chains, was synthesized from 3HQ (Scheme 13) in three steps. We envisaged that 5HQ might self-assemble (Figure 28) in the first instance with 1 equiv of the [BBIPYBIPXYCY]$^{4+}$ cyclophane, affording a [2]pseudorotaxane [5HQ·BBIPYBIPXYCY]$^{4+}$, and then with another equivalent [BBIPYBIPXYCY]$^{4+}$ cyclophane, forming a [3]-pseudorotaxane [BBIPYBIPXYCY·5HQ·BBIPYBIPXYCY]$_2^{8+}$.

When 5HQ is mixed in acetone solution with an equimolar proportion of [BBIPYBIPXYCY][PF_6]$_4$, a deep orange color develops as the tetracationic cyclophane, which is sparingly soluble in acetone, slowly dissolves. The presence of a CT band, centered on 468 nm, is characteristic of the formation of the [2]pseudorotaxane [5HQ·BBIPYBIPXYCY][PF_6]$_4$. Evaporation of the solvent from the sample gave a reddish-orange glassy solid which was subjected to analysis by FAB mass spectrometry. Two peaks were observed at *m/z* 2317 and 2172, corresponding to the loss of one and two PF_6^- counterions, respectively, from the [2]pseudorotaxane [5HQ·

Scheme 13

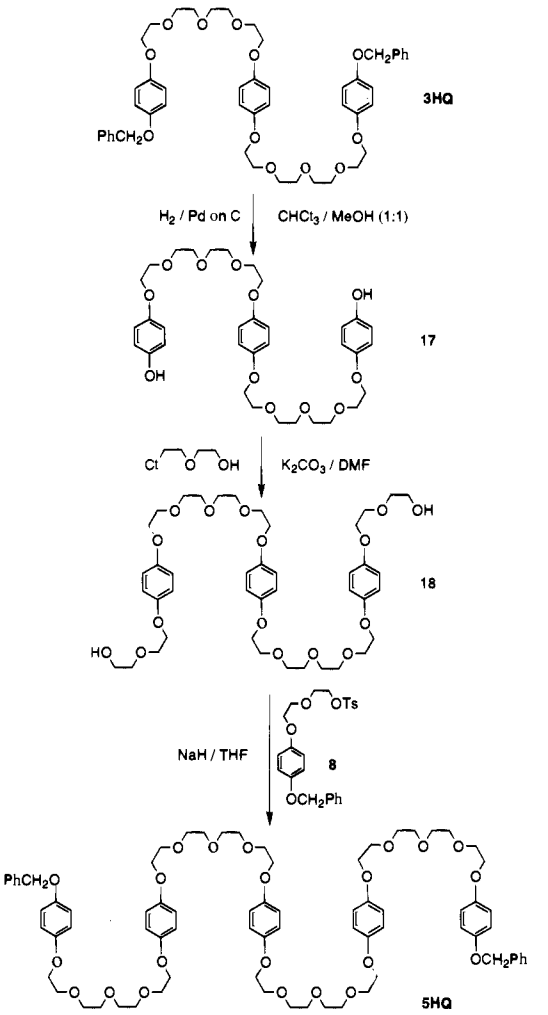

BBIPYBIPXYCY][PF_6]$_4$. The peak observed at *m/z* 2055 corresponds to the loss of one PF_6^- counterion from the same [BBIPYBIPXYCY]$_2$[PF_6]$_8$ cluster observed for the smaller [2]-pseudorotaxanes.

The 400 MHz ^{1}H NMR spectrum of [5HQ·BBIPYBIPXYCY]-[PF_6]$_4$, recorded in CD_3COCD_3 at 293 K, is characterized by extensive line broadening as a result of exchange between different species in solution which is becoming slow on the ^{1}H NMR time scale. On cooling the solution down to 233 K, the spectrum becomes considerably sharper. The most notable feature of the ^{1}H NMR spectrum recorded at 233 K is the appearance of two resonances for the benzylic methylene protons of *unequal* intensity. At room temperature, the benzylic methylene protons resonate as one singlet at δ 4.98, but, on cooling down to 233 K, broadening of this single resonance is observed, followed by the appearance of the two singlets of unequal intensity. The hydroquinone proton resonances undergo considerable line sharpening as the temperature is lowered from 293 K to 233 K. At 233 K, resonances corresponding to hydroquinone ring protons are observed in three regions of the spectrum. A group of resonances corresponding to two of the five hydroquinone rings in 5HQ is observed in the range δ 6.70 to 6.90, while resonances arising from another two of the five hydroquinone rings in 5HQ are observed in the range δ 6.20 to 6.60, and finally a broad resonance at δ 3.65, which accounts for the last of the five hydroquinone rings of 5HQ, has been identified by a saturation transfer experiment performed at 260 K. Further, the presence of the three resonances, which are observed at 233 K for the α-CH and β-CH protons of the [BBIPYBIPXYCY]$^{4+}$ component of the [2]pseudorotaxane, was

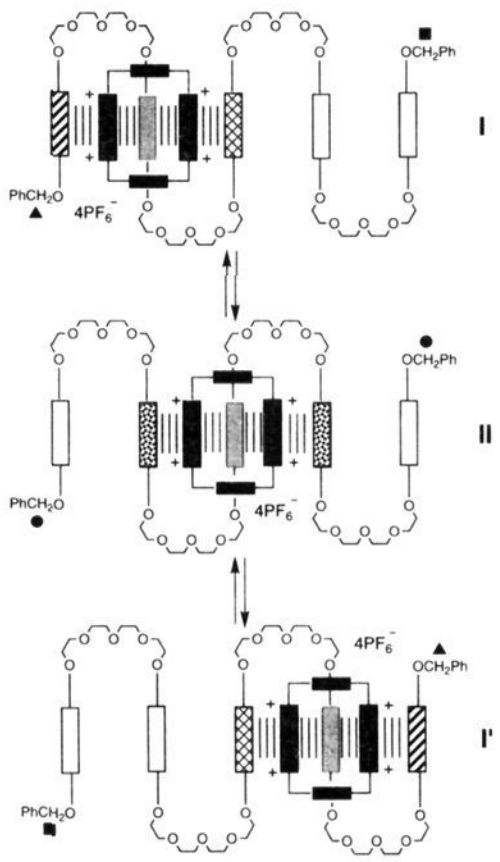

Figure 29. The possible translational isomers (I/I′ and II) of [5HQ·BBIPYBIXYCY][PF_6]$_4$.

confirmed by an $^1H-^1H$ COSY experiment performed in CD_3COCD_3 at 233 K, three cross peaks being observed for the spin–spin relationship between the α-CH and β-CH protons. Decoupling difference experiments performed at 233 K indicate that the hydroquinone ring protons resonating in the region δ 6.20 to 6.60 are, in fact, three overlapping AA′BB′ systems. In addition, irradiation of the hydroquinone ring proton resonances in the range δ 6.70 to 6.90 in an NOE difference experiment produces a positive enhancement in the resonances for the benzylic methylene protons, indicating that the hydroquinone rings, which resonate in the range δ 6.70 to 6.90, are associated with the termini of the 5HQ molecule. All of these observations may be rationalized by considering (Figure 29) all the possible translational isomers for the [2]pseudorotaxane [5HQ·BBIPYBIPXYCY][PF_6]$_4$. At 233 K in CD_3COCD_3 solution, the [2]pseudorotaxane exists as a mixture of two translationally isomeric superstructures (I/I′ and II in Figure 29) which are in slow exchange on the ^1H NMR time scale. There are three classes of hydroquinone ring present in the superstructures shown in Figure 29. The hydroquinone rings which are unshaded are located in positions remote from the [BBIPYBIPXYCY]$^{4+}$ cyclophane, and so the protons on these hydroquinone rings would be expected to resonate close to the chemical shift (δ 6.80) of the hydroquinone rings in free 5HQ. The second class of hydroquinone rings are those which enter into a $\pi-\pi$ stacking interaction with the external π-surface of the 4,4′-bipyridinium dications of [BBIPYBIPXYCY]$^{4+}$ (striped, cross-hatched, and dotted in Figure 29). Thus, the resonances for these protons should be shifted to higher field as a result of the effect of the 4,4′-bipyridinium dication ring current on the hydroquinone rings. The final kinds of hydroquinone rings are those included within the cavity of the [BBIPYBIPXYCY]$^{4+}$ cyclophane (shaded in Figure 29). The resonances observed for the hydroquinone ring protons in the 400 MHz ^1H NMR spectrum of [5HQ·BBIPYBIPXYCY][PF_6]$_4$ can now be assigned. The signals observed in the region δ 6.70 to 6.90 are the resonances corresponding to the unshaded hydroquinone rings in Figure 29. The three AA′BB′ systems, observed in the range δ 6.20 to 6.60, arise from the resonances of the protons on the striped, cross hatched, and dotted hydroquinone rings in Figure 29 which enter into a $\pi-\pi$ stacking interaction with [BBIPYBIPXYCY]$^{4+}$. Finally, the broad resonance, observed

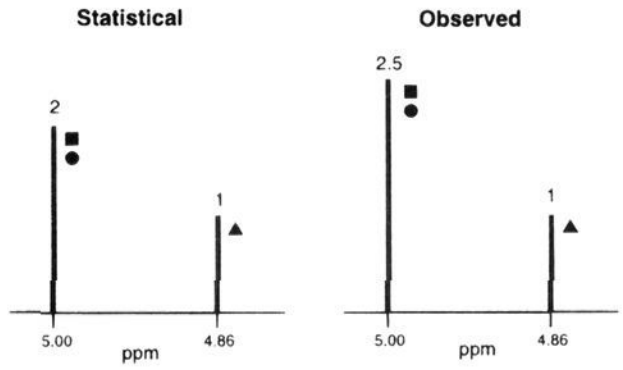

Figure 30. The statistical versus the observed integrated ratios for the benzylic methylene protons of 5HQ in [5HQ·BBIPYBIXYCY][PF_6]$_4$ in CD_3COCD_3 solution below 253 K.

in the saturation transfer experiment, can be assigned to the protons on the hydroquinone ring, shaded in Figure 29, which is included within the cavity of the [BBIPYBIPXYCY]$^{4+}$ cyclophane. Further, the translational isomer I/I′ and II provide three constitutionally different environments for the bipyridinium dications of [BBIPYBIPXYCY]$^{4+}$ within the $\pi-\pi$ stacked portion of the superstructure, which is in accord with the resonances observed for the protons on these units in the ^1H NMR spectrum at 233 K. Although there are three constitutionally different benzylic methylene environments (▲, ●, and ■) within I/I′ and II, there are only two markedly different magnetic environments. One set of benzylic methylene protons (▲) are attached to a hydroquinone ring which is associated via a $\pi-\pi$ interaction with the [BBIPYBIPXYCY]$^{4+}$ cyclophane. It is therefore reasonable to expect the resonance for these protons to experience some upfield shift as a result of the shielding effect of the tetracationic cyclophane. We can therefore assign the resonance observed at δ 4.86 to these benzylic methylene protons (▲). The other two sets of benzylic methylene protons (● and ■), however, lie in locations remote from the influence of [BBIPYBIPXYCY]$^{4+}$ and would therefore be expected to resonate close to the chemical shift of these protons in free 5HQ. Thus, we may assign the resonance at δ 5.00 to these benzylic methylene protons (● and ■).

There appears to be some enhancement of the population of translational isomer II relative to that of the degenerate pair I/I′ as judged from the integration of the benzylic methylene proton resonances. The signal observed at δ 5.00 has an integrated area[40] some 2.5 times that of the signal resonating at δ 4.86. If the populations of the translational isomers I/I′ and II were distributed statistically, the expected integral ratio for these signals is 2:1. The enhancement of the resonance at δ 5.00 must therefore arise from a surplus of translational isomer II since this translational isomer contains benzylic methylene protons (■) which appear only in this resonance (Figure 30), while the degenerate pair (I/I′) contains benzylic methylene protons (▲ and ●) which contribute to both resonances. Further evidence for this nonstatistical population of translationally-isomeric states comes from an iterative computer line shape analysis[41] of the exchange broadened resonance for the benzylic methylene protons at 273 K. This analysis affords a good fit with respect to experimental data only when a population of 40% is assigned to translational isomer II and 30% to each of the degenerate pair I and I′. Table 14 summarizes the results of the analysis. A much poorer match with the experimental data is obtained when the populations of the translational isomers are allowed to assume their statistical value of $33^1/_3$%. The reason for this very slight preference for the more symmetrical isomer is not obvious.

When 5HQ was mixed in acetone solution with 2 molar equiv of [BBIPYBIPXYCY][PF_6]$_4$, a deep red color developed rapidly, as a result of the appearance of a CT absorption band in the visible region of the spectrum centered on 468 nm and characteristic of the formation of a complex between hydro-

Table 14. Calculated[a] Best-Fit Thermodynamic Parameters for the Equilibration of I/I′ and II in [5HQ·BBIPYBIXYCY][PF_6]$_4$

process	k_{273}/s^{-1} [b]	$\Delta G^{\ddagger}_{273}$ (kcal mol^{-1})[c]
I/I′ → II	57	13.3
II → I/I′	43	13.4

[a] Calculated from an iterative least-squares line shape analysis (ref 27) of the benzylic methylene region of the ^{1}H NMR spectrum of [5HQ·BBIPYBIXYCY][PF_6]$_4$ at 273 K in CD_3COCD_3. [b] First order rate constant for the exchange process at 273 K. [c] Free energy of activation for the exchange process at 273 K.

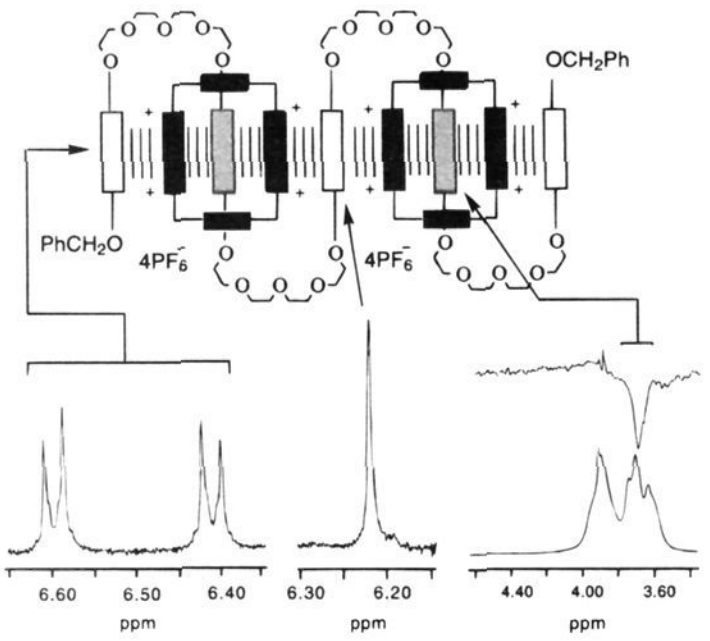

Figure 31. Partial 400 MHz ^{1}H NMR spectra, recorded in CD_3COCD_3, of [BBIPYBIXYCY·5HQ·BBIPYBIXYCY][PF_6]$_8$ showing the $\pi-\pi$ stacked structure of the [3]pseudorotaxane and the behavior of the signals corresponding to the protons on the hydroquinone rings of 5HQ at 233 K.

quinone rings and [BBIPYBIPXYCY]$^{4+}$. The simplicity of the ^{1}H NMR spectrum at 233 K of [BBIPYBIPXYCY·5HQ·-BBIPYBIPXYCY][PF_6]$_8$ in CD_3COCD_3 requires that the [3]-pseudorotaxane must exist in solution as the highly symmetric completely π-stacked superstructure (Figure 31). Within the completely π-stacked superstructure of [BBIPYBIPXYCY·-5HQ·BBIPYBIPXYCY][PF_6]$_8$, the hydroquinone rings fall into three categories. There are two hydroquinone rings at the termini of the 5HQ chain (unshaded in Figure 31) which interact with only one 4,4′-bipyridinium dication of the [BBIPYBI-PXYCY]$^{4+}$ cyclophanes. The protons on these hydroquinone rings resonate as an AA′BB′ system (δ 6.60 and 6.42) in the ^{1}H NMR spectrum recorded at 233 K (Figure 31, leftmost spectrum). The central hydroquinone ring of the 5HQ chain interacts dynamically with two 4,4′-bipyridinium dications of two separate [BBIPYBIPXYCY]$^{4+}$ cyclophanes. The protons on these hydroquinone rings resonate as a singlet at δ 6.22 at 233 K (Figure 31, center spectrum). Finally, two hydroquinone rings are included within the cavities of the two [BBIPYBI-PXYCY]$^{4+}$ cyclophanes present in the structure. The resonances for the protons on these rings may be identified by means of a saturation transfer experiment (Figure 31 rightmost spectrum) performed in CD_3COCD_3 solution at 263 K. Irradiation of the signals in the range δ 6.40 to 6.60 resulted in some transfer of saturation to a broad resonance centered on δ 3.70. This experiment also revealed a strong positive enhancement (NOE) of the signal for the benzylic methylene protons at δ 4.85, confirming the assignment of the AA′BB′ system in the range δ 6.40 to 6.60 as arising from the hydroquinone rings at the termini of the 5HQ chain. In addition, a ^{1}H−^{1}H COSY experiment, performed at 233 K, revealed that the α-CH and β-CH protons of the [BBIPYBIPXYCY]$^{4+}$ component each resonate as two doublets at this temperature. Interestingly, on cooling the CD_3COCD_3 solution from 233 down to 193 K, a strong upfield shift is observed[42] in the resonance for protons on the central hydroquinone ring (δ 6.22 at 233 K becomes δ 6.00 at 193 K) of 5HQ, indicating a stronger dynamic interaction with the 4,4′-bipyridinium dications located toward the center of the superstructure.

The spontaneous formation of the [3]pseudorotaxane [BBIPYBIPXYCY·5HQ·BBIPYBIPXYCY][PF_6]$_8$ demonstrates that it is possible to self-assemble a superstructure, which is reasonably large at a termolecular level, simply by employing two different molecular components which, by virtue of their mutual recognition properties, are capable of organizing themselves in a delicately controlled and stepwise manner. Assuming the completely $\pi-\pi$ stacked superstructure (Figure 31) for [BBIPYBIPXYCY·5HQ·BBIPYBIPXYCY][PF_6]$_8$ in solution, the [3]pseudorotaxane is ca. 3.0 nm long and ca. 1.5 nm in diameter, with a molecular weight of 3562, i.e., it is a superstructure on the nanometer scale, yet it forms spontaneously in a highly ordered manner—without the need for external templates—on simply mixing the components under the appropriate conditions. Such systems may be viewed as prototypes for a more general class of tertiary structures assembled by this kind of modular approach.

Conclusion. The successful self-assembly of a range of [2]-catenanes and [*n*]pseudorotaxanes, with variable constitutions, demonstrates the efficiency and utility of self-assembly strategies, based on the molecular recognition displayed between π-electron rich and π-electron deficient subunits, for the construction of highly ordered superstructures which are either stabilized only by noncovalent bonding interactions—the [*n*]-pseudorotaxanes—or additionally by mechanical interlocking—the [2]catenanes. The use of "intelligent" components which have mutually complementary recognition features is paramount to the success of self-assembly strategies aimed at the fabrication of synthetic nanometer-scale structures.

Experimental Section

General Methods. Reagents were purchased from Aldrich Chemical Company and were used as received without purification. Solvents were used as supplied, with the exception of the following. Dimethylformamide (DMF) was distilled from calcium hydride under reduced pressure, acetonitrile (MeCN) was distilled from P_2O_5, and tetrahydrofuran (THF) was distilled under nitrogen from sodium benzophenone ketyl. Tetraethylene glycol bistosylate,[43] BHEEPB, BPP34C10, [BBIPYPXY][PF_6]$_2$, [BBIPYBIPXYCY][PF_6]$_4$, [BBIPYMXY][PF_6]$_2$, and [BBIPYBIMXYCY][PF_6]$_4$ were prepared using published procedures.[12,18c] Reactions involving the use of ultrahigh pressures were carried out in Teflon vessels using a custom-built ultrahigh pressure press manufactured by PSIKA Pressure Systems Limited of Glossop in the UK. Thin-layer chromatography (TLC) was performed on aluminium sheets (10 × 5 cm) coated with Merck 5735 Kieselgel 60F. Developed plates were air-dried, scrutinized under a UV lamp, and, if necessary, then either sprayed with cerium(IV)sulfate-sulfuric acid reagent and heated to ca. 100 °C or developed in an iodine tank. Kieselgel 60 (0.040−0.063 mm mesh, Merck 9385) was used to perform column chromatography. Microanalyses were performed by the University of Birmingham Microanalytical Service. Melting points were determined on an Electrothermal 9200 melting point apparatus and are uncorrected. Mass spectra (MS) were obtained from either Kratos Profile or MS80RF instruments, the latter being equipped with a fast atom bombardment (FAB) facility (using a Krypton primary atom beam in conjunction with a 3-nitrobenzyl alcohol matrix). FABMS were recorded in the positive-ion mode at a scan speed of 30s per decade. Electrospray positive mass spectra (ESMS) were obtained employing a VB Prospec triple focusing magnetic sector instrument operating at 4 kV accelerating voltage and fitted with an electrospray ion source. ^{1}H Nuclear magnetic resonance (NMR) spectra were recorded on Jeol FX-90Q (90 MHz), Bruker AC300 (300 MHz), or Bruker AMX400 (400 MHz) spectrometers (using the deuterated solvent as lock and residual solvent or tetramethylsilane as internal reference). ^{13}C NMR spectra were

recorded on a Bruker AC300 (75 MHz) or AMX 400 (100 MHz) spectrometers using a JMOD pulse sequence (assuming $^1J_{CH}$ = 143 Hz). For all the catenanes displaying translational isomerism resonances and integrals for the ^{1}H and ^{13}C NMR spectra are quoted for the major isomer, which is present in >95% in solution.

1,4,7,10,13-Pentaoxa[13]metacyclophane (MP16C5),[21] 1,4,7,10,-13,20,23,26,29,32-decaoxa[13.13]metacyclophane (BMP32C10),[19] and 1,4,7,10,13,20,23,26,29,32,39,42,45,48,51-pentadecaoxa-[13.13.13]-metacyclophane (TMP48C15). Cesium carbonate (40.56 g, 124 mmol) was suspended in dry DMF (500 mL), and the suspension was degassed with a flow of nitrogen for 15 min, during which time cesium tosylate (11.06 g, 36.4 mmol) and tetrabutylammonium iodide (1.53 g, 4.1 mmol) were added. The temperature of the mixture was raised to 80 °C with vigorous stirring, and a degassed solution of tetraethylene glycol bistosylate (16.55 g, 32.9 mmol) and 1,3-dihydroxybenzene (3.62 g, 32.9 mmol) in dry DMF (150 mL) was added over 3 days. After a further 2 days stirring at 80 °C under nitrogen, the reaction mixture was filtered at the pump, and the solid was washed with DMF (100 mL). After evaporation of the solvent in vacuo, the mixture was partitioned between PhMe (200 mL) and H_2O (200 mL). The aqueous layer was washed with PhMe (200 mL), and the combined organic layers were dried ($MgSO_4$). Evaporation of the solvent afforded a residue which was subjected to column chromatography [SiO_2, Me_2CO−hexane (2:3)] to yield in order of elution from the column—(a) MP16C5 as a colorless oil (4.80 g, 54%): EIMS 268 (M^+); ^{1}H NMR [$CDCl_3$, 300 MHz] δ 3.52−3.59 (4H, m), 3.60−3.65 (4H, m), 3.74 (4H, t), 4.24 (4H, t), 6.47−6.54 (2H, m), 7.04−7.12 (2H, m); ^{13}C NMR [$CDCl_3$, 75 MHz] δ 68.8, 70.4, 70.7, 70.8, 103.8, 110.1, 129.4, 160.3; (b) BMP32C10 as a white solid (0.75 g, 8.4%): mp 72−74 °C; FABMS 536 (M^+); ^{1}H NMR [$CDCl_3$, 300 MHz] δ 3.60−3.75 (16H, m), 3.81 (8H, t), 4.06 (8H, t), 6.44−6.57 (6H, m), 7.10 (2H, t); ^{13}C NMR [$CDCl_3$, 75 MHz] δ 67.5, 69.7, 70.7, 70.9, 101.9, 107.2, 129.8, 160.0; and (c) TMP48C15 as a white solid (0.15 g, 1.7%): mp 54−56 °C; FABMS 805 ([M + H]$^+$); ^{1}H NMR [$CDCl_3$, 300 MHz] δ 3.64−3.74 (24H, m), 3.82 (12H, t), 4.08 (12H, t), 6.47−6.52 (9H, m), 7.09−7.18 (3H, m); ^{13}C NMR [$CDCl_3$, 75 MHz] δ 67.5, 69.7, 70.7, 70.9, 101.9, 107.2, 129.8, 160.0.

1,3-Bis[2-(2-hydroxyethoxy)ethoxy]benzene (BHEEMB). 1,3-Dihydroxybenzene (13.0 g, 118.1 mmol) was added directly to a degassed stirred suspension of K_2CO_3 (50.0 g, 362.6 mmol) in dry MeCN (300 mL) which was heated to 50 °C in a nitrogen atmosphere. After an additional 20 min, 2-(2-chloroethoxy)ethanol (40.1 g, 326.6 mmol) was added dropwise over 30 min. The reaction mixture was heated under reflux and stirred for a further 7 days. After cooling to room temperature, the reaction mixture was filtered, and the solid residue was washed with DMF (150 mL) and EtOAc (100 mL). The solvent was removed in vacuo, and the residue was partitioned between CH_2Cl_2 (250 mL) and aqueous 10% NaOH (150 mL). The organic phase was washed with aqueous 10% NaOH (100 mL) and saturated aqueous NaCl (150 mL) and then dried ($MgSO_4$). The solvent was removed in vacuo to leave a light brown solid. Column chromatography [SiO_2: Me_2CO−hexane (1:1)] afforded BHEEMB as a fine white solid (14.2 g, 43%): mp 48−49 °C; EIMS 286 (M^+); ^{1}H NMR [$CDCl_3$, 300 MHz] δ 3.65−3.70 (4H, m), 3.74−3.79 (4H, m), 3.84−3.88 (4H, m), 4.10−4.15 (4H, m), 6.51−6.56 (3H, m), 7.14−7.21 (1H, m); ^{13}C NMR [$CDCl_3$, 75 MHz] δ 61.8, 67.5, 69.7, 72.6, 101.9, 107.3, 129.9, 159.9. Anal. ($C_{14}H_{22}O_6$) C, H.

1,4-Bis{2-(2-(2-(2-toluene-*p*-sulfonylethoxy)ethoxy)ethoxy)ethoxy}-benzene (1). 1,4-Dihydroxybenzene (2.5 g, 22.6 mmol) was added as a solid to a stirred suspension of K_2CO_3 (62.8 g, 454.6 mmol) in dry MeCN (450 mL) heated at 60 °C under nitrogen. After an additional 30 min, a solution of tetraethylene glycol bistosylate (68.9 g, 137.3 mmol) in dry MeCN (150 mL) was added dropwise over 15 min. The reaction mixture was brought to reflux and stirred for a further 3 days. After cooling down to room temperature, the reaction mixture was filtered, and the solid residue was washed with EtOAc (100 mL). The solvent was removed under vacuum, and the residue was partitioned between PhMe (250 mL) and aqueous 10% NaOH (300 mL). The organic phase was washed with H_2O (2 × 400 mL), dried ($CaCl_2$), and concentrated in vacuo. Column chromatography [SiO_2:CH_2Cl_2−EtOAc (95:5)] afforded **1** as a yellow oil (7.1 g, 41%): FABMS 770 (M^+); ^{1}H NMR [$CDCl_3$, 300 MHz] δ 2.43 (6H, s), 3.47−3.68 (20H, m), 3.74−3.79 (4H, m), 6.85 (6H, s), 7.44−7.48 (4H, m), 7.77−7.82 (4H, m); ^{13}C NMR [$CDCl_3$, 75 MHz] δ 21.6, 68.1, 68.7, 69.3, 69.9, 70.6, 70.7, 70.8, 115.6, 128.0, 129.8, 133.1, 144.8, 153.1. Anal. ($C_{36}H_{50}S_2O_{14}$) C, H.

1,4,7,10,13,20,23,26,29,32-Decaoxa[13]para[13]metacyclophane (PPMP33C10) and 1,4,7,10,13,20,23,26,29,32,39,42,45,48,51,58,61,-64,67,70-eicosaoxa[13]meta[13]para[13]meta[13]paracyclophane (BPPBMP66C20). Following the procedure described for the synthesis of BMP32C10, 1,3-dihydroxybenzene (0.44 g, 4.00 mmol) was added directly to a degassed stirred suspension of Cs_2CO_3 (26.1 g, 80.1 mmol), CsOTs (3.0 g, 13.5 mmol), and tetrabutylammonium iodide (0.4 g, 1.1 mmol) in dry DMF (250 mL), which was heated at 80 °C under nitrogen. After an additional period of 1 h, a degassed solution of **1** (3.0 g, 4.00 mmol) and CsOTs (3.1 g, 13.9 mmol) in dry DMF (150 mL) was added dropwise over 1 h. The temperature of the reaction mixture was increased to 100 °C, and stirring was continued for 2 days. After cooling to room temperature, the reaction mixture was filtered and the solid residue washed with CH_2Cl_2 (100 mL). The combined organic phases were concentrated in vacuo, and the residue, dissolved in CH_2Cl_2 (250 mL), was washed with H_2O (250 mL). The aqueous phase was extracted with CH_2Cl_2 (2 × 150 mL). The combined organic phases were dried ($CaCl_2$) and concentrated in vacuo. Column chromatography [SiO_2: Me_2CO−CH_2Cl_2−hexane (1:0.5:1)] afforded PPMP33C10 as a clear oil (1.1 g, 51%): FABMS 575 ([M + K])$^+$, 559 ([M + Na])$^+$, 536 (M^+); ^{1}H NMR [$CDCl_3$, 300 MHz] δ 3.58−3.66 (16H, m), 3.75−3.83 (8H, m), 3.99−4.08 (8H, m), 6.47−6.50 (2H, m), 6.52−6.53 (1H, d), 6.61 (4H, s), 7.14 (1H, t); ^{13}C NMR [$CDCl_3$, 75 MHz] δ 68.3, 68.9, 70.2, 70.3, 71.3, 71.3, 71.4, 101.9, 107.6, 116.3, 130.5, 154.0, 161.1. Anal. ($C_{28}H_{40}O_{10}$) C, H. BPPBMP66C20 was also afforded as a clear oil (0.23 g, 11%): FABMS 1112 ([M + K]$^+$), 1073 (M^+); ^{1}H NMR [$CDCl_3$, 300 MHz] δ 3.62−3.71 (32H, m), 3.74−3.83 (16H, m), 3.91−4.08 (16H, m), 6.44−6.49 (6H, m), 6.79 (2H, s), 7.07−7.14 (2H, m); ^{13}C NMR [$CDCl_3$, 75 MHz] δ 67.4, 68.1, 68.2, 69.6, 69.7, 70.7, 70.8, 101.5, 107.1, 115.5, 115.7, 129.8, 153.1, 160.0. Anal. ($C_{56}H_{80}O_{20}$) C, H.

9,18,29,38-Tetraazonia[1.1.0]para[1]meta[1.0]paracyclophane Tetrakishexafluorophosphate [BBIPYPXYMXYCY][PF_6]$_4$. 1,4-Bis-(bromomethyl)benzene (0.42 g, 1.59 mmol), [BBIPYMXY][PF_6]$_2$ (1.12 g, 1.59 mmol), and BHEEPB (1.00 g, 3.49 mmol) were dissolved in dry DMF (30 mL), and the reaction mixture was stirred at room temperature for 4 weeks. The reaction mixture was poured into Et_2O (300 mL), and the precipitate was filtered off under gravity. The solid was partitioned between H_2O (100 mL) and CH_2Cl_2 (300 mL), and the aqueous layer was extracted continuously for 5 days with CH_2Cl_2. A saturated solution of NH_4PF_6 (10 mL) was added to the separated aqueous layer, precipitating a white solid, which was filtered and then subjected to column chromatography [SiO_2:MeOH−NH_4Cl (aqueous, 2N)−$MeNO_2$ (7:2:1)]. The fractions containing the products (as monitored by TLC) were concentrated under vacuum and taken up in H_2O, before the hexafluorophosphate salt was precipitated by addition of a saturated aqueous solution of NH_4PF_6. The product was isolated as a white solid (122 mg, 7%): mp > 250 °C; FABMS 955 ([M − PF_6]$^+$), 810 ([M − 2PF_6]$^+$), 665 ([M − 3PF_6]$^+$); ^{1}H NMR [CD_3COCD_3, 300 MHz], δ 6.18 and 6.19 (8H, overlapping s), 7.70 (1H, t), 7.82 (4H, s), 7.89 (1H, s), 7.95 (2H, d), 8.40 (4H, d), 8.45 (4H, d), 9.30−9.39 (8H, overlapping d). Anal. ($C_{36}H_{32}N_4F_{26}P_4$), C, H, N.

{[2]-[1,4,7,10,13,20,23,26,29,32-Decaoxa[13.13]para-cyclophane][9,18,29,38-tetraazonia[1.1.0]para[1]meta[1.0]-paracyclophane]catenane} Tetrakishexafluorophosphate ({[2]-[BPP34C10][BBIPYPXYMXYCY]catenane}[PF_6]$_4$). Method A. 1,4-Bis(bromomethyl)benzene (31 mg, 0.12 mmol), [BBIPYMXY]-[PF_6]$_2$ (80 mg, 0.11 mmol), and BPP34C10 (201 mg, 0.38 mmol) were dissolved in dry DMF (5 mL), and the resulting solution was stirred at room temperature for 7 days. The solvent was removed under vacuum, and the residue was dissolved in a mixture of MeOH−NH_4Cl (aqueous, 2N)−$MeNO_2$−Me_2CO (7:2:1:10) and subjected to column chromatography [SiO_2:MeOH−NH_4Cl (aqueous 2N)−$MeNO_2$ (7:2:1)]. The fractions containing the products (as monitored by TLC) were combined and concentrated under vacuum to give a residue which was dissolved in H_2O. The catenanes were precipitated from these solutions by addition of a saturated aqueous NH_4PF_6 solution. The [2]catenane was isolated as a red solid (74 mg, 40%): mp > 250 °C; FABMS 1636 (M)$^+$, 1491 ([M − PF_6]$^+$), 1346 ([M − 2PF_6]$^+$), 1201 ([M − 3PF_6]$^+$); ^{1}H NMR [CD_3COCD_3, 400 MHz] δ 3.37−3.43 (4H, m), 3.60−3.70

(6H, m), 3.72−3.79 (4H, m), 3.79−3.85 (4H, m), 3.83−4.03 (16H, m), 4.30−4.52 (2H, bm), 6.03 (4H, s), 6.10 (4H, s), 6.27 (4H, s), 7.87 (1H, t), 7.98 (1H, s), 8.04 (4H, s), 8.12−8.20 (6H, m), 8.25 (4H, d), 9.15 (4H, d), 9.27 (4H, d); ^{13}C NMR [CD_3COCD_3, 101 MHz] δ 65.2, 65.7, 67.2, 68.5, 70.5, 70.6, 70.7, 71.1, 71.3, 71.4, 114.4, 116.0, 116.3, 126.1, 126.5, 132.0, 133.3, 134.9, 135.1, 137.8, 145.6, 146.4, 146.9, 151.3, 153.1. Anal. ($C_{64}H_{72}N_4O_{10}F_{24}P_4$) C, H, N. Single crystals, suitable for X-ray crystallography, were grown by vapor diffusion of *i*-Pr_2O into a solution of the catenane in MeCN.

Method B. Using conditions identical to those described in method A, 1,3-bis(bromomethyl)benzene (32 mg, 0.12 mmol), [BBIPYPXY]-$[PF_6]]_2$ (86 mg, 0.12 mmol), and BPP34C10 (211 mg, 0.39 mmol) were dissolved in dry DMF (5 mL), and the resulting solution was stirred at room temperature for 7 days. Workup and column chromatography yielded the [2]catenane (35 mg, 18%) which gave identical analytical data to the products isolated using method A.

Method C. Using a procedure identical to that employed[12] in the high pressure synthesis of {[2]-[BPP34C10]-[BBIPYBIPXYCY]-catenane}$[PF_6]_4$, the {[2]-[BPP34C10]-[BBIPYPXYMXYCY]catenane}-$[PF_6]_4$ was prepared from 1,3-bis(bromomethyl)benzene (52 mg, 0.20 mmol), [BBIPYMXY]$[PF_6]_2$ (132 mg, 0.19 mmol), and BPP34C10 (299 mg, 0.56 mmol) in 59% yield (181 mg). It had identical analytical data to that described for the [2]catenane isolated using method A.

{[2]-[1,4,7,10,13,20,23,26,29,32-Decaoxa[13.13]paracyclophane]-[9,18,29,38-tetraazonia[1]meta[1.0]para[1]meta[1.0]paracyclophane]-catenane} Tetrakishexafluorophosphate ({[2]-BPP34C10]-[BBIPYBIMXYCY]catenane}$[PF_6]_4$). 1,3-Bis(bromomethyl)benzene (48 mg, 0.18 mmol), [BBIPYMXY]$[PF_6]_2$ (128 mg, 0.18 mmol), and BPP34C10 (267 mg, 0.50 mmol) were dissolved in dry DMF (5 mL) in a Teflon high pressure reaction vessel which was subjected to a pressure of 10 kbar for 3 days at 20 °C. Following the purification procedure described above for {[2]-[BPP34C10]-[BIPYPXY-BIPYMXYCY]catenane}$[PF_6]_4$ (method A), the [2]catenane was isolated as a red solid (82 mg, 28%): mp > 250 °C; FABMS 1491 ($[M - PF_6]^+$), 1346 ($[M - 2PF_6]^+$), 1201 ($[M - 3PF_6]^+$); ^{1}H NMR [CD_3COCD_3, 400 MHz, 318 K] δ 3.40−3.44 (4H, m), 3.65−3.69 (4H, m), 3.75−3.90 (16H, m), 3.95−3.99 (4H, m), 4.07−4.11 (4H, m), 4.41 (4H, bs), 6.13 (8H, s), 6.31 (4H, s), 7.87 (2H, t), 8.04 (2H, s), 8.17 (4H, d), 8.23 (8H, d), 9.13 (8H, d); ^{13}C NMR [CD_3COCD_3, 101 MHz] δ 65.4, 67.1, 68.5, 70.5, 70.9, 71.2, 71.3, 114.8, 116.0, 126.1, 132.2, 134.1, 135.0, 146.3, 146.8, 151.5, 153.1. Anal. ($C_{64}H_{72}N_4O_{10}F_{24}P_4$) C, H, N. Single crystals, suitable for X-ray crystallography, were grown by vapor diffusion of *i*-Pr_2O into a solution of the catenane in MeCN.

{[2]-[1,4,7,10,13,20,23,26,29,32-Decaoxa[13]para[13]meta-cyclophane][9,18,29,38-tetraazonia-[1.1.0.1.1.0]paracyclophane]ca-tenane} Tetrakishexafluorophosphate ({[2]-[PPMP33C10][BBIP-YBIPXYCY]catenane}$[PF_6]_4$). 1,4-bis(bromomethyl)benzene (35.3 mg, 0.13 mmol) was added directly to a solution of PPMP33C10 (202.3 mg, 0.38 mmol) and [BBIPYPXY]$[PF_6]_2$ (107.2 mg, 0.15 mmol) in dry DMF (5 mL). The reaction mixture was stirred for 18 days, producing a peach-colored suspension. The solvent was removed under reduced pressure. Following the same purification procedure as that described above for {[2]-[BPP34C10][BIPYPXYBIPYMXYCY]-catenane}$[PF_6]_4$ (method A), the [2]catenane was isolated as a red solid (35.2 mg, 15%): mp > 275 °C; FABMS 1636 $(M)^+$, 1491 ($[M - PF_6]^+$), 1346 ($[M - 2PF_6]^+$), 1201 ($[M - 3PF_6]^+$); ^{1}H NMR [CD_3COCD_3, 400 MHz] δ 3.35−3.45 (4H, m), 3.51−3.63 (4H, bs), 3.70−3.86 (12H, m), 3.89−4.09 (16H, m), 5.46−5.57 (1H, bs), 6.03 (8H, s), 6.24−6.33 (2H, bd), 7.01−7.15 (1H, bt), 8.04 (8H, s), 8.14 (8H, d), 9.34 (8H, d); ^{13}C NMR [CD_3COCD_3, 400 MHz] δ 65.6, 67.7, 68.5, 70.6, 70.7, 70.9, 71.2, 71.5, 71.8, 101.7, 108.4, 114.0, 126.5, 131.4, 131.9, 137.9, 145.9, 147.2, 151.2, 160.7. Anal. ($C_{64}H_{72}N_4O_{10}F_{24}P_4$) C, H, N. Single crystals, suitable for X-ray crystallography, were grown by vapor diffusion of *i*-Pr_2O into a solution of the catenane in MeCN.

{[2]-[1,4,7,10,13,20,23,26,29,32-Decaoxa[13]para[13]meta-cyclophane][9,18,29,38-tetraazonia-[1.1.0]para[1]meta[1.0]-paracyclophane]catenane} Tetrakishexafluorophosphate ({[2]-[PPMP33C10][BBIPYPXYMXYCY]catenane}$[PF_6]_4$). 1,4-Bis(bromomethyl)benzene (38.0 mg, 0.14 mmol) was added directly to a solution of PPMP33C10 (205.8 mg, 0.38 mmol) and [BBIPYMXY]-$[PF_6]_2$ (107.0 mg, 0.15 mmol) in dry DMF (5 mL). The reaction mixture was stirred for 14 days, producing a red-colored suspension. The solvent was removed under reduced pressure. Following the same purification procedure as that described above for {[2]-[BPP34C10]-[BIPYPXYBIPYMXYCY]catenane}$[PF_6]_4$ (method A), the [2]catenane was isolated as a red solid (67.6 mg, 27%): mp > 280 °C; FABMS 1636 $(M)^+$, 1491 ($[M - PF_6]^+$), 1346 ($[M - 2PF_6]^+$), 1201 ($[M - 3PF_6]^+$); ^{1}H NMR [CD_3COCD_3, 400 MHz] δ 3.35−3.42 (4H, s), 3.55−3.60 (4H, bs), 3.76−4.05 (28H, m), 5.56 (1H, s), 6.00 (4H, s), 6.07 (4H, s), 6.28 (2H, d), 7.05−7.14 (1H, bt), 7.87 (1H, t), 8.01 (5H, s), 8.11−8.26 (10H, m), 9.20 (4H, d), 9.30 (4H, d); ^{13}C NMR [CD_3COCD_3, 101 MHz] δ 64.1, 64.5, 66.2, 67.3, 69.5, 69.6, 69.8, 70.1, 70.2, 70.5, 100.4, 107.3, 113.3, 125.0, 125.3, 130.4, 130.9, 132.2, 133.7, 134.0, 136.7, 144.7, 145.5, 146.0, 150.2, 159.6. Anal. ($C_{64}H_{72}N_4O_{10}F_{24}P_4$) C, H, N.

{[2]-[1,4,7,10,13,20,23,26,29,32-Decaoxa[13]para[13]meta-cyclophane][9,18,29,38-tetraazonia[1]meta[1.0]para[1]meta[1.0]-paracyclophane]catenane} Tetrakishexafluorophosphate ({[2]-[PPMP33C10][BBIPYBIMXYCY]catenane}$[PF_6]_4$). 1,3-Bis(bromomethyl)benzene (38.6 mg, 0.15 mmol) was added directly to a solution of PPMP33C10 (193.7 mg, 0.36 mmol) and [BBIPYMXY]-$[PF_6]_2$ (104.5 mg, 0.15 mmol) in dry DMF (5 mL) in a Telfon high pressure reaction vessel. The reaction mixture was subjected to 12 kbar pressure at 20 °C for 2 days, producing a red-colored suspension. The solvent was removed under reduced pressure. Following the same purification procedure as that described above for {[2]-[BPP34C10]-[BIPYPXYBIPYMXYCY]catenane}$[PF_6]_4$ (method A), the [2]catenane was isolated as a red solid (4.2 mg, 1.7%): mp > 280 °C; FABMS 1491 ($[M - PF_6]^+$), 1346 ($[M - 2PF_6]^+$), 1201 ($[M - 3PF_6]^+$); ^{1}H NMR [CD_3COCD_3, 400 MHz] δ 3.34−3.42 (4H, m), 3.52−3.59 (4H, m), 3.73−4.10 (24H, m), 4.39 (4H, bs), 5.69 (1H, d), 6.11 (8H, s), 6.24−6.27 (2H, d), 6.99−7.06 (1H, t), 7.80−7.91 (2H, bt), 8.02 (1H, s), 8.03−8.16 (12H, m), 9.19 (8H, d); ^{13}C NMR [CD_3COCD_3, 101 MHz] δ 63.7, 64.9, 65.1, 66.9, 68.1, 70.1, 70.5, 70.8, 70.9, 71.1, 71.3, 100.9, 108.2, 125.8, 128.3, 128.4, 128.6, 130.1, 131.3, 131.9, 133.9, 134.0, 134.7, 134.8, 146.4, 146.8, 151.3, 160.5.

{[2]-[1,4,7,10,13,20,23,26,29,32-Decaoxa[13.13]metacyclophane]-[9,18,29,38-tetraazonia[1.1.0.1.1.0]paracyclophane]catenane} Tetrakishexafluorophosphate ({[2]-[BMP32C10][BBIPYBIPXYCY]-catenane}$[PF_6]_4$). 1,4-Bis(bromomethyl)benzene (30.7 mg, 0.12 mmol), BMP32C10 (151.0 mg, 0.28 mmol), and [BBIPYPXY]$[PF_6]_2$ (82.0 mg, 0.12 mmol) were dissolved in dry DMF (4 mL), and the reaction mixture was stirred 7 days, producing a yellow-colored suspension. Following the purification procedure described above for {[2]-[BPP34C10]-[BBIPYPXYMXYCY]catenane}$[PF_6]_4$ (method A), the [2]catenane was isolated as a yellow solid (33.0 mg, 17%): mp > 250 °C; FABMS 1490 ($[M - PF_6]^+$), 1345 ($[M - 2PF_6]^+$), 1200 ($[M - 3PF_6]^+$); ^{1}H NMR [CD_3COCD_3, 400 MHz, 253 K] δ 1.73 (1H, bt), 3.05 (1H, t), 3.45−3.55 (4H, m), 3.65−3.95 (28H, m), 4.76 (2H, dd), 5.61 (1H, bt), 5.95−6.10 (10H, m), 6.71 (1H, t), 8.04 (8H, bd), 8.25−8.40 (8H, m), 9.38 (8H, bd); ^{13}C NMR [CD_3COCD_3, 101 MHz, 233K] δ 64.9, 65.1, 67.3, 67.4, 69.8 (×2), 70.1 (×2), 70.5, 71.1, 99.4, 100.5, 105.8, 106.8, 126.1, 127.1, 128.2, 130.9, 131.3, 131.4, 137.9, 138.3, 145.1, 145.6, 146.8, 146.9, 157.7, 160.0. Anal. ($C_{64}H_{72}N_4O_{10}F_{24}P_4$) C, H, N.

{[2]-[1,4,7,10,13,20,23,26,29,32-Decaoxa[13.13]metacyclophane]-[9,18,29,38-tetraazonia[1.1.0]para[1]meta[1.0]paracyclophane]-catenane} Tetrakishexafluorophosphate ({[2]-[BMP32C10]-[BBIPYPXYMXYCY]catenane}$[PF_6]_4$). 1,4-Bis(bromomethyl)benzene (25.3 mg, 0.10 mmol), BMP32C10 (244.3 mg, 0.46 mmol), and [BBIPYMXY]$[PF_6]_4$ (68.2 mg, 0.10 mmol) were dissolved in dry DMF (5 mL). The reaction mixture was stirred for 7 days, and following the same purification procedure as that described above for {[2]-[BPP34C10][BBIPYPXYMXYCY]catenane}$[PF_6]_4$ (method A), the [2]-catenane was isolated as a yellow solid (19.3 mg, 12%): mp > 250 °C; FABMS 1490 ($[M - PF_6]^+$), 1345 ($[M - 2PF_6]^+$), 1200 ($[M - 3PF_6]^+$); ^{1}H NMR [CD_3COCD_3, 400 MHz, 263 K] δ 2.68 (1H, bs), 3.62−4.01 (33H, m), 4.51 (2H, bs), 5.81 (1H, bs), 6.05−6.08 (10H, m), 6.89 (1H, bs), 7.93 (1H, t), 7.97 (1H, bs), 8.06 (4H, bs), 8.08 (2H, d), 8.16 (4H, bs), 8.18 (4H, d), 9.13 (4H, d), 9.18 (4H, d); ^{13}C NMR [CD_3COCD_3, 101 MHz, 243 K] δ 64.7, 65.1, 67.1, 67.5, 69.7, 69.9, 70.5, 70.6, 78.5, 78.8, 79.2, 105.2, 106.4, 126.0, 127.3, 131.5, 131.6, 134.6, 135.6, 138.5, 145.3, 146.3, 146.7, 147.3, 157.4, 160.0.

1,5-Bis[2-(hydroxyethoxy)ethoxy]naphthalene (3). 1,5-Dihydroxynaphthalene (NP) (4.50 g, 30 mmol) was added to a vigorously stirred slurry of K_2CO_3 (15.53 g, 112 mmol) in dry DMF (400 mL) under an

atmosphere of nitrogen. After stirring for 1 h at 80 °C, 2-(2-chloroethoxy)ethanol (8.75 g, 70.3 mmol) in dry DMF (50 mL) was added slowly during 2 h. The reaction mixture was maintained under these conditions for 3 days, after which time it was filtered, and the solvent removed under vacuum, giving a very dark brown oil. The residue was partioned between $CHCl_3$ and saturated NaCl solution, and the pH of the aqueous layer adjusted to <2 using dilute HCl. The organic layer was separated, washed once with dilute $NaHCO_3$ solution, twice with H_2O, and dried ($MgSO_4$), before the solvent was removed under vacuum. The residual red-brown oil was subjected to column chromatography (CH_2Cl_2/MeOH, 98:2) on silica gel. The fractions containing the product were combined and concentrated to afford **3** as a yellow solid (4.35 g, 46%): mp 91−91 °C; EIMS 336, (M^+); ^{1}H NMR [$CDCl_3$, 300 MHz] δ 2.33 (2H, br s), 3.74−3.79 (8H, m), 3.92−3.98 (4H, m), 4.28−4.33 (4H, m), 6.90 (2H, d), 7.30 (2H, t), 7.80 (2H, d); ^{13}C NMR [$CDCl_3$, 75 MHz] δ 61.9, 68.0, 69.8, 69.8, 72.6, 105.9, 114.7, 125.2, 126.8, 154.3. Anal. ($C_{18}H_{24}O_6$) C, H.

1-[2-(2-Hydroxyethoxy)ethoxy]-4-benzyloxybenzene (6). 4-Benzyloxyphenol **4** (28.33 g, 141.7 mmol) was added with stirring to a suspension of K_2CO_3 (55.2 g, 400 mmol) in dry DMF (400 mL) under nitrogen, and the temperature of the reaction mixture was raised to 50 °C. 2-(2-Chloroethoxy)ethanol (18.7 g, 150 mmol) was added in dry DMF (150 mL) over 3 h, and the reaction mixture was stirred at 75 °C under nitrogen. After 4 days, the reaction was allowed to cool, and the solvent was removed in vacuo to leave a reddish-brown residue which was partitioned between $CHCl_3$ and H_2O. The organic layer was washed well with H_2O and then dried ($MgSO_4$). Removal of the solvent yielded a pink solid, which was recrystallized from CH_2Cl_2/light petroleum (bp 60−80 °C), giving **6** (37.8 g, 93%): mp 67−69 °C; EIMS 288, (M^+); ^{1}H NMR [$CDCl_3$, 300 MHz] δ 2.54 (1H, bs), 3.74 (4H, m), 3.83 (2H, m), 4.10 (2H, m), 5.02 (2H, s), 6.87 (4H, m), 7.38 (5H, m);); ^{13}C NMR [$CDCl_3$, 75 MHz] δ 61.9, 67.8, 68.3, 70.4, 71.7, 115.3, 116.1, 125.3, 125.4, 127.4, 137.6, 153.2, 153.9. Anal. ($C_{17}H_{20}O_4$) C, H.

1-Benzyloxy-5-{2-(2-hydroxyethoxy)ethoxy}naphthalene (7). The title compound was prepared from 1-benzyloxy-5-hydroxynaphthalene[44] **5** (3.28 g, 13.1 mmol) and 2-(2-chloroethoxy)ethanol (2.04 g, 16.4 mmol) by employing an identical procedure to that used for the preparation of **6**, giving **7** as a tan-colored solid (4.21 g, 95%): mp 67−69 °C; EIMS 338, (M^+); ^{1}H NMR [$CDCl_3$, 400 MHz] δ 2.41 (2H, br s), 3.65−3.68 (2H, m), 3.71−3.74 (2H, m), 3.90−3.93 (2H, m), 4.20−4.24 (2H, m), 5.18 (2H, s), 6.80 (1H, d), 6.87 (1H, d), 7.29−7.41 (5H, m), 7.47 (2H, d), 7.86 (1H, d), 7.94 (1H, d); ^{13}C NMR [$CDCl_3$, 75 MHz] δ 61.9, 68.0, 69.8, 70.2, 72.7, 105.9, 106.1, 114.5, 114.9, 125.1, 125.3, 126.9, 127.0, 127.4, 127.9, 128.6, 137.2, 154.3, 154.4. Anal. ($C_{21}H_{24}O_4$) C, H.

1-[2-(2-Toluene-*p*-sulfonylethoxy)ethoxy]-4-benzyloxybenzene (8). Toluene-*p*-sulfonyl chloride (19.1 g, 103 mmol) in CH_2Cl_2 (100 mL) was added slowly to a stirred solution of **6** (22.6 g, 79 mmol) and Et_3N (25 mL) in CH_2Cl_2 (150 mL). The reaction mixture was maintained at <5 °C during the addition and then allowed to warm up to room temperature before being stirred for 18 h. The organic layer was washed with dilute HCl, with H_2O, and then finally dried ($MgSO_4$). The solvent was removed in vacuo to yield the product as an off-white solid. Recrystallization from Et_2O/light petroleum (bp 60−80 °C) gave **8** as a colorless solid (27.2 g, 78%): mp 77−78 °C; EIMS 442, (M^+); ^{1}H NMR [$CDCl_3$, 300 MHz] δ 2.42 (3H, s), 3.74 (4H, m), 3.83 (2H, m), 4.10 (2H, m), 5.02 (2H, s), 6.87 (4H, m), 7.38 (5H, m), 7.29 (2H, d), 7.78 (2H, d); ^{13}C NMR [$CDCl_3$, 75 MHz] δ 21.7, 67.4, 68.8, 69.3, 70.1, 70.4, 114.9, 115.3, 125.1, 125.2, 126.9, 127.1, 127.4, 132.5, 144.8, 153.9, 154.1. Anal. ($C_{24}H_{26}O_6S$) C, H.

1-Benzyloxy-5-{2-(2-toluene-*p*-sulfonylethoxy)ethoxy}naphthalene (9). The title compound was prepared from toluene-*p*-sulfonyl chloride (2.86 g, 14.9 mmol) and **7** (4.20 g, 79 mmol) by employing an identical procedure to that used for the preparation of **7**, giving **9** as an off-white solid (4.63 g, 76%): mp 101−113 °C; EIMS 492, (M^+), ^{1}H NMR [$CDCl_3$, 400 MHz] δ 2.34 (3H, s), 3.80−3.84 (2H, m), 3.89−3.93 (2H, m), 4.18−4.23 (4H, m), 5.24 (2H, s), 6.81 (1H, d), 6.92 (1H, d), 7.22 (2H, d), 7.32 7.43 (5H, m), 7.53 (2H, d), 7.76 (2H, d), 7.81 (1H, d), 7.94 (1H, d); ^{13}C NMR [$CDCl_3$, 75 MHz] δ 21.6, 67.9, 69.0, 69.4, 70.0, 70.2, 105.8, 106.1, 114.6, 114.9, 125.1, 125.2, 126.8, 126.9, 127.4, 127.9, 128.0, 128.6, 129.8, 133.0, 137.2, 144.8, 154.3, 154.4. Anal. ($C_{28}H_{28}O_6S$) C, H.

1,4-Bis[2-[2-[2-[2-(4-benzyloxyphenoxy)ethoxy]ethoxy]ethoxy]-ethoxy]benzene (3HQ). 1,4-Bis[2-(2-hydroxyethoxy)ethoxy]benzene[12] **2** (5.2 g, 26.2 mmol) was added dropwise with stirring to a suspension of NaH (2.33 g, 58.2 mmol) and anhydrous THF (130 mL) under nitrogen at room temperature during 30 min. The reaction mixture was warmed up to 50 °C over 1 h. After hydrogen evolution had subsided, **8** (26 g, 53.5 mmol) in anhydrous THF (100 mL) was added, and the reaction mixture was stirred under nitrogen for 5 days at 75 °C. H_2O (10 mL) was added to destroy unreacted hydride, and the solvent was removed in vacuo. Recrystallization of the crude product from MeOH/Me_2CO gave 3HQ as a colorless solid (13.8 g, 71%): mp 93−94 °C; FABMS 826, (M^+); ^{1}H NMR [$CDCl_3$, 300 MHz] δ 3.77 (16H, m), 3.82 (8H, m), 4.04 (8H, m), 5.00 (4H, s), 6.80 (4 H, s), 6.83 (8H, m), 7.44 (10H, m); ^{13}C NMR [$CDCl_3$, 75 MHz] δ 68.1, 69.9, 70.7, 70.8, 115.6, 115.7, 115.8, 127.5, 127.9, 128.6, 137.3, 153.2. Anal. ($C_{48}H_{58}O_{12}$) C, H.

1,5-Bis[2-[2-[2-[2-(4-benzyloxyphenoxy)ethoxy]ethoxy]ethoxy]-ethoxy]naphthalene (2HQNP). The title compound was prepared from 1,5-bis[2-(2-hydroxyethoxy)ethoxy]naphthalene[45] **3** (3.12 g, 10 mmol) and **8** (8.61 g, 20 mmol) by employing an identical procedure to that used for the preparation of 3HQ, giving 2HQNP as a colorless solid (5.69 g, 70%): mp 107−109 °C; FABMS 876, (M^+); ^{1}H NMR [$CDCl_3$, 300 MHz] δ 3.67−3.73 (12H, m), 3.77−3.82 (8H, m), 3.95−4.08 (8H, m), 4.28 (4H, t), 5.00 (4H, s), 6.79−6.90 (10H, m), 7.30−7.45 (12H, m), 7.86 (2H, m); ^{13}C NMR [$CDCl_3$, 75 MHz] δ 68.0, 68.1, 69.9, 70.7, 70.8, 70.9, 71.0, 105.8, 114.7, 115.7, 115.8, 125.1, 126.9, 127.5, 127.8, 128.5, 136.5, 153.2, 154.4. Anal. ($C_{52}H_{60}O_{12}$) C, H.

1,4-Bis[2-[2-[2-[2-(5-benzyloxy-1-naphthoxy)ethoxy]ethoxy]ethoxy]-ethoxy]benzene (2NPHQ). The title compound was prepared from 1,4-bis[2-(2-hydroxyethoxy)ethoxy]benzene[12] **2** (110 mg, 0.39 mmol) and **9** (381 mg, 0.78 mmol) by employing an identical procedure to that used for the preparation of 3HQ, giving 2NPHQ as a colorless solid (189 mg, 53%): mp 117−119 °C; FABMS 926, (M^+); ^{1}H NMR [$CDCl_3$, 300 MHz] δ 3.58−3.67 (12H, m), 3.69−3.76 (8H, m), 3.89−3.97 (8H, m), 4.17−4.25 (4H, m), 5.15 (4H, s), 6.72 (4H, s), 6.77 (2H, d), 6.84 (2H, d), 7.24−7.39 (10H, m), 7.45 (4H, m), 7.80 (2H, d), 7.84 (2H, d); ^{13}C NMR [$CDCl_3$, 75 MHz] δ 67.9, 69.0, 69.4, 70.0, 70.2, 105.8, 106.1, 114.6, 114.9, 125.1, 125.2, 127.4, 127.9, 128.0, 128.6, 129.8, 137.2, 154.3, 154.4. Anal. ($C_{56}H_{62}O_{12}$) C, H.

1,5-Bis[2-[2-[2-[2-(5-benzyloxy1-naphthoxy)ethoxy]ethoxy]ethoxy]-ethoxy]naphthalene (3NP). The title compound was prepared from 1,5-bis[2-(2-hydroxyethoxy)ethoxy]naphthalene[45] **3** (5.2 g, 26.2 mmol) and **9** (26 g, 53.5 mmol) by employing an identical procedure to that used for the preparation of 3HQ, giving 3NP as a tan-colored solid (13.8 g, 71%): mp 122−125 °C; FABMS 976, (M^+); ^{1}H NMR [$CDCl_3$, 300 MHz] δ 3.59−3.68 (12H, m), 3.69−3.78 (8H, m), 3.88−3.95 (8H, m), 4.19−4.27 (4H, m), 5.22 (4H, s), 6.80 (2H, d), 6.85 (2H, d), 6.93 (2H, d), 7.24−7.40 (16H, m), 7.75 (2H, d), 7.80 (2H, d), 7.86 (2H, d); ^{13}C NMR [$CDCl_3$, 75 MHz] δ 67.9, 69.0, 69.4, 70.0, 70.2, 105.8, 106.1, 114.6, 114.9, 125.1, 125.2, 127.4, 127.9, 128.0, 128.6, 129.8, 137.2, 154.3, 154.4. Anal. ($C_{60}H_{64}O_{12}$) C, H.

1,11-Bis{4-[2-(2-hydroxyethoxy)ethoxy]phenoxy}-3,6,9-trioxaundecane (13). 2-(2-Chloroethoxy)ethanol (28 mL, 266 mmol) in DMF (30 mL) was added to a slurry of K_2CO_3 (53 g, 384 mmol), DMF (200 mL), and 1,11-bis(4-hydroxyphenoxy)-3,6,9-trioxaundecane[12] **12** (15.0 g, 39.6 mmol) which had been stirring at room temperature under nitrogen for 30 min. The slurry was warmed up slowly to 80 °C and then stirred for 7 days at 80 °C under nitrogen. The slurry was filtered, the cake was washed well with DMF, and the solvent was removed in vacuo, yielding a brown oil which was purified by flash chromatography on silica gel (EtOAc/CH_2Cl_2, 1:1). The colorless solid was recrystallized from EtOAc/CH_2Cl_2/light petroleum (bp 60−80 °C) giving **13** (22.1 g, 83%): mp 66−68 °C; FABMS 554, (M^+); ^{1}H NMR [CD_3COCD_3, 300 MHz] δ 2.37 (2H, bs), 3.77 (16H, m) 3.82 (8H, m), 4.04 (8H, m), 6.85 (8H, s); ^{13}C NMR [CD_3COCD_3, 75 MHz] δ 68.8, 68.9, 70.3, 70.4, 71.2, 71.3, 71.3, 116.2, 116.3, 116.5, 152.2, 153.1, 154.0. Anal. ($C_{28}H_{42}O_{11}$) C, H.

1-Chloro-11-hydroxy-3,6,9-trioxaundeance (14). 1,11-Dihydroxy-3,6,9-trioxaundecane (117 g, 600 mmol) in $CHCl_3$ (250 mL) was added to dry C_5H_5N (250 mL), and the solution was cooled to 0 °C. The solution was protected from moisture by means of a $CaCl_2$ guard tube. $SOCl_2$ (95.2 g, 800 mmol) was added dropwise over 6 h, the temperature of the reaction mixture never rising above 2 °C during the

addition. The reaction mixture was then allowed to warm up to room temperature before being heated to 60 °C for 3 h. The solvent was removed in vacuo, and the residual oil was partitioned between $CHCl_3$ and H_2O. The organic layer was washed with H_2O (4 × 200 mL), and the aqueous layer was re-extracted with $CHCl_3$ (4 × 150 mL). The combined organic extracts from this procedure were evaporated to dryness, the residual oil was carefully distilled using a large, heated, glass Vigreux column, and the fraction (41 g, 32%) with boiling point 157−161 °C (0.9 mmHg) was collected. GCMS showed this clear oil to contain 96% of **14**—the remaining 4% being 1,11-dihydroxy-3,6,9-trioxaundecane. This material was used without further purification: EIMS 212, (M^+); ^{1}H NMR [$CDCl_3$, 300 MHz] δ 3.42 (1H, br s), 3.60−3.79 (16H, m).

1,11-Bis{4-[2-(2-(2-hydroxyethoxy)ethoxy)ethoxy)ethoxy]-phenoxy}-3,6,9-trioxaundecane (15). 1,11-Bis(4-hydroxyphenoxy)-3,6,9-trioxaundecane[12] **12** (10.0 g, 18.1 mmol) in dry MeCN (50 mL) was added to a vigorously stirred suspension of K_2CO_3 (20.0 g, 144.8 mmol) in anhydrous MeCN (100 mL) under an atmosphere of nitrogen. The reaction mixture was heated to 80 °C for 2 h, and then **14** (11.5 g, 54.2 mmol) in dry MeCN (50 mL) was added dropwise over a further period of 2 h. The reaction mixture was stirred at 80 °C under nitrogen for a further 72 h, before being cooled and filtered. The solid residue was washed well with MeCN. The filtrate was evaporated to dryness, and the residue was subjected to flash chromatography (SiO_2:$CHCl_3$/MeOH 96:4) to give **15** as an off-white solid (22.1 g, 67%): mp 55−57 °C; FABMS 730, (M^+); ^{1}H NMR [$CDCl_3$, 300 MHz] δ 2.34 (2H, br s), 3.56−3.61 (8H, m), 3.62−3.74 (20H, m), 3.79−3.85 (8H, m), 4.04−4.10 (12H, m), 6.83 (8H, s); ^{13}C NMR [$CDCl_3$, 75 MHz] δ 61.5, 68.1, 68.7, 69.3, 69.9, 70.6, 70.7, 70.8, 115.2, 115.6, 123.3, 127.9, 128.6, 129.8, 153.1, 153.3.

1,11-Bis{4-[2-(2-(2-(toluene-*p*-sulfonyl)ethoxy)ethoxy)ethoxy)-ethoxy]phenoxy}-3,6,9-trioxaundecane (16). Toluene-*p*-sulfonyl chloride (7.12 g, 37.18 mmol) in CH_2Cl_2 (100 mL) was added slowly to a stirred solution of **15** (11.38 g, 15.59 mmol) and Et_3N (25 mL) in CH_2Cl_2 (150 mL). The reaction mixture was maintained at <0 °C during the addition and then allowed to warm up to room temperature and stirred for 36 h. The organic layer was washed with dilute hydrochloric acid and with water and then finally dried ($MgSO_4$). The solvent was removed in vacuo to yield an off-white solid which was purified by column chromatography (SiO_2:$CHCl_3$/MeOH, 99:1) to give **16** as a colorless oil (11.2 g, 69%). This oil solidified very slowly to give a colorless solid: mp 67−69 °C; FABMS 1038, (M^+); ^{1}H NMR [$CDCl_3$, 300 MHz] δ 2.43 (6H, s), 3.56−3.61 (8H, m), 3.62−3.74 (20H, m), 3.79−3.85 (8H, m), 4.04−4.10 (8H, m), 4.14−4.19 (4H, m), 6.83 (8H, s), 7.33 (4H, d), 7.79 (4H, d); ^{13}C NMR [$CDCl_3$, 75 MHz] δ 30.8, 68.1, 68.7, 69.3, 69.9, 70.6, 70.7, 70.8, 115.2, 115.6, 123.3, 127.9, 128.6, 129.8, 133.1, 144.8, 153.1. Anal. ($C_{50}H_{70}O_{19}S_2$) C, H.

1,11-Bis{4-[2-[2-[2-(4-benzyloxyphenoxy)ethoxy]ethoxy]ethoxy]-ethoxy]phenoxy}-3,6,9-trioxaundecane (4HQ). Route I. The title compound was prepared from **13** (257 mg, 0.46 mmol) and **8** (449 mg, 1.02 mmol) by employing an identical procedure to that used for the preparation of 3HQ, giving 4HQ as a colorless solid (257 mg, 51%): mp 99−100 °C; FABMS 1094, (M^+); ^{1}H NMR [$CDCl_3$, 300 MHz] δ 3.77 (24H, m), 3.82 (12H, m), 4.04 (12H, m), 5.00 (4H, s), 6.80 (8H, s), 6.84 (8H, m), 7.44 (10H, m); ^{13}C NMR [$CDCl_3$, 75 MHz] δ 68.1, 69.8, 69.9, 70.7, 70.8, 115.6, 115.7, 115.8, 127.5, 127.9, 128.5, 156.2. Anal. ($C_{62}H_{78}O_{17}$) C, H.

Route II. 4-Benzyloxyphenol **4** (275 mg, 2.22 mmol) in dry MeCN (20 mL) was added to a vigorously stirred slurry of K_2CO_3 (2.76 g, 20 mmol) in dry MeCN (80 mL) under a nitrogen atmosphere over a period of 20 min. This mixture was heated at 80 °C for 2 h. **16** (1.04 g, 1 mmol) in dry MeCN (25 mL) was then added dropwise over 3 h, and the reaction mixture was heated under reflux for 3 days. The solution was cooled and filtered, and the solid residue was washed well with MeCN. The filtrate was evaporated to dryness, and the residual solid purified by column chromatography (SiO_2:$CHCl_3$/MeOH, 99:1) to give 4HQ as a colorless solid (797 mg, 73%). This compound gave identical physical and spectroscopic data to that reported above.

1,4-Bis[2-[2-[2-[2-(hydroxyphenoxy)ethoxy]ethoxy]ethoxy]-benzene (17). 3HQ (10 g, 12.1 mmol) was subjected to hydrogenolysis in $CHCl_3$/MeOH (1:1) (300 mL) using 10% Pd on charcoal (1 g). The reaction mixture was stirred under hydrogen for 24 h before it was filtered through a bed of Hyflo supercel to remove the catalyst. The filter cake was washed well with MeOH. Removal of the solvent gave the product which was recrystallized from aqueous EtOH, giving **17** as colorless crystals (7.1 g, 90%): mp 77−78 °C; FABMS 646, (M^+); ^{1}H NMR [$CDCl_3$, 300 MHz] δ 3.64 (16H, m), 3.76 (8H, m), 4.03 (8H, m), 6.75 (8H, m), 6.84 (4H, s), 7.68 (2H, s); ^{13}C NMR [$CDCl_3$, 75 MHz] δ 68.8, 68.9, 70.3, 70.4, 71.2, 71.3, 71.3, 116.2, 116.3, 116.5, 152.2, 153.1, 154.0. Anal. ($C_{34}H_{46}O_{12}$) C, H.

1,4-Bis{2-{2-{2-{2-{[2-(2-hydroxyethoxy)ethoxy]phenoxy}ethoxy}-ethoxy}ethoxy}ethoxy}benzene (18). 2-(2-Chloroethoxy)ethanol (2.12 g, 17 mmol) in DMF (30 mL) was added to a slurry of K_2CO_3 (7.73 g, 56 mmol), DMF (200 mL), and **17** (5 g, 7.74 mmol) which had been stirred at room temperature under nitrogen for 30 min. The slurry was warmed up slowly to 80 °C and then stirred for 7 days at 80 °C under nitrogen. The slurry was filtered, the cake was washed well with DMF, and the solvent was removed in vacuo leaving a brown oil which was purified by flash chromatography (SiO_2:EtOAc/CH_2Cl_2, 1:1) to give a colorless solid. Recrystallization from CH_2Cl_2/light petroleum (bp 60−80 °C) gave **18** as a colorless solid (4.64 g, 73%): mp 59−61; FABMS 822, (M^+); ^{1}H NMR [$CDCl_3$, 300 MHz] δ 2.31 (2H, bs), 3.64 (24H, m), 3.74 (12H, m), 4.03 (12H, m), 6.80 (4H, s), 6.83 (8 H, m); ^{13}C NMR [$CDCl_3$, 75 MHz] δ 61.2, 66.9, 67.6, 68.8, 68.9, 70.3, 70.4, 71.2, 71.3, 71.3, 116.2, 116.3, 116.5, 152.2, 153.1, 154.0.

1,4-Bis{2-{2-{2-{[2-[2-[2-(4-benzyloxyphenoxy)ethoxy]ethoxy]-ethoxy]ethoxy]phenoxy}ethoxy}ethoxy}ethoxy}ethoxy}benzene (5HQ). The title compound was prepared from **18** (460 mg, 0.56 mmol) and **8** (545 mg, 1.23 mmol) by employing an identical procedure to that used for the preparation of 3HQ, giving 5HQ as a colorless solid (442 mg, 58%): mp 77−79 °C; FABMS 1362, (M^+); ^{1}H NMR [$CDCl_3$, 400 MHz] δ 3.73 (32H, m), 3.80 (16H, m), 4.04 (16H, m), 5.02 (4H, s), 6.80 (12H, s), 6.83 (8H, m), 7.45 (10H, m); ^{13}C NMR [$CDCl_3$, 75 MHz] δ 68.8, 68.9, 70.3, 70.4, 71.2, 71.3, 71.3, 116.2, 116.3, 116.5, 152.2, 153.1, 154.0. Anal. ($C_{76}H_{98}O_{22}$) C, H.

Procedures for ^{1}H NMR and ^{13}C NMR Spectroscopic Studies of Complexation. Solutions of complexes with a 1:1 or 1:2 molar ratio of π-electron rich to π-electron deficient components were made up in deuterated solvents 24 h before the spectra were recorded to allow time for radical quenching to occur. Concentrations were in the range 3 × 10^{-3}−9 × 10^{-3} mol L^{-1}. Unless otherwise stated, all chemical shift changes, Δδ, are quoted in ppm for 1:1 or 1:2 complexes and were calculated using the equation $\Delta\delta = \delta(\text{complex}) - \delta(\text{free})$.

Procedure for UV Spectrophotometric Titrations. The change in the optical density of a solution of a complex was recorded as the relative concentration of one component (usually the guest) of the complex was increased with respect to the other component (the cyclophane host). All stability constants were determined in dry MeCN or Me_2CO solution at 300 K. In a typical experiment, a solution of the cyclophane was made up in a volumetric flask and its optical density recorded in a 1 cm path length cuvette. The contents of the cuvette were then transferred back into the volumetric flask, and the cuvette was rinsed with solvent. The washings were added to the volumetric flask. A known quantity of the guest was added to the solution, and the excess of solvent volume was removed by evaporation in a stream of dry nitrogen. The optical density of this solution of the complex was recorded, and the procedure was repeated until no significant change in optical density was observed when a further guest was added. Molar ratios of guests to cyclophanes used were in the range 0.1:1 to 30:1 for strong complexes and in the range 5:1 to 300:1 for weak complexes. The data were treated by the use of a nonlinear curve fitting program running on an Apple Macintosh SE/30 microcomputer. The values for K_a quoted are the average of two determinations.

Electrochemistry. The electrochemical experiments were performed as described elsewhere.[12]

X-ray Crystallography. X-ray diffraction measurements were performed on a Nicolet R3m diffractometer with graphite-monochromated Cu Kα radiation with ω scans. The crystal data and data collection parameters are presented in Table 15. Lattice parameters were determined by least-squares fits from 18 to 22 centered reflections. Intensities were corrected for the decay of two control reflections, measured every 50 reflections, and for Lorentz and polarization factors but not for absorption.

The structures were solved by direct methods and refined by full-matrix least-squares. Reflections with $|F_0| > 3\sigma(|F_0|)$ were considered to be observed and were included in the refinements (based on F_0). A

Table 15. Crystal Data and Data Collection Parameters

data	A[a]	B[a]	C[a]
formula	$C_{74}H_{72}O_{t0}N_4P_4F_{24}$	$C_{74}H_{69}N_8O_{t0}P_4F_{24}$	$C_{78.75}H_{72}O_{t0}N_{t1.25}P_4F_2$
solvent	5MeCN	4MeCN	7.25MeCN + 0.25H_2O
molecular weight	1827.3	1810.5	1915.9
lattice type	monoclinic	triclinic	triclinic
space group	*C2/c*	$P\bar{1}$	$P\bar{1}$
T, K	291	291	293
cell dimensions			
a, Å	49.47(7)	12.669(5)	14.280(10)
b, Å	13.945(16)	15.553(4)	17.740(2)
c, Å	28.88(3)	21.801(9)	20.260(2)
α, deg		84.50(2)	77.66(9)
β, deg	119.16(2)	82.00(2)	74.61(7)
γ, deg		78.21(2)	69.22(8)
V, Å^3	17400	4154	4586
Z	8	2	2
D_c, g cm^{-3}	1.39	1.45	1.39
F(000)	7480	1850	1958
μ, mm^{-t}	1.78	1.86	1.73
θ range, deg	2−55	2−58	1.5−55
no. unique reflections			
measured	11636	10811	11348
observed	4543	7173	4919
no. variables	841	1100	831
R, %	13.94	9.98	15.1
R_w, %	13.71	9.66	15.7
weighting factor *f*	0.0005	0.0005	0.0005
extinction *g*	0.00017(3)	0.0017(2)	0.001(2)

[a] A = {[2]-[BPP34C10][BBIPYPXYMXYCY]catenane}$[PF_6]_4$, B = {[2]-BPP34C10][BBIPYBIMXYCY]catenane}$[PF_6]_4$, and C = {[2]-[PPMP33C10][BBIPYBIPXYCY]-catenane}$[PF_6]_4$.

weighting function of the form $w^t = \sigma^2(F) + pF^2$ was applied. Leading hydrogen atoms on methyl groups attached to sp^2 carbon atoms were, where possible, located from the ΔF maps. Methyl groups were refined as idealized rigid bodies. In compound C, the hydrogen atoms of the included MeCN molecules could not be located; they were therefore omitted from the computations. Depending on data quality and the data:parameter ratio, hydrogen atoms were either included in the refinement or placed in calculated positions (C−H distance 0.96 Å) and allowed to ride on their parent carbon atoms (U(H) = 1.2U_{eq}(C)).

Parameters refined were the overall scale factor, isotropic extinction parameter g (correction of F_c where $F^* = F_c[1.0 + 0.002gF^2/\sin(2\theta)]^{0.25}$), positional and anisotropic thermal parameters for the full occupancy non-hydrogen atoms. Refinements converged with shift: error ratios less than unity for all variables, except occassionally for disordered atoms. Final difference Fourier maps showed no significant features. All calculations were carried out using the SHELXTL program system.[46]

Acknowledgment. This research was supported by the Engineering and Physical Sciences Research Council, the Wolfson Foundation, and Zeneca Pharmaceuticals in the United Kingdom. A NATO Collaborative Research Grant [(SRG 920666) from the Supramolecular Chemistry Program] between Miami and Birmingham helped to support the electrochemical studies reported in the Paper.

JA9438977